# *Using Pickering Stabilisation as a Tool for the Fabrication of Supra-Colloidal Structures*

**Patrick James Colver MChem**

PhD Thesis

University of Warwick

Chemistry Department

December 2008

## *Table of Contents*

# *Tables, Figures and Equations*

## Chapter 1:



## Chapter 2:



## Chapter 3:

## Chapter 4:

## Chapter 5:

## Chapter 6:



## Chapter 7

## Appendix

## *Acknowledgements*

I would like to thank the entire Bon group who I have worked with for making my time fun and interesting. I would like to thank Catheline Colard for her help with the Ludox systems. I also want to Thank Assoc. Prof. Stefan Bon for his continued encouragement and help through out my PhD who without there would probably be no completed thesis. I would like to thank Wang Tao and Prof J. Keddie for the use of their facilities at the University of Surrey and all the help and input given in the work with the pressure sensitive adhesives. I acknowledge S. York, S. Schumann and Dr. N. Wilson for help with microscopy, D. Hammond for running thermal gravimetric analysis measurements on my samples and the EPSRC for funding. I would like to thank P. Wright and K. Randell for transport arrangements, Capt. S. Colver for his literary suggestions, E. Colver for her valued logical thinking and focus. Most importantly I would like to thank H. Keens for keeping me sane and giving constant support.

## *Declaration*

I declare that I am the major contributor to all work in this thesis except for the work in chapter 3 on the jamming of the interface of droplets passed through a capillary which was done in collaboration with S. Mookhoek from DELFT, NL. Also the pressure sensitive adhesives section in chapter 6 which was done in collaboration with Professor J. Keddie and Wang Tao from Surrey University, UK. Lastly the zeta potential graph (Chapter 5, Figure 6) was produced by C. Colard. Any work previously published is referenced on the opening page of each chapter.

Signed_____Date_____

**Patrick Colver**

## *Summary*

We have shown the use of Pickering stabilisation (the stabilisation of an interface with solid particles) in the creation of different materials. This gave us access to structures not possible in normal surfactant systems. These materials have some unique properties: For instance by using the high forces holding the Pickering particles at an oil-water-interface we can create interesting droplet morphologies. The non-spherical droplets obtained this way have potential uses in materials such as self healing composites. Additionally we developed the first Pickering miniemulsion system by using Laponite clay as the stabiliser. We went on to then demonstrate the improvements the latex can impart on the properties of pressure sensitive adhesives as well as increasing the thermal stability of the encapsulated polymer. We also created the first Pickering poly(HIPE) material and have shown that it is possible to produce structures which can be used in applications such as microfiltration. Finally the first purely Pickering emulsion polymerisation system was also designed using Ludox particles as a charged stabiliser. We could then create interesting shell morphologies by post treating the armoured latex particles.

## *Abbreviations*

| | |
|---|---|
| **acrylonitrile** | **(ACN)** |
| **2,2'-azobisisobutyronitrile** | **(AIBN)** |
| **butyl acrylate** | **(BA)** |
| **butyl methacrylate** | **(BMA)** |
| **cation exchange capacity** | **(cec)** |
| **cetyl trimethyl ammonium bromide** | **(CTAB)** |
| **dodecylbenzenesulfonic acid, sodium salt** | **(DDBSS)** |
| **dynamic mechanical thermal analysis** | **(DMTA)** |
| **dimethylaminoethyl methacrylate** | **(DMAEMA)** |
| **dioctadecyl dimethyl ammonium bromide** | **(DODAB)** |
| **di-*tert*-butylperoxyoxalate** | **(DTBPO)** |
| **divinylbenzene** | **(DVB)** |
| **ethyl methacrylate** | **(EMA)** |
| **high internal phase emulsion** | **(HIPE)** |
| **interpenetrating network** | **(IPN)** |
| **potassium persulfate** | **(KPS)** |
| **lauryl acrylate** | **(LA)** |
| **lauryl methacrylate** | **(LMA)** |
| **methyl acrylate** | **(MA)** |
| **methacrylic acid** | **(MAA)** |
| **medium internal phase emulsion** | **(MIPE)** |
| **methyl methacrylate** | **(MMA)** |

| | |
|---|---|
| **nuclear magnetic resonance** | **(NMR)** |
| **polydispersity** | **(PDi)** |
| **pressure sensitive adhesive** | **(PSA)** |
| **sodium dodecyl sulphate** | **(SDS)** |
| **field emission – scanning electron microscope** | **(FE-SEM)** |
| **sorbitan monolaureate** | **(SPAN 20)** |
| **sorbitan monooleate** | **(SPAN 80)** |
| **styrene** | **(St)** |
| **single walled carbon nanotube** | **(SWNT)** |
| **transmission electron microscope** | **(TEM)** |
| **thermal gravimetric analysis** | **(TGA)** |
| **2,2'-azobis(2-methyl propionamidine) dihydrochloride** | **(V-50)** |
| **2,2'-azobis(2,4-dimethyl valeronitrile)** | **(V-65)** |

## *Materials*

Methyl methacrylate, methyl acrylate, *n*-butyl methacrylate, *n*-butyl acrylate, ethyl methacrylate, lauryl methacrylate, lauryl acrylate, octyl acrylate, divinylbenzene, methacrylic acid, ethylene glycol dimethacrylate, acrylonitrile, styrene and 2-ethylhexyl methacrylate were purchased from Aldrich or subsidiary companies at 99% (except DVB which is 80% technical grade) or greater purity and were passed through a basic alumina (activated, basic, Brockmann I) column before use in order to remove inhibitors. Hostasol methacrylate was kindly provided by the group of Prof. D. Haddleton. *n*-Hexadecane was purchased from Aldrich, and sodium chloride was purchased from BDH, both at reagent-grade purity. Ammonia was purchased from Fisher at S.G. 0.88 (35%) concentration in water. All were used as supplied. The clay used was Laponite RD and was kindly donated by Rockward Additives Ltd. AIBN, V-65 and V-50 were kindly donated by Wako Initiators and were used as supplied. Ludox TM40 colloidal silica (40 wt% suspension in water), sodium hydroxide (NaOH), potassium persulfate (KPS) p.a.>99.0% and hydrochloric acid aqueous solution (HCl (aq)) analaR, and sodium dodecyl sulfate (SDS) were purchased from BDH. Cetyltrimethylammonium bromide 99+% (CTAB) and dioctadecyldimethylammonium bromide (DODAB) were purchased from ACROS organics. Olive oil was obtained from the shelf of the local Costcutter supermarket. Oxalyl chloride puriss., ≥99.0%, purum, packed in PTFE bottles, ~5.5 M in decane (over molecular sieve 4Å) (anhydrous)pentane, sodium 4-styrenesulfonate and sodium hydrogen carbonate were purchased from Aldrich or subsidiaries. Pyridine also purchased from Aldrich was stored with half its volume of NaOH pellets in a sealed bottle.

# *Chapter 1: Introduction to Pickering Stabilisation*[1]

Manipulation of materials in order to build useful structures has been done for thousands of years. When you start from a bulk material you can shape it either by carving or etching, or via molding. These shaped objects can then be used as building blocks to subsequently form more complex materials, made via assembly of the individual parts. The preparation of the building blocks follows a top-down approach. This method of producing materials can become complex if the targeted object and individual building blocks become small, *i.e.* of micro- or nano-sized dimensions. Interest in small materials was initiated by a ground breaking lecture given by physicist Richard Feynman in 1959 entitled ''There is plenty of room at the bottom'' in which he addressed the problem of manipulating and controlling things on a tiny scale, with the example of printing the entire 24 volumes of Encyclopedia Britannica on the head of a pin. To easily manipulate materials at this tiny scale a different approach must be used and is called bottom-up, and has great potential. In this, the individual building blocks are synthesized via chemical procedures. This can be a complex task in itself, but the real challenge comes from arranging these individual components into the desired suprastructure. The latter process is referred to as assembly, and there are two ways to achieve this, either directed or spontaneous.

[1] Part of this chapter has already been published: Patrick J. Colver, Tao Chen and Stefan A. F. Bon, *Macromol.Symp.* **2006**, *245-246*, 34-41.

Directed requires an external force to manipulate the building blocks into the desired structure. The most intuitive way of directing building blocks is to be able to physically move them via micromanipulation. In 1986 Ashkin *et al.* showed that light could be used to trap and move particles, a technique referred to as optical tweezers.[1] With holographic optical tweezer arrays it is possible to manipulate and order multiple particles at the same time.[2] Electric fields can be used for o*n*-chip manipulation and assembly of colloidal particles, as recently reviewed by Velev and Bhatt.[3] Winkleman *et al.* showed that 100 μm glass microspheres could assemble into ordered arrays on patterned electrodes under the influence of an applied electric field.[4] Electrodeposition of latexes has been used for years in the coatings industry.[5] Spontaneous assembly, or self-assembly is slightly different. This is where the building blocks can form a structure without being directly manipulated. There are a few ways in which this can be accomplished: Convective flow can be used to assemble colloids into highly ordered lattices, thereby producing photonic crystals.[6] Van Blaaderen showed that uniform FCC crystals can be formed from simple gravity deposition of microspheres on an underlying perforated substrate having a hexagonal arrangement of particle-sized holes.[7] Capillary forces can be used to guide directed assembly of objects/colloids. Whitesides demonstrated the mesoscale assembly of hexagonal disks at the interface of water and perfluorodecalin. By altering which sides of the disks were hydrophilic or hydrophobic, control of the self-assembly process driven

by capillarity was gained. This resulted in a number of different suprastructures.[8] A similar approach was undertaken by Suzuki *et al.*, who, through self assembly of particles with two hemispheres of different wettabilities, created "necklaces" of linked particles.[9] On a much smaller scale, molecules can be tuned to self-assemble via hydrogen bonds to create hydroge*n*-bonded polymers which will self-heal.[10] In a similar vain much work has been conducted on using DNA to cause selective self-assembly. By tuning the hydrogen bonding sites on a particle with amino acids it has been shown that it is possible to arrange particles with a desired partner.[11-13] A more widespread and simple technique for spontaneous self-assembly is the use of Pickering stabilisation [14,15], this is where solid colloidal particles will self assemble onto an interface in order to reduce the overall energy of the system. Weitz and co-workers published a paper on the stabilisation of droplets and coined the term "colloidosome" to describe the suprastructure[16]. Although this lacks the control of some of the other methods, this process has been known for over a century and has recently grown into a big area of interest for many researchers and industries around the world and has great versatility for making different materials. The work I will be reporting in this thesis, uses Pickering stabilisation as its basis.

When particles, instead of surfactant molecules, are used to stabilize an emulsion it is termed a Pickering emulsion.[15] A colloidal particle is a particle that does not feel the affect of gravity and is only influenced by

Brownian motion. Colloidal particles are generally in the size range of 10-1000 nm and can come in many types. Natural colloids can be clays, proteins or even bacteria. Synthetic colloids can be organic; microgel particles or dendrimers. They can also be inorganic *i.e.* metal (oxide) nanoparticles like CdSe or $TiO_2$.

The theory behind a Pickering emulsion is that the particles adsorb at the interface and form a colloidosome in order to lower the total interfacial energy. This is seen by looking at the energy of the interfaces available: Pieranski examined the 3 energies of the created interfaces; particle/oil(p/o) particle/water(p/w) and oil/water(o/w)[17].

$$E_{P/O} = \gamma_{P/O} \cdot 2\pi R^2 (1 - \hat{z}) \qquad \textbf{Equation 1}$$

$$E_{P/W} = \gamma_{P/W} \cdot 2\pi R^2 (1 - \hat{z}) \qquad \textbf{Equation 2}$$

$$E_{O/W} = \gamma_{O/W} \cdot \pi R^2 (1 - \hat{z}^2) \qquad \textbf{Equation 3}$$

Where σ is the respective surface tension and ž=z/R is the displacement (z) of the particle from centre of particle radius R. This allows the calculation of the position of the particle at its lowest energy, and in turn allows the calculation of the type of emulsions most favourably formed:

$$E_{init} = \gamma_{O/W} \cdot \mathrm{A}_{O/W} + 4\pi R^2 \gamma_{W/P} \qquad \textbf{Equation 4}$$

$$E_{final} = \gamma_{O/W} (\mathrm{A}_{O/W} - \pi R^2) + 2\pi R^2 (\gamma_{W/P} + \gamma_{O/P}) \qquad \textbf{Equation 5}$$

This in turn shows that the energy has been reduced and equation 5 can be rewritten as:

$$E_{final} = E_{init} - \pi R^2[\gamma_{O/W} + 2(\gamma_{O/P} - \gamma_{W/P})] \qquad \textbf{Equation 6}$$

This equation can then be used to calculate the total amount of energy saved from the interface change[18]. Figure 1 shows the energies for a standard system involving water and *n*-hexadecane as the two phases and 200 nm polystyrene particles. The calculated energies were divided by Brownian motion ($k_BT$) in order to make these values dimensionless.

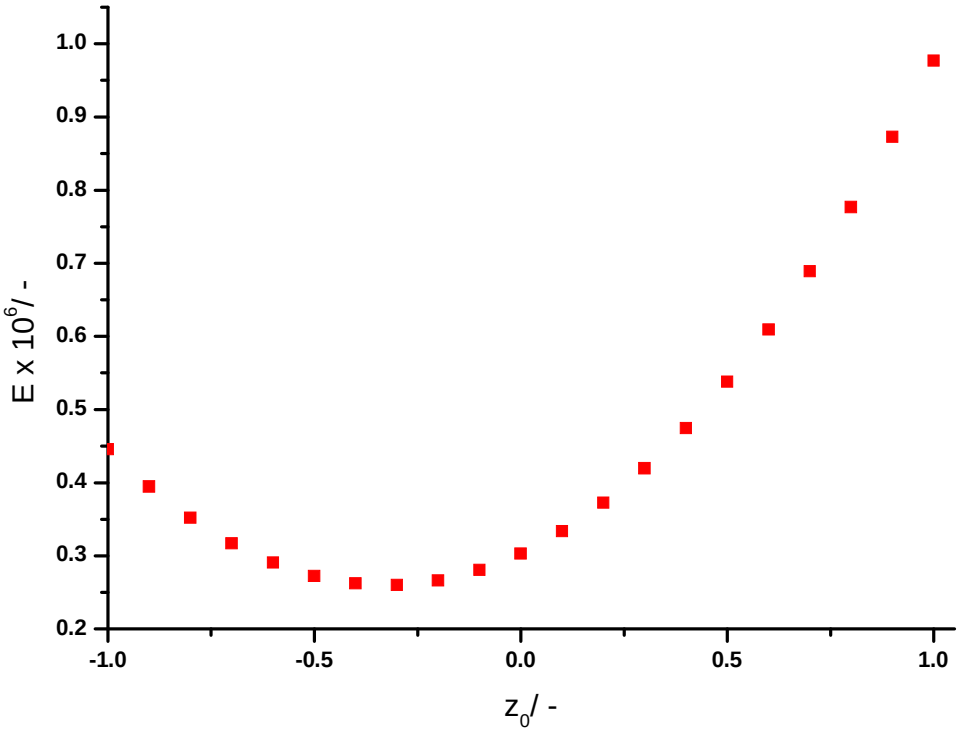


**Figure 1:** Graph showing the energy E, the calculated energy divided by Brownian motion $k_BT$, at different displacements, $z_0$, of the particle, where z=-1 is fully in the *n*-hexadecane phase and 1 is fully in the water phase

Figure 1 shows that the energy needed to remove the particle from the interface is at least 200,000 times that of thermal energy ($k_BT$) and can be up to 700,000 $k_BT$. However, it can also be seen that if the particle was more hydrophobic or hydrophilic the minimum would be shifted. This

implies that if the particle is more stable in one phase the minimum could be greater or less than +/-1, respectively.

This approach does not take into account the angle that the adsorbed particle will form at the interface when a droplet is formed. Binks has shown that the energy required to remove a particle from an interface is[19]:

$$E_{\gamma} = \pi R^2 \gamma (1 \pm \cos\theta)^2 \qquad \textbf{Equation 7}$$

Where $\gamma$ is the interfacial tension between the water and oil phases and $\theta$ is the contact angle made between oil and particle (see Figure 2):

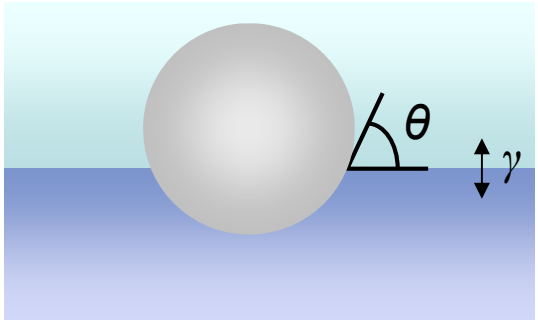


**Figure 2**: Diagram showing a particle at an interface and its contact angle.

The final method for calculating the stabilisation energy adds an extra energy term to the interfacial stabilisation. Another stabilising/destabilising effect is that of image charges. Image charges are a theoretical way of calculating the charge density around an interface (for example a particle). Instead of a boundary of charge, the charges are separated into points. These points are called image charges and, when added up, they completely counter the charge on the particle. The position and size of an image charge can be calculated by Green's

function,[20] which calculates spatial charge density with respect to the dielectric constant of the medium. In a homogeneous solution there is no dependence on spatial coordinates and charge, so there are no defined image charges. When an interface between two materials of different dielectric constants is considered, a dependence on spatial coordinates is now generated. More of the counter ions to the charge will move to the area with a larger dielectric constant, this then induces a macroscopic variation in charge. For a charged particle approaching a planar interface of two liquids of different dielectric constants, two effective charges are generated: One on the particle and one of the same magnitude equidistant on the other side of the interface. The charge on the opposite side of the interface is the generated image charge and has an attraction according to Coulomb's law: "The magnitude of the electrostatic force between two point electric charges is directly proportional to the product of the magnitudes of each charge and inversely proportional to the square of the distance between the charges". The forces involved have been calculated theoretically for spheres with charge double layers by Klein and Grünberg.[21] and were somewhat corroborated by their experimental work measuring these forces by total internal reflection microscopy.[22] This showed that when a particle in an apolar solvent moves towards an interface with a polar one, the image charge has an opposite charge to the particle: This generates an attractive force. For the opposite system the image charge has the same charge as the particle,

creating repulsion. Unrefuted evidence of this stabilising force was shown by van Blaaderen, who showed that, in a generated colloidal crystal of poly(methyl methacrylate) spheres in oil, particles form a monolayer touching (but not imbedded in) the interface between the oil and water.[55] This is attributed to the attraction due to the image charge, since the polymer spheres are not wetted by the water. The role of image charges in the stabilisation of colloidal systems has been expertly reviewed recently.[23]

The major factor that controls the energies involved in the three methods is the particle charge. In solution the surface charge of the particle is neutralised by oppositely-charged ions that will fix around the particle surface, this is called the Stern layer. Other oppositely-charged ions will be attracted to the colloidal particle but will be slightly repelled by the Stern layer; these particles form the diffuse layer. Together these form what is called as a double layer. This double layer causes an electro-kinetic potential between the surface of the colloid and any point in the mass of the suspending liquid. This voltage difference is on the order of millivolts and is referred to as the surface potential. The particle's mobility when a potential is applied is related to the dielectric constant and viscosity of the suspending liquid and to the electrical potential at the boundary between the moving particle and the liquid. This boundary is called the slip plane and is usually defined as the point where the Stern layer and the diffuse layer meet. The Stern layer is considered to be

rigidly attached to the colloid, while the diffuse layer is not. As a result, the electrical potential at this junction is related to the mobility of the particle and is called the zeta potential. Although zeta potential is an intermediate value, it is sometimes considered to be more significant than surface potential as far as electrostatic repulsion is concerned.[24] Typically particles with zeta potentials of greater than +30 mV or less than -30 mV are colloidally stable. These are considered to be the minimum values before the energy of Brownian motion is strong enough to force the particles to become close enough for the Van der Waals forces to overcome the repulsion. When a colloidal particle is used as a Pickering stabiliser it actually benefits the system for the zeta potential to be between +/-30 mV. This is because the particle has to sit on the interface between the two phases, and if the particle is too stable in one phase this will not happen; this is equivalent to the minimum in Figure 1 being outside -/+1.

There are a few examples in which the stability of a Pickering emulsion can be controlled by manipulating the wettability of the stabilising particle. Binks *et al.* showed that the stability of a Pickering emulsion could be controlled by changing the solution pH and using polystyrene latex particles with surface amine groups as Pickering stabiliser.[25] Another interesting paper by Ngai *et al*. who created a temperature and pH responsive Pickering system by using a crosslinked PNIPAM-co-PMAA microgel latex as stabiliser.[26] The water solubility of the PNIPAM

was modified by changing the temperature of the system. This is due to the fact PNIPAM has an LCST of 32 °C in aqueous medium[27]. In addition the charge on the MAA groups can be changed by modifying the pH of the system as the carboxyl groups become deprotonated above pH 4. Li and Stover have reported a doubly pH-responsive system using alumina-coated silica particle and charged potassium hydrogen phthalate species, which only binds to the silica at pH 3.5-5.5. Thus for pH lower than 3.5 or higher than 5.5 the Pickering emulsions are not stable.[28] The solution pH has also been used to control the type of droplet that is stabilised. Schmitt *et al.* showed that by using the same particles and varying the solution pH, small sparsely-covered droplets or large well-covered droplets could be made.[29] Wettability isn't the only factor that can control stability. Fuller *et al.* showed in some ground breaking work that magnetic particles could be used as a Pickering stabiliser. This gives an emulsion which can be reversibly broken via an external stimulus, and also the Pickering particles can be easily reclaimed.[30]

Pickering stabilisation allows for the production of very interesting materials. One example has already been shown creating magnetic latex particles. Recently Salonen showed the production of liquid crystal-like solutions created from solid-stabilised emulsions.[31] The use of Pickering stabilisation has also been used to create Janus-type particles[9] (particles with two or more different faces[32]). In industrial processes control over the particle size distribution is very important. By using limited droplet

coalescence Arditty *et al.* created very monodisperse droplets of sizes ranging from micrometre to millimetre sizes.[29,33] Limited droplet coalescence works by creating more interface than the Pickering stabiliser can cover. The droplets then coalesce until enough interface is covered. Another industrial application has been shown by Syngenta who released a patent on the use of solid-stabilised droplets of pesticides.[34] Later we will discuss solid-stabilised porous materials with structures not accessible using usual conventional surfactants, which are currently being investigated for commercial use.[35] In a similar vein Clegg *et al.* have created stable bicontinous emulsions which are only stable due to the high stabilising force of Pickering.[36-38]

The basic theory of how Pickering emulsions work has been discussed, but the major downfall of this technique is that if one of the phases is removed, the balance of surface energies is broken and the structure falls apart. This is a fatal flaw if the generated structures need to be dried or moved into a different medium. To overcome this, the structures must be stabilised or "scaffolded". There are a few ways in which this can be accomplished:

**Table 1:** Scaffolding Strategies

| Physical Scaffolding | Chemical Scaffolding |
|---|---|
| • Solidification of inner liquid phase<br>• Jamming and/or 2D crystallisation<br>• Autohesion/Film formation<br>• Physisorption of polymers<br>• Formation of an Interpenetrating Polymer Network (IPN) | • Interfacial polymerisation<br>• Chemisorption of polymers |

Firstly the liquid core could be solidified to make the structure more rigid. Paunov followed an intuitive approach by using gelation of agarose in the water phase. [39] The Bon group has used a similar technique by polymerising the internal phase of colloidosomes of styrene and hexadecane stabilised by silica particles. This work creates hybrid organic/inorganic particles.[40] A similar approach was first used with less success by Xin *et al*.[41] Chiu *et al.* also used this technique to create polyaniline/ZnO composite particles.[42] By replacing the inorganic particles with polymer microgels a more stable system is created as the building blocks are irreversibly attached to the interface via a interpenetrating polymer network (IPN).[43] This method was unwittingly used by Wiley in his patents during the 1950's making stable suspension polymerisations.[44-47] Recently a paper by Stone and co-workers demonstrated that by "jamming" the interface of a droplet with particles, a stable crystal structure or "armoured" colloidosome could be formed[48]. This was possible due to the strong adhesive forces holding the particles

to the interface. More examples of jammed structures are given in a later chapter. In the first paper to coin the term "colloidosome", Weitz *et al.* managed to stabilise latex based Pickering emulsions by autohesion. Colloidosomes were prepared by heating above the glass transition temperature ($T_g$) of the latex particles. This allowed deformation and polymer-polymer interdiffusion to reinforce the latex superstructure. [49] One of the simplest ways of physically binding the building blocks to one another at the droplets interface is by physisorption of polymers. Weitz showed a very elegant way of doing this[49] when a droplet containing poly-L-Lysine was stabilised by colloidal latex particles; polymer chains then adsorb onto the latex particles, locking neighbours together, giving a rigid yet flexible scaffold.

An alternative approach to physical scaffolding is to chemical scaffold the structure. One very good way of doing this was performed by Russell, when CdSe QDs stabilised by polymerisable ligands were polymerised using ROMP[50] and in a different paper also by normal free radical polymerisation.[51] Van der Zwaag showed the preparation of a complex Pickering composite material stabilised by an isocyanate–alcohol interfacial polymerization reaction.[52] hollow magnetic colloidosomes have been made and scaffolded using a sol-gel process to deposit a silica shell onto the interface of an oil-in-water emulsion stabilised my magnetic nanoparticles.[53] Cauvin *et al.* recently showed the

chemisorption of reactive polymers to colloidosomes made from inorganic pigments.[54]

In the following chapters we will endeavour to show that many interesting and useful structures can be prepared via Pickering emulsification. We will also show that, by using a Pickering route, materials can be created that are not available using conventional methods surfactant methods.

(1) A. Ashkin, J. M. D., J. E. Bjorkholm, and S. Chu, *Opt. Lett.* **1986**, *11*, 288.
(2) Eric, R. D.; Gabriel, C. S.; Matthew, T. D.; Steven, A. S.; David, G. G. *Rev. Sci. Instrum.* **2001**, *72*, 1810-1816.
(3) Velev, O. D.; Bhatt, K. H. *Soft Matter* **2006**, *2*, 738-750.
(4) Winkleman, A.; Gates, B. D.; McCarty, L. S.; Whitesides, G. M. *Adv. Mater.* **2005**, *17*, 1507-1511.
(5) Koch, R. L., II *Products Finishing (Cincinnati, OH, United States)* **1967**, *31*, 45-53.
(6) Lee, J. A.; Meng, L.; Norris, D. J.; Scriven, L. E.; Tsapatsis, M. *Langmuir* **2006**, *22*, 5217-5219.
(7) van Blaaderen, A.; Ruel, R.; Wiltzius, P. *Nature* **1997**, *385*, 321-324.
(8) Bowden, N.; Choi, I. S.; Grzybowski, B. A.; Whitesides, G. M. *J. Am. Chem. Soc.* **1999**, *121*, 5373-5391.
(9) Suzuki, D.; Tsuji, S.; Kawaguchi, H. *J. Am. Chem. Soc.* **2007**, *129*, 8088-8089.
(10) Cordier, P.; Tournilhac, F.; Soulie-Ziakovic, C.; Leibler, L. *Nature* **2008**, *451*, 977-980.
(11) Kim, A. J.; Biancaniello, P. L.; Crocker, J. C. *Langmuir* **2006**, *22*, 1991-2001.
(12) Liang, H.; Angelini Thomas, E.; Ho, J.; Braun Paul, V.; Wong Gerard, C. L. *J. Am. Chem. Soc.* **2003**, *125*, 11786-7.
(13) Tkachenko Alexei, V. *Phys. Rev. Lett.* **2002**, *89*, 148303.
(14) Ramsden, W. *Proc. R. Soc.* **1903**, *72*, 156-164.
(15) Pickering, S. U. *Journal of the Chemical Society, Transactions* **1907**, *91*, 2001-21.
(16) Dinsmore, A. D.; F., H. M.; Nikolaides, M. G.; Marquez, M.; Bausch, A. R.; Weitz, D. A. *Science* **2002**, *298*, 1006-1009.
(17) Pieranski, P. *Phys. Rev. Lett.* **1980**, *45*, 569.
(18) C. Zeng, H. B., A. D. Dinsmore *Solid State Commun.* **2006**.
(19) Binks, B. P.; Lumsdon, S. O. *Langmuir* **2000**, *16*, 8622-8631.
(20) Jackson, J. D. *Classical Electrodynamics*; Third ed.; John Wiley & Sons, Inc., 1999.
(21) Klein, R.; Von Grunberg, H. H. *Pure Appl. Chem.* **2001**, *73*, 1705-1719.
(22) von Grunberg, H. H.; Helden, L.; Leiderer, P.; Bechinger, C. *J. Chem. Phys.* **2001**, *114*, 10094-10104.
(23) Hatlo, M. M.; Lue, L. *Soft Matter* **2008**, *4*, 1582-1596.
(24) http://www.malverninstruments.com.
(25) Amalvy, J. I.; Armes, S. P.; Binks, B. P.; Rodrigues, J. A.; Unali, G. F. *Chem. Commun.* **2003**, 1826-1827.
(26) Ngai, T.; Behrens, S. H.; Auweter, H. *Chem. Commun.* **2005**, *3*, 331-333.
(27) Wu, C. *Polymer* **1998**, *39*, 4609-4619.
(28) Li, J.; Stover, H. D. H. *Langmuir* **2008**, *24*, 13237-13240.
(29) Arditty, S.; Whitby, C. P.; Binks, B. P.; Schmitt, V.; Leal-Calderon, F. *Eur. Phys. J.: E* **2003**, *11*, 273-281.
(30) Melle, S.; Lask, M.; Fuller, G. G. *Langmuir* **2005**, *21*, 2158-2162.
(31) Salonen, A.; Muller, F.; Glatter, O. *Langmuir* **2008**, *24*, 5306-5314.
(32) Perro, A.; Reculusa, S.; Ravaine, S.; Bourgeat-Lami, E.; Duguet, E. *J. Mater. Chem.* **2005**, *15*, 3745-3760.
(33) Arditty, S.; Schmitt, V.; Giermanska-Kahn, J.; Leal-Calderon, F. *J. Colloid Interface Sci.* **2004**, *275*, 659-664.
(34) Fowler, J.; (Syngenta Participations AG, Switz.). Application: WO WO, 2008, p 43pp.
(35) Colver, P. J.; Bon, S. A. F. *Chem. Mater.* **2007**, *19*, 1537-1539.

(36) Clegg, P. S.; Herzig, E. M.; Schofield, A. B.; Horozov, T. S.; Binks, B. P.; Cates, M. E.; Poon, W. C. K. *J. Phys.: Condens. Matter* **2005**, *17*, S3433-S3438.

(37) Clegg, P. S.; Herzig, E. M.; Schofield, A. B.; Egelhaaf, S. U.; Horozov, T. S.; Binks, B. P.; Cates, M. E.; Poon, W. C. K. *Langmuir* **2007**, *23*, 5984-5994.

(38) Clegg, P. S.; Herzig, E. M.; Schofield, A. B.; Egelhaaf, S. U.; Horozov, T. S.; Binks, B. P.; Cates, M. E.; Poon, W. C. K. *Los Alamos Natl. Lab., Prepr. Arch., Condens. Matter* **2006**, 1-12

(39) Cayre, O. J.; Noble, P. F.; Paunov, V. N. *J. Mater. Chem.* **2004**, *14*, 3351-3355.

(40) Chen, T.; Colver, P. J.; Bon, S. A. F. *Adv. Mater.* **2007**, *19*, 2286-2289.

(41) Liu, Y.; Chen, X.; Wang, R.; Xin, J. H. *Mater. Lett.* **2006**, *60*, 3731-3734.

(42) Jeng, J.; Chen, T.-Y.; Lee, C.-F.; Liang, N.-Y.; Chiu, W.-Y. *Polymer* **2008**, *49*, 3265-3271.

(43) Bon, S. A. F.; Cauvin, S.; Colver, P. J. *Soft Matter* **2007**, *3*, 194-199.

(44) Wiley, R. M.; (Dow Chemical Co.). US, 1959.

(45) Wiley, R. M.; (Dow Chemical Co.). US, 1959.

(46) Wiley, R. M. *J. Colloid Sci.* **1954**, *9*, 427-437.

(47) Wiley, R. M.; (Dow Chemical Co.). DE, 1957.

(48) Subramaniam, A., B.; Abkarian, M.; Stone, H. A. *Nat. Mater.* **2005**, *4*, 553-556.

(49) Gordon, V. D.; Chen, X.; J.W., H.; Bausch, A. R.; Marquez, M.; Weitz, D. A. *J. Am. Chem. Soc.* **2004**, *126*, 14117-14122.

(50) Skaff, H.; Lin, Y.; Tangirala, R.; Breitenkamp, K.; Boker, A.; Russell, T. P.; Emrick, T. *Adv. Mater.* **2005**, *17*, 2082-2086.

(51) Lin, Y.; Skaff, H.; Boker, A.; Dinsmore, A. D.; Emrick, T.; Russell Thomas, P. *J. Am. Chem. Soc.* **2003**, *125*, 12690-1.

(52) Mookhoek, S. D.; Blaiszik, B. J.; Fischer, H. R.; Sottos, N. R.; White, S. R.; van der Zwaag, S. *J. Mater. Chem.* **2008**, *18*, 5390-5394.

(53) Shen, S.-L.; Wu, W.; Guo, K.; Meng, H.; Chen, J.-F. *Colloids and Surfaces A: Physicochem. Eng. Aspects* **2007**, *311*, 99-105.

(54) Shirley, I. M.; Heming, A. M.; Bon, S. F.; Cauvin, S. M. P.; (Syngenta Limited, UK). Application: WO, 2008, p 13pp.

(55) Leunissen, M. E., van Blaaderen, A., Hollingsworth, A. D., Sullivan M. T., Chaikin, P. M., *PNAS*, **2007,** *8,* 2585-2590

## *Chapter 2: Water-in-oil Pickering High Internal Phase Emulsions – Fabrication of Poly"colloido"(HIPE)s*[†]

In the previous chapter we briefly discussed creating Pickering structures with the dispersed phase being a hydrophobic monomer and the external continuous phase being water, which can be polymerised to give individual armoured particles. Prime examples were our previous work in preparing hollow supracolloidal structures using microgels as solid-stabilizers which are scaffolded by interpenetrating polymer networks (IPNs)[1], and our silica-armoured polymer capsules,[2] along with many other examples shown in the previous chapter. However, it is also possible, by tuning the wettability of the Pickering stabiliser, to create either water-in-air or water-in-oil emulsions. Binks showed this by changing an air-in-water foam into a water-in-air "dry water" system. This was done by changing the wettability of the stabilising silica particles, thereby causing a transitional inversion, or by increasing the water and air ratio causing a catastrophic inversion.[3] Tervoort *et al.* has shown a simple method to modify metal oxide nanoparticles in order to create water-in-oil emulsions.[4] By doing this one creates individual droplets of water in a continuous phase of monomer. Solidification of the continuous phase, in the present case through polymerisation, would create a porous monolithic structure, generically referred to as cellular materials. Different types of porous materials have been made using this

[†] Part of this chapter has been published: Patrick J. Colver and Stefan A. F. Bon, *Chem.Mater.* **2007,** *19(7)*, 1537-1539

system for many years:[5] These materials can have a porous structure, which consists of closed cells and/or open cells, with the latter referring to a system in which the pores are interconnected. This porous feature makes these materials interesting for a wide range of applications, such as supports for catalysts (high surface area), mechanical scaffolds *e.g.* for tissue growth, materials for electrical, sound and heat insulation (high porosity), 3D batteries and optical band-gap materials.[6] Pine *et al.* showed the preparation of uniform macro-porous silica, titania and poly(acrylamide) which were synthesized around a concentrated dispersion of liquid emulsion droplets with narrow particle size distribution.[7] Titania foams have been shown to have excellent photocatalytic activity[8] and, using the method developed by Pine's group, can be used to produce photonic crystals.[9] Binks reported the preparation of macroporous silica using solid-stabilised/Pickering emulsions as templates. These materials had either cellular, bicontinuous or colloidal gel type morphologies, depending on the type of emulsion used.[10] More recently, Sun *et al.* showed by the vapour deposition of water onto a hydrophobic oil that Pickering honeycombs could be produced using silica as stabiliser.[11] Sherrington and co-workers have produced numerous examples of porous supports for reactions.[39]

Most of these examples have limited porosity (less than 74%). By creating materials with much higher porosity you can greatly increase the interface of the substrate, vastly improving properties such as catalytic

activity or functional separation. Cellular polymers formed by creation of a High Internal Phase Emulsion (HIPE) and subsequent polymerisation of the continuous phase, are often referred to as poly(HIPE), and were pioneered by Bartl,[12,13] Lissant[14] and Barby.[15] A High Internal Phase Emulsion, or gel emulsion, has a volume fraction for the dispersed phase greater than 0.74, which is the maximum packing density for monodisperse hard spheres. The porous polymer materials are generally formed via templates of water-in-monomer gel emulsions stabilised with surfactants such as sorbitan monooleate (SPAN 80),[16] or a mixture of nonionic, anionic, and cationic surfactants: sorbitan monolaureate (SPAN 20), dodecylbenzenesulfonic acid sodium salt (DDBSS), and cetyltrimethylammonium bromide (CTAB).[17]

We developed, for the first time, the concept of using particle-stabilised, or Pickering, emulsions as a template to manufacture poly(HIPE)s. [18] At the same time we published this work, Bismarck *et al.* published on the use of carbon nanotubes as solid stabilizers to create poly(MIPE)s in an attempt to create a conducting porous material.[19] They later extended this work into the production of titania[20] and silica[21] stabilised poly(HIPES). Tervoort and coworkers have also published some interesting papers in this area, creating many different types of porous materials.[22] Closely related are the recently reported Pickering foams, in which air is used as the internal phase. These are made by modifying silica or clay particles

with surfactants and then using the particles in the same way as surfactants are used in normal HIPE manufacture.[23,24]

Because the particles are effectively irreversibly adhered to the interface in these Pickering systems, they are stable for many months. This characteristic can produce a number of benefits in poly(HIPE) manufacturing, which are not achievable when using conventional low-molecular weight surfactants. The use of Pickering-stabilised emulsion droplets as templates will functionalise the cell walls of the poly(HIPE)s with a layer of solid particles. The irreversible adhesion of the particles to the interface of the emulsion droplets allows the functionalisation of individual cells with different types of particles via one simple synthetic procedure. Another advantage of having particles on the interface rather than surfactants is that the functionalised material will have a larger surface area due to its rough nature.[1] This creation of different micro-environments amongst the cells could be of great potential benefit in the design of porous monoliths for multi-step reactions or filtration processes. We demonstrate this principle by using a combination of fluorescently-labelled and non-labelled cross-linked latex particles as stabilisers; in three possible poly(HIPE) designs illustrated in Figure 1.

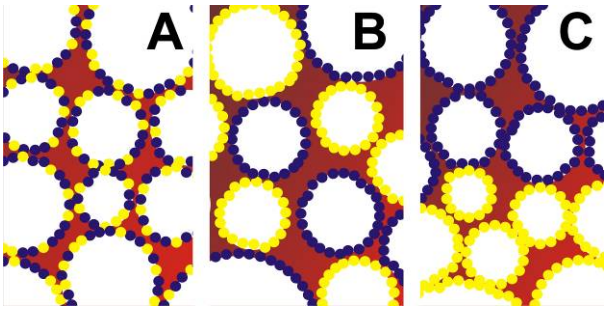


**Figure 1:** Three possible designs using two different particles as Pickering stabilisers of cellular polymer monoliths. *2D* Projections are from the side (y,z-plane). In example A the particles are randomly distributed over each water droplet, or cell; B shows a random blend of two Pickering emulsions with each droplet stabilised by only one type of particle; in C we pack one Pickering emulsion on top of the other creating distinct zones or layers, in the cellular monolith.

The synthesis strategy can be set out in three consecutive steps:

(i) Microgels of submicron dimensions synthesised via miniemulsion polymerisation were used as solid stabilisers to create Pickering water-in-oil emulsions.[1,25,26] When a good solvent for the polymer is used, the crosslinking of these latex particles is essential, in order to prevent disintegration via swelling once assembled at the liquid-liquid interface, which will ultimately result in loss of Pickering stabilization. For the poly(HIPE)s containing two different types of particle stabilisers we used both hostasol-labelled and non-labelled microgels. As a tag we used 2-(6-methacryloyloxyhexyl)-thioxantheno[2,1,9-dej]iso-quinoline-1,3-dione, a hostasol methacrylate derivative.[27] A variety of monomers were used to make up the oil phase, such as divinylbenzene, mixtures of styrene/divinylbenzene, *n*-butyl and mixtures of *n*-lauryl methacrylate/ethylene glycol dimethacrylate. The oil phase also included *ca.* 1.0 wt% of a radical initiator, being di-tert-butylperoxyoxalate[28] or 2,2'-

azobis(2,4-dimethyl valeronitrile) (V-65). The microgel-stabilised water-in-oil emulsions were generated by vigorous handshaking. Note that the microgels are dispersed in the aqueous phase prior to mixing. Also in some cases the room temperature initiator, di-tert-butylperoxyoxalate, was used when monomer and water evaporation, or the formation of air bubbles, caused the creation of large voids or induced destabilisation.

(ii) The Pickering emulsions were allowed to settle via gravitation/buoyancy, typically for about 1 hour with occasional gentle shaking to increase the packing efficiency. According to Stokes' law (1851) this is the time needed for a "hard sphere" of water with a diameter of 10 μm to descend 4.36 cm in toluene, conditions which are easily met for our monolith designs:

$$V_S = \frac{2}{9}\frac{(\rho_p - \rho_f)}{\mu} g \cdot R^2 \qquad \textbf{Equation 1}$$

Equation 1 shows the equation that corresponds to Stokes' law. Where $V_s$ is the terminal velocity of the droplet of water (m/s), $\rho_p$ is the density of the water droplet (998 kg/m$^3$), $\rho_f$ is the density of the continuous medium (taken to be toluene at 867 kg/m$^3$), μ is the viscosity of the continuous medium (0.59 x 10$^{-3}$ Pa s), g is the acceleration due to gravity (9.81 m s$^{-2}$) and R is the mean radius of the droplet (m).

Since the emulsion droplet size distributions were not monodisperse, this allowed for the generation of high internal phase Pickering emulsion layers (vol. fraction > 0.74). A pre-made mixture of hostasol-labelled

(yellow) and non-labelled (white) microgels dispersed in the water phase was used for system **A**. The random blend of emulsion droplets each stabilised with one type of particle, **B**, was generated by gentle mixing of two pre-made Pickering emulsions via tumbling by hand of the vials. For the layered systems, **C**, one high internal phase Pickering emulsion template was carefully placed on top of the other using a pipette.

(iii) The stacked high internal phase Pickering emulsions were subsequently polymerised via radical polymerisation of the continuous monomer phase either at ambient temperature using di-*tert*-butylperoxyoxalate, or at 51$^{o}$C using V-65 as initiator. Note that in all experiments the excess bulk phase of pure monomer was not removed. Typically the polymerisation was allowed to proceed for a minimum of four initiator half-lives. The poly(HIPE) monoliths produced were obtained by removal of the cylindrical glass reaction vessel and were dried in air and subsequently under vacuum. In case of isolated cell structures the monoliths were crushed.

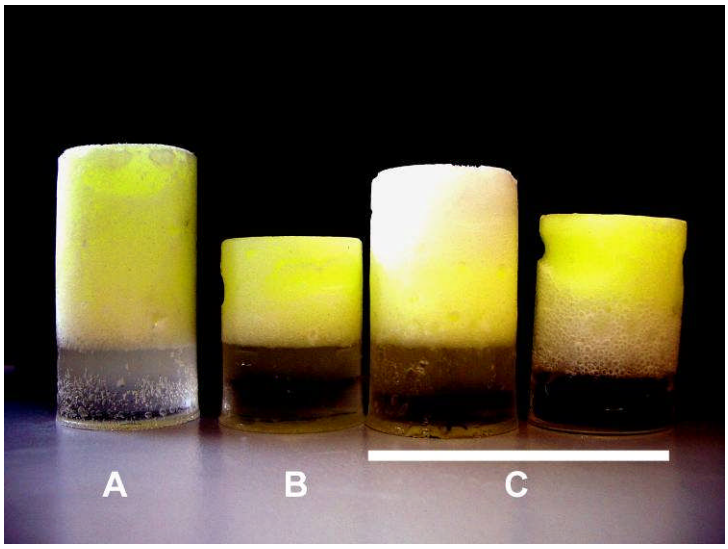


**Figure 2:** Collection of poly(*n*-butyl methacrylate) based cellular polymer monoliths produced via Pickering high internal phase emulsions after removal of reaction vial. The monoliths are placed upside down. The clear bottom layer in the image is bulk polymer

Figure 2 depicts three possible monolith scenarios using two different particle stabilisers, the continuous phase being poly (*n*-butyl methacrylate). This polymer was used as it made analysis easier, because the monoliths were easier to cut for FE-SEM analysis. From the two monoliths on the right, it is evident that schematic design **C** has been achieved with the hostasol-labelled microgels imbedded at the bottom and the top of the cellular monolith, respectively. To distinguish between designs **A** and **B**, we performed confocal microscopy. The results are given in Figure 3 for scenario **B**. From this image it can be clearly seen that only a fraction of the cells are covered with fluorescent microgels, in the image coloured yellow. The location of the yellow "rings" shows that the fluorescent particles are located mostly at the cell interfaces. Moreover, it proves that no interchange of particles between the

Pickering-stabilised emulsion droplets occurs on the time scale of the in situ polymerisation, otherwise all cells would show some fluorescent emission. These findings are to be expected, since the energy well at the liquid-liquid interface is too large for the particles to escape.

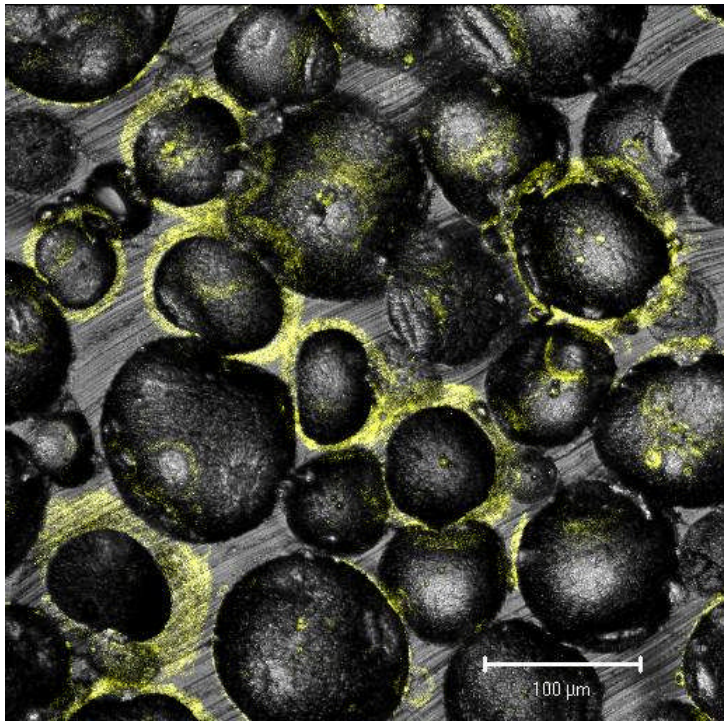


**Figure 3:** Cumulative projection of z-slices obtained via dual channel confocal microscopy. The first channel (white) represents the reflected light signals of the Pickering poly(HIPE), whereas the second channel (yellow) exclusively shows the fluorescent emission

In order to prove that the materials we have made are indeed poly(HIPE) materials, their porosity must be calculated. To do this, the clear bulk polymer phase was removed from the monoliths, after which their overall density was calculated via gravimetry, assuming cylindrical cellular polymer monolith geometry and a known density of the scaffold polymer. All Pickering poly(HIPE) materials showed had volume fraction of air of between 0.76-0.87.

When various monomers are used as the continuous phase, different properties can be imbibed into the structure. For instance, upon evaporation of the water under vacuum the monoliths made from poly(*n*-butyl methacrylate) buckled. Clearly, the pure poly(*n*-butyl methacrylate) scaffold is not robust enough to withstand pressure differences/capillary forces upon drying.

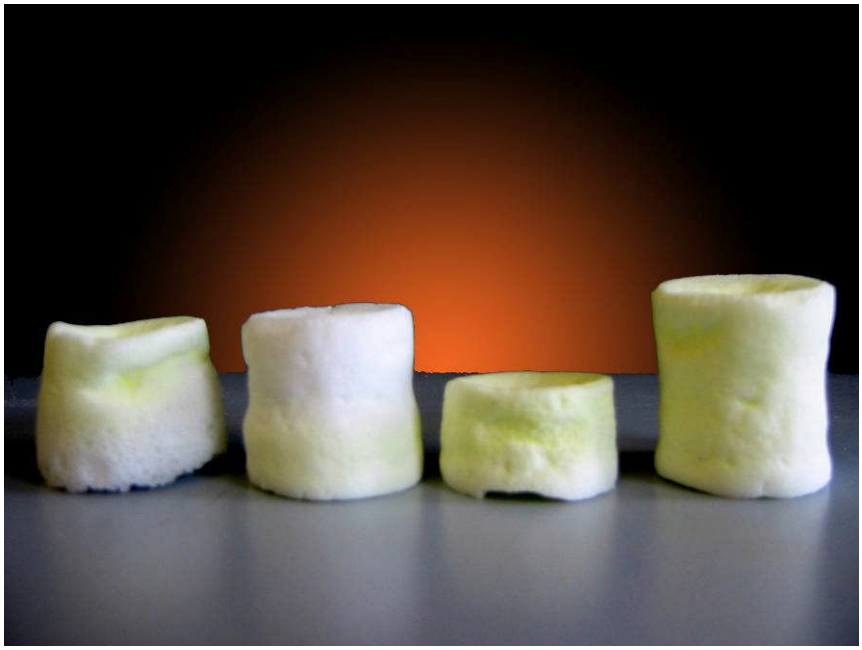

**Figure 4:** Image showing the buckling of the 4 PBMA Poly(HIPE) materials shown in figure 2 after drying

Permanent shape deformation of the cellular monoliths were not observed when 10.1% divinylbenzene was used as a comonomer, or in the cases of pure divinylbenzene or its mixtures with styrene, or in the case of a mixture of *n*-lauryl methacrylate and ethylene glycol dimethacrylate (4.7 wt%). The pure divinylbenzene monolith gave the highest porosity of 87 %. This is probably due to the DVB having the highest density change during polymerisation, causing volume contraction of the continuous phase while the internal phase remains the same size.

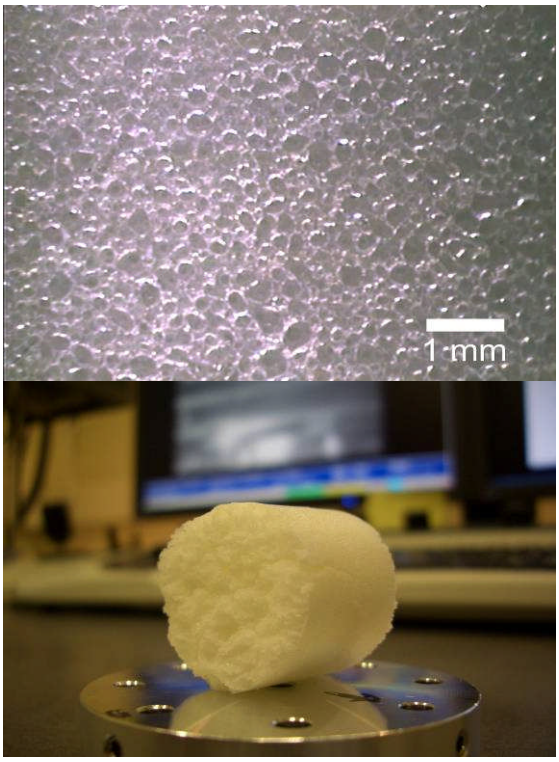


**Figure 5:** Images of pure poly(DVB) HIPE. Top shows an optical microscope image of the porous structure, while bottom shows the whole monolith.

The latter *n*-lauryl methacrylate plus ethylene glycol dimethacrylate cellular monolith was very flexible and spongy. Elastomeric poly(HIPE) materials have been made before by Cameron and Sherrington using conventional surfactants.[29]

An important parameter to control in our system is the cell size. As in normal surfactant poly(HIPE) systems this can be controlled by varying the amount of microgel particles used. As a crude indication for cell dimensions, *i.e.* the diameter of the Pickering-stabilised emulsion droplets, we can use equation 2:

$$D = \pi \cdot Cov \cdot \left( \frac{1}{w_{part}} \right) \cdot \left( \frac{\rho_{part}}{\rho_{water}} \right) d_{part} \qquad \textbf{Equation 2}$$

In which *Cov* represents the coverage expressed as the ratio of the effective area covered by the particle stabilisers and the total area of the water droplet, $w_{part}$ is the weight fraction of particle stabilisers used with respect to the amount of water phase, $\rho_{water}$ and $\rho_{part}$ being the densities of the water phase and the microgel particles in g cm$^{-3}$, and $D$ and $d_{part}$ are the diameters of the emulsion droplet and the particle stabilisers in µm. In case of the preparation of a purely divinylbenzene-scaffolded cellular monolith (see experimental) we assume full coverage, *Cov* = 1. This would in theory produce a poly(HIPE) having cells with an average diameter of approximately 400 µm. From figure 6 it can be observed that this approximate value is of the right order of magnitude.

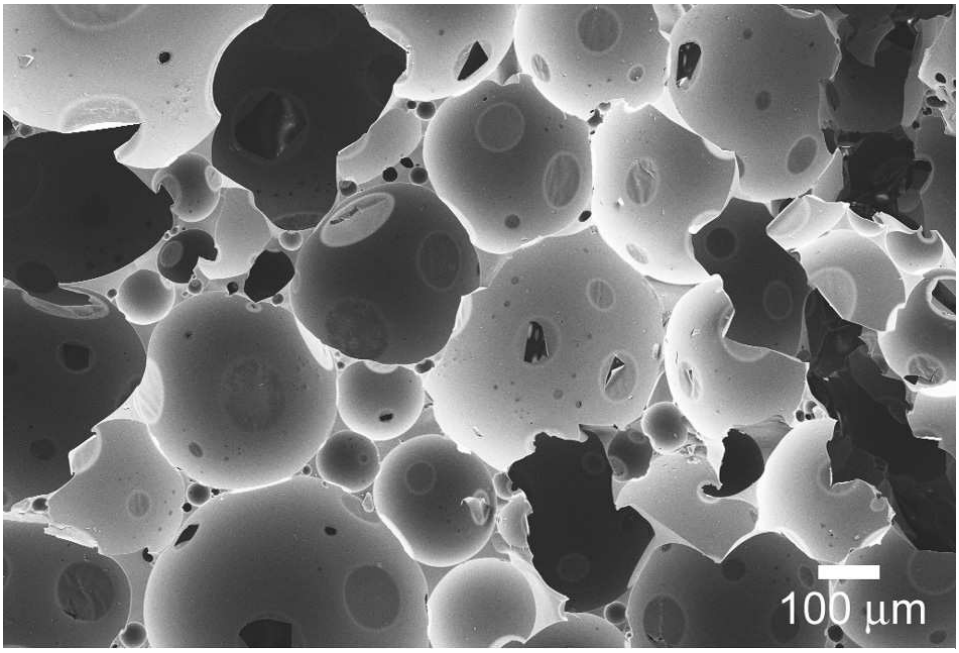


**Figure 6:** FE-SEM image of cellular monoliths scaffolded with poly(divinyl benzene).

The cellular structure in our Pickering Poly(HIPE)s can be open and/or closed. In the case of the poly(divinylbenzene) monoliths, we see from FE-SEM analysis (Figure 6) that cells sometimes are interconnected, but in most cases a thin film is present at the points of contact of two cells. This thin film occasionally is broken, as can clearly be observed from the image. It seems logical that these films are present since Pickering emulsions are highly stable, even upon direct contact. We envisage that these films could be used as pressure release valves in two pack systems where each individual cell is filled with different reagents, provoking a desired chemical reaction upon rupture.

Figure 3 already indicated that the fluorescent particles are present at the interface of the cells. A question arising is whether we have a film with particles on both sides, or a monolayer of particles at the point of contact

between two cells. The latter was recently observed by Horozov and Binks.[30] In all of our cases we have not been able to find bridging monolayers.

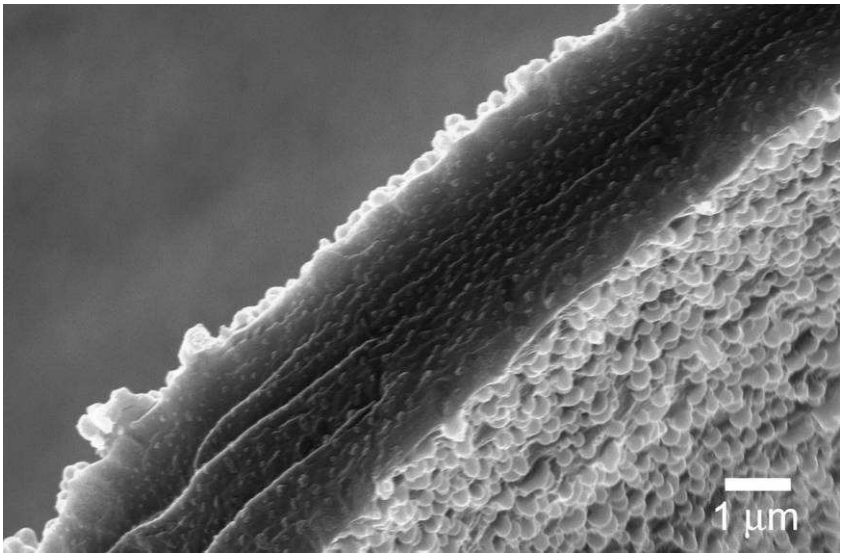


**Figure 7:** FE-SEM image of point of contact between two cells in Pickering Poly(HIPE). It can be seen that particles are presents on both sides of the 3 µm interconnecting film

As clearly can be seen from Figure 7, microgel building blocks are present at both sides of the interconnecting scaffolding polymer. The absence of monolayer films could however be an artefact, as these films would be very thin and could quite easily break under the stresses of drying and sample preparation. This film breaking was observed in some cases when we tried to examine some films more closely under SEM.

It is also possible, due to the high stability of these emulsions, to increase their porosity by forcing greater packing density by putting the liquid HIPE into a centrifuge tube and spinning the emulsion and forcing the heavier water to the bottom of the tube. It was found that our emulsions could withstand forces up to 3000 times gravity. By removing the

resulting excess monomer forced to the top, poly(HIPE) materials could be made with 80-90 % porosity without the need for a 1 hr settling period. These materials however were not as robust as the HIPEs made previously. This can be seen in Figure 8.

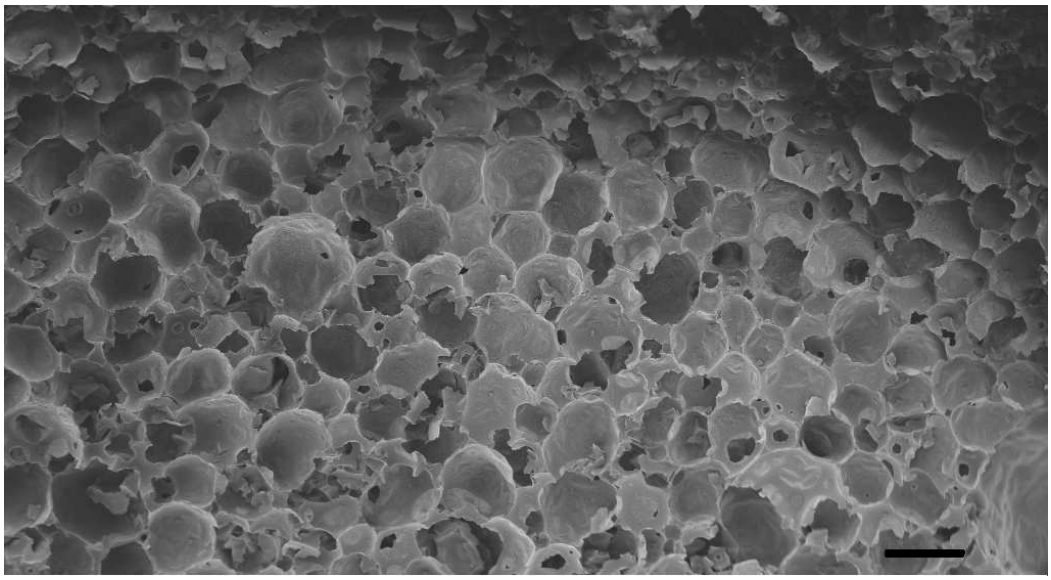

**Figure 8:** FE-SEM image showing a polymerised HIPE after centrifugation. Of note are the thin walls which can be seen to have crumbled.

A potential application of the poly(HIPE) monolith is as a scaffold for tissue regeneration, as shown by Cameron.[31] Another potential use is that of a monolithic stationary phase in separation science. This was first shown by Bhumgara,[32] but much subsequent work has been done by Frechet and co-workers who have shown monoliths made from many types of materials to separate different materials.[33-37] However, because of the stability of our Pickering system we can go one further than these systems. One major problem in making poly(HIPE) filtration devices is that when the capillaries get small the forces involved are so great that the emulsion structure is destroyed. Due to the greater stability of our

solid-stabilised system it is possible to create microfiltration devices. The method for producing these differs little from the bulk system. The basic inverse Pickering emulsion is created and a capillary is then inserted into the medium. The capillary forces cause the emulsion to rise up the tube. (It is this high force that breaks down standard foams. This is because, for capillary action to occur, the attractive force between a substrate and a fluid needs to be greater than intermolecular forces, *i.e.* the forces holding a surfactant at an interface). The monomer/water HIPE can then be polymerised thermally or via a photo-initiator to create a solid porous structure inside the capillary.

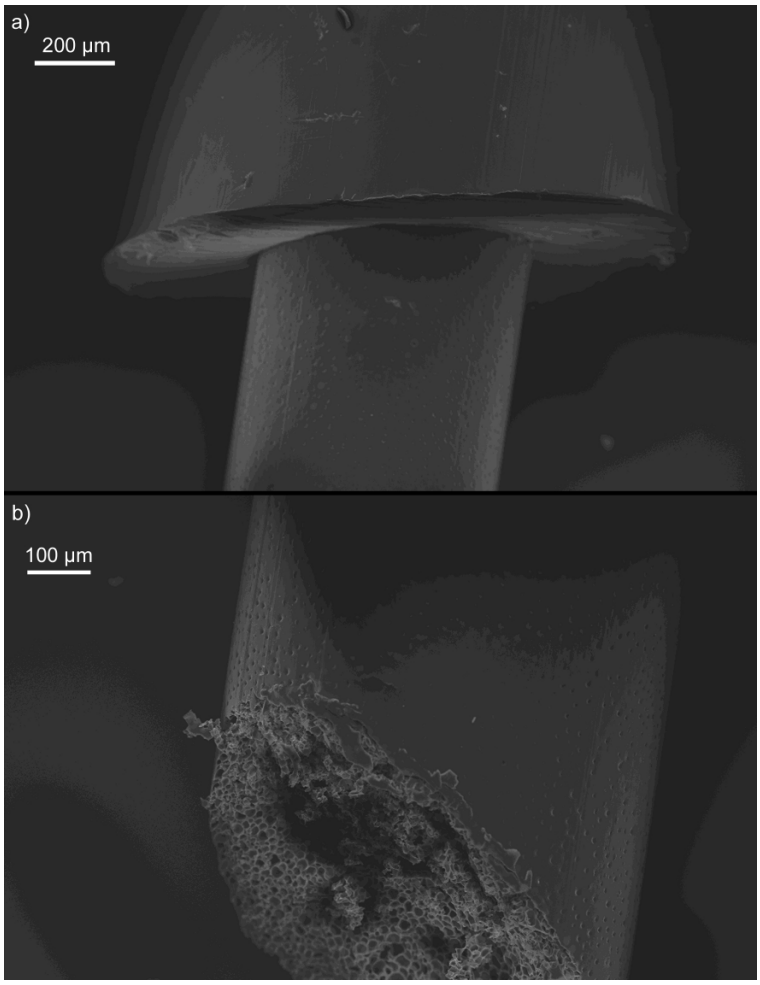


**Figure 9:** a) FE-SEM image showing the solid polymer HIPE protruding from a PTFE tube and b) the porous end of the HIPE

Figure 9 shows the successful polymerisation of a solid-stabilised poly(HIPE) inside a 750 µm I.D. tube. Note however that the cellar structure generated is not interconnecting. This is because the pores generated to create the HIPE needed to be much smaller in order to get sufficient porosity in a small tube. This has the result of decreasing the settling rate of the emulsion, meaning less packing density is achieved. There are a couple of ways this could be potentially overcome. Firstly centrifugation could be used, or secondly a filter could be used to allow the extraction of continuous phase while retaining the particle-stabilised

droplets. Another issue which can be seen in this system, as can be seen from Figure 8a, is the contraction of the continuous phase during polymerisation. This causes the HIPE material to pull away from the inside of the capillary. This problem can be overcome in a couple of ways; either by modifying the inside of the capillary to polymerise along with the continuous phase, or by making the material of the capillary from a material that will swell with monomer to create an interpenetrating network of polymer chains.

## *Conclusion*

It has been shown that Pickering-stabilised Poly(HIPE)s can be made with different morphologies that are not possible with standard surfactant-stabilised HIPEs. It has also been shown that there is potential use for these structures to be used in microfiltration. More work is being done in collaboration with Dr. Emily Hilders' group in Tasmania on overcoming the remaining obstacles involved in this application.[38]

## *Experimental*

### General conditions

pH measurements were performed using a Knick pH meter 765 Calimetic. Miniemulsions were formed using a shear force created by a Branson 450W digital sonifier. Micro*n*-sized colloidosomes were generated via handshaking or using an IKA WERKA, Ultra Turrax, T25 basic. Centrifugation was performed using a Sigma Sciquip 2-16 with a

Sigma 12151 adapter at 1000g for 2 times 5 min. Excess organic phase was removed with a pipette. Dynamic light scattering and zeta potentials measurements were performed on a Malvern Instruments Zetasizer 3000HSA. FE-SEM images were taken on a ZEISS supra 55VP FEGSEM under high vacuum EHT = 5 kV WD = 4 mm. Confocal imaging was performed on a ZEISS LSM 510 confocal microscope with a 458 nm, 477 nm and 488 nm wavelength argon ion laser with two active channels: One with a LP 505 filter (detects fluorescence) and another with no filter (detects reflectance).

**Pickering Particle Formation**

Poly(ethyl methacrylate-b-2-(dimethylamino)ethyl methacrylate) ($M_n$(SEC) = 17800, $M_w/M_n$ = 1.24, $H^1$-NMR DMAEMA:EMA molar ratio = 88:60) (0.4047 g, $0.23x10^{-4}$ mol, 4 %wt)[1] *n*-hexadecane (0.4545 g, 4 %wt) MMA (9.1111 g, $0.9x10^{-1}$ mol) and DVB (1.0520 g, $0.8x10^{-2}$ mol) (total 10% solids), was added to a 250 mL beaker and mixed until all had dissolved. Deoxygenated distilled water (85 mL) was added to the organic mixture. While stirring the mixture, the pH was lowered to pH 4.5 by adding conc. HCl (aq) dropwise. While under ice and stirring the mixture was sonicated at 70% amplitude for 6 mins 30 secs in 1 min intervals with a 30 second rest, with the temperature controlled to a 40 $^oC$ maximum to minimise monomer evaporation. The mixture was decanted into a 250 mL round bottom flask and sealed with a Suba seal. The mixture was purged with nitrogen for 10 minutes while an oil bath heated it to 45 $^oC$.

After ten minutes the mixture was subjected to positive nitrogen pressure and V-044 initiator (0.0542 g, $1.6 \times 10^{-4}$ mol) dissolved in deoxygenated water (2 mL) was injected into the emulsion. After 24 hrs the mixture was and allowed to cool. Particle formed had $Z_{average}$=153 nm PDi=0.03, determined by dynamic light scattering.

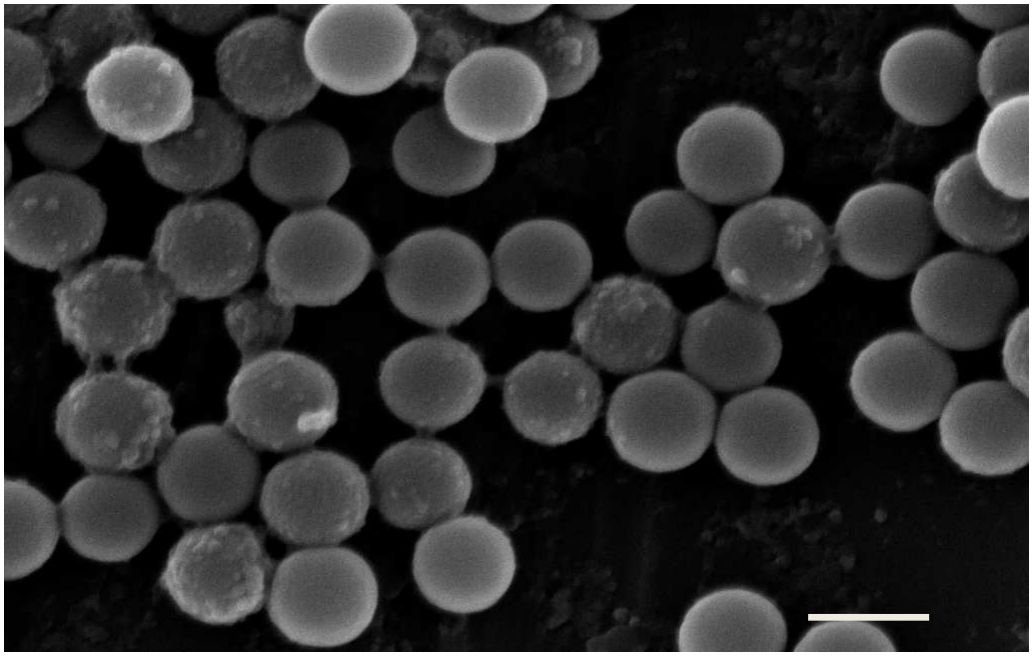

**Figure 10:** FE-SEM image of DVB-poly(methyl methacrylate) latex spheres used for generating poly(HIPEs). Scale bar 200 nm

## Inverse Pickering Emulsion Formation

*Preparation of poly(divinylbenzene) HIPE:* The PMMA microgel particles (0.01 g) were dispersed in water (8.5 g, 46 wt%) at pH 9. Next divinylbenzene (10.0 g, 54 wt%) containing V-65 (0.05 g) as initiator was added and the mixture was shaken to generate the Pickering emulsion. The Pickering emulsion was allowed to settle for 1 hour, during which the emulsion was gently agitated to improve the packing density of the droplets. The excess amount of divinylbenzene was removed from the

top with a pipette. The resulting high internal phase emulsion was then allowed to polymerise at 51 $^{o}$C for 24 h. The poly(HIPE) was allowed to dry first in air and then under vacuum. This was done to remove the water. The overall porosity of this poly(HIPE) was 82%.

All other poly(HIPE) materials mentioned were formed in the same way except the monomer type was exchanged.

**Synthesis of di-tert-butylperoxyoxalate:**

This compound was prepared using the procedure reported by Bartlett *et al*[28]. Tert-butyl hydroperoxide (5.5 M solution, 18.85 g) dry pyridine (12 mL) and anhydrous *n*-pentane (120 mL) were charged into a 500 mL round bottom flask under nitrogen, which had previously been dried in an ovenset to 150 °C. This mixture was cooled below -10 °C using a solution of saturated calcium chloride cooled to just above freezing by liquid nitrogen. Oxalyl chloride (0.077 M, 9.75 g) in 80 mL anhydrous pentane was added dropwise during stirring over a period of 1 h while keeping the temperature under -5 °C. The mixture was then stirred for another 1.5 h then allowed to reach room temperature. The finished reaction mixture was filtered and the filtrate was recrystalised in frozen *n*-heptane. The resulting crystals of DTBPO were filtered then collected.

**CAUTION: This compound is an explosive hazard and, therefore, the use of metal equipment should be avoided to exclude possible induced**

**decomposition. Moreover, the compound should be handled with extreme care – avoid scratching and shaking – and should always be stored in a freezer (255 K) immediately after use, preferably in a plastic container.**

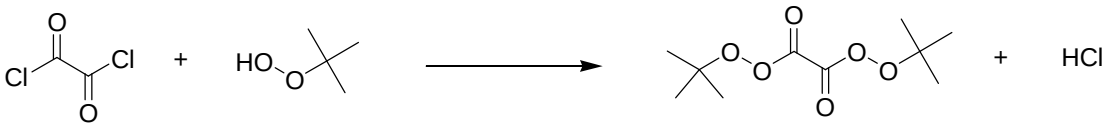


**Figure 11:** Schematic showing the reaction to form the low temperature DTBPO initiator

Yield: 30%

$H^1$NMR: 300 Hz ($CDCl_3$) δ 7.2600 (s, $CDCl_3$), 1.3707 (s, 18H, all H's), 1.2658 (s, 3Heq, self-terminated radical)

$C^{13}$NMR: 300 Hz ($CDCl_3$) δ 169.0116 (C=O), δ 85.6531 (tertiary C centre), δ 76.3623-77.2152 ($CDCl_3$), δ 30.9819 (self-terminated radical $CH_3$), δ 25.7806 ($6CH_3$)

(1) Bon, S. A. F.; Cauvin, S.; Colver, P. J. *Soft Matter* **2007**, *3*, 194-199.
(2) Chen, T.; Colver, P. J.; Bon, S. A. F. *Adv. Mater.* **2007**, *19*, 2286-2289.
(3) Binks, B. P.; Murakami, R. *Nat. Mater.* **2006**, *5*, 865-869.
(4) Akartuna, I.; Studart, A. R.; Tervoort, E.; Gonzenbach, U. T.; Gauckler, L. J. *Langmuir* **2008**, *24*, 7161-7168.
(5) Zhang, H.; Cooper, A. I. *Soft Matter* **2005**, *1*, 107-113.
(6) Gibson, L. J.; Ashby, M. F. *Cellular Solids: Structure and properties*; second ed.; Cambridge University Press, 1999.
(7) Imhof, A.; Pine, D. J. *Chem. Eng. Technol.* **1998**, *21*, 682-685.
(8) Zhao, Y.; Zhang, X.; Zhai, J.; Jiang, L.; Liu, Z.; Nishimoto, S.; Murakami, T.; Fujishima, A.; Zhu, D. *Microporous Mesoporous Mater.* **2008**, *116*, 710-714.
(9) Manoharan, V. N.; Imhof, A.; Thorne, J. D.; Pine, D. J. *Adv. Mater. (Weinheim, Germany)* **2001**, *13*, 447-450.
(10) Binks, B. P. *Adv. Mater.* **2002**, *14*, 1824-1827.
(11) Sun, W.; Ji, J.; Shen, J. *Langmuir* **2008**, *24*, 11338-11341.
(12) Bartl, H.; Bonin, W. v. *Makromole. Chem.* **1962**, *57*, 74-95.
(13) Bartl, H.; Bonin, W. v. *Makromole. Chem.* **1963**, *66*, 151-156.
(14) Lissant, K. J.; Mayhan, K. G. *J. Colloid Interfac. Sci.* **1973**, *42*, 201-208.
(15) Barby, D.; Haq, Z. 1982.
(16) Williams, J. M. *Langmuir* **1991**, *7*, 1370-1377.
(17) Barbetta, A.; Cameron, N. R. *Macromolecules* **2004**, *37*, 3188-3201.
(18) Binks, B. P. *Curr. Opin. Colloid Interface Sci* **2002**, *7*, 21-41.
(19) Menner, A.; Verdejo, R.; Shaffer, M.; Bismarck, A. *Langmuir* **2007**, *23*, 2398-2403.
(20) Menner, A.; Ikem, V.; Salgueiro, M.; Shaffer, M. S. P.; Bismarck, A. *Chem. Commun.* **2007**, 4274-4276.
(21) Ikem, V. O.; Menner, A.; Bismarck, A. *Angew. Chem. Int. Ed.* **2008**, *47*, 8277-8279.
(22) Studart, A. R.; Gonzenbach, U. T.; Akartuna, I.; Tervoort, E.; Gauckler, L. J. *J. Mater. Chem.* **2007**, *17*, 3283-3289.
(23) Zhang, S.; Lan, Q.; Liu, Q.; Xu, J.; Sun, D. *Colloids Surf. Physicochem. Eng. Aspects* **2008**, *317*, 406-413.
(24) Binks, B. P.; Kirkland, M.; Rodrigues, J. A. *Soft Matter* **2008**, *4*, 2373-2382.
(25) Fujii, S.; Read, E. S.; Binks, B. P.; Armes, S. P. *Adv. Mater.* **2005**, *17*, 1014-1018.
(26) Ngai, T.; Behrens, S. H.; Auweter, H. *Chem. Commun.* **2005**, *3*, 331-333.
(27) Tronc, F.; Li, M.; Lu, J.; Winnik, M. A.; Kaul, B. L.; Graciet, J.-C. *J. Polym. Sci. Part A: Polym. Chem.* **2003**, *41*, 766-778.
(28) Bartlett, P. D.; Benzing, E. P.; Pincock, R. E. *J. Am. Chem. Soc.* **1960**, *82*, 1762-1768.
(29) Cameron, N. R.; Sherrington, D. C. *J. Mater. Chem.* **1997**, *7*, 2209-2212.
(30) Horozov, T. S.; Binks, B. P. *Angew. Chem. Int. Ed.* **2006**, *45*, 773-776.
(31) Christenson, E. M.; Soofi, W.; Holm, J. L.; Cameron, N. R.; Mikos, A. G. *Biomacromolecules* **2007**, *8*, 3806-3814.
(32) Bhumgara, Z. *Filtr. Sep.* **1995**, *32*, 245-51.
(33) Viklund, C.; Svec, F.; Frechet, J. M.; Irgum, K. *Biotechnol. Progr.* **1997**, *13*, 597-600.
(34) Petro, M.; Svec, F.; Gitsov, I.; Frechet, J. M. *Anal. Chem.* **1996**, *68*, 315-21.
(35) Peters, E. C.; Petro, M.; Svec, F.; Frechet, J. M. *Anal. Chem.* **1997**, *69*, 3646-9.
(36) Svec, F.; Frechet, J. M. *Science* **1996**, *273*, 205-11.
(37) Xie, S.; Svec, F.; Frechet, J. M. *J. Chromatogr. A* **1997**, *775*, 65-72.
(38) http://fcms.its.utas.edu.au/scieng/chem/pagedetails.asp?lpersonId =2475.
(39) Guyot, A., Hodge, P., Sherrington, D. C., Widdecke, H., *Reactive Polymers*, **1992**, *3*, 233-259

## *Chapter 3: Pickering Droplets – Control of Morphology*[*]

Non-spherical shapes are of great interest for several reasons. For instance objects with a high surface area to volume are much more effective in self healing composite materials. This can be seen by looking at the work by White *et al.* who showed a composite material which could be used for the self healing of cracks.[1]

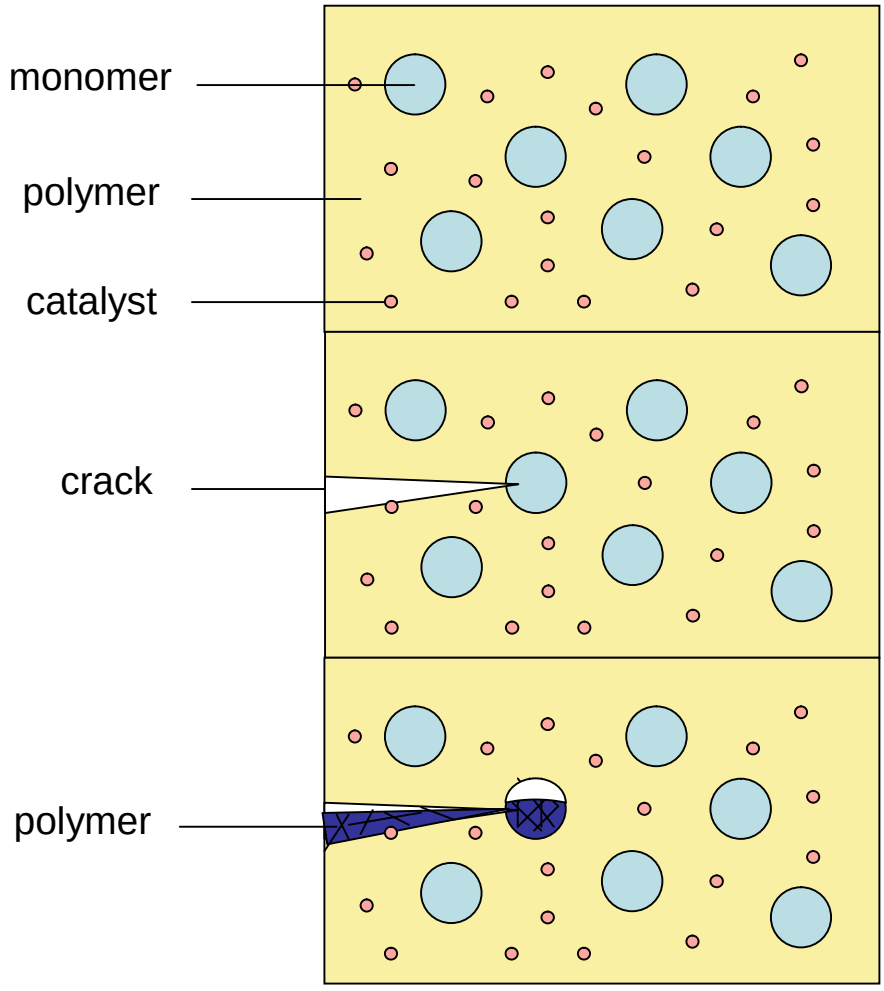


**Figure 1:** Reproduction of the self healing material designed by White *et al.* showing crack propagation and subsequent healing due to catalytic polymerisation

[*] Part of this Chapter was published Stefan A. F. Bon, Steven D. Mookhoek, Patrick J. Colver, Hartmut R. Fischer, and Sybrand van der Zwaag, *Eur.Polym.J.* **2007**, *43(11),* 4839-4842

The main flaw with this system was that in order to get an effective chance of crack propagating onto a capsule a high volume % of capsule must be added. This amount of additive dramatically reduces the effectiveness of the material. By increasing the aspect area of the capsule the chance of cracks propagating onto the correct area is increased, meaning less material need be added.

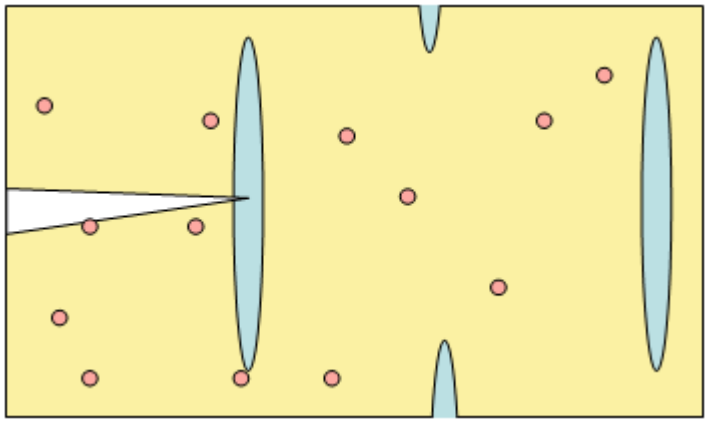

**Figure 2:** Diagram showing the improved chance of crack propagating through an elongated capsule.

Obviously this technique would only work for materials with one direction of propagation, but this is possible for materials with a force constantly applied along one direction.

A second bonus for having a higher surface area to volume ratio is that a non-spherical object will have a high surface area with which to interact with its environment, making them of interest for substrate interactions and chromatographic applications. They are also subject to the "brazil nut effect"[2,3] causing separation from similarly sized spherical shapes.

Many techniques have been used to generate non-spherical shapes. Okubo has shown by controlling the phase separation of monomers

during stepwise polymerisation of latex particles, many interesting shapes can be produced, one example being "octopus particles".[4] another technique to create non-spherical particles is to physically manipulate them. Kumacheva has shown that by creating droplets in a microfluidic device and forcing them through a narrower capillary than the diameter of the droplet, non-spherical shapes could be obtained by then polymerising the droplet inside the capillary.[5] A similar technique has been used to create magnetic discs or plugs.[6] Another technique using a similar principle was designed in 1990 to create rod shaped polystyrene particles. Styrene was dispersed in an elastomeric matrix. The matrix was then stretched deforming the styrene and this was then polymerised to lock in the structure.[7] Recently some very interesting work has been published where non-spherical particles were generated by assembling particles into the pores of a honeycombed structure and heating the material up until the cluster of particles film-form and generate well-defined multi-lobed particles.[8] Stone showed by compressing two Pickering stabilised bubbles into each other an elongated non-spherical bubble could be produced.[9] This is because a "jammed" interface was generated, meaning that the bubble could not return to its spherical shape, as doing so would require the removal of particles from the interface which we have already shown would require a very large force. A similar principle of jamming an interface was manipulated to generate the stable bijels mentioned in the earlier chapter.[10] We will show two

methods of our own, utilising this jamming of interfaces to non-spherical droplets. The first method we will demonstrate relies on a microfluidic approach by passing spherical oil droplets dispersed in water through a long narrow cylindrical tube or capillary with internal diameter being considerably smaller that the diameter of the droplets. By doing this, the oil droplet will deform by forming a plug of oil through the capillary. Normally the deformed droplets will re-adapt, within a very short time span, to their spherical shape upon exit from this confined environment. However, when we use Pickering stabilisers we can prevent the droplets from relaxing back to their spherical shape.

Pushing Pickering stabilized droplets through a narrow capillary will create an enlarged surface area as a result of droplet deformation. The key to this production route is to use an excess amount of Pickering stabilizers either dispersed in water or within the oil droplets and to push the solution through a capillary. To ensure an excess of particles a simple coverage calculation can be done in order to find the maximum number of particles that can fit on the desired interface. Knowing this number makes it possible to add an excess of particles. We can use a modified version of the equation used in the previous chapter.

$$Coverage = \frac{A_{part}^{Cov}}{A_{oil}} = \frac{1}{\pi} \cdot \left( \frac{w_{part}}{w_{oil}} \right) \cdot \left( \frac{\rho_{oil}}{\rho_{part}} \right) \cdot \left( \frac{R_{oil}}{R_{part}} \right) \qquad \textbf{Equation 1}$$

Where A is the area, $w$ is the weight, $\rho$ is the density and R is the radius of the particles and the oil droplets. In order to calculate the mass of

Pickering particles 100% coverage (1.0) is assumed as a jammed interface is desired. Under our experimental conditions, where typically 0.1 g of submicrometer-sized Pickering stabilizers (diameter approx. 200 nm) are used for 2.0 g of oil phase dispersed as millimeter-sized droplets in approximately 11 g of water, the radii ratio ($R_{oil}/R_{part}$) is in the order of $10^4$ thereby easily securing a large excess of Pickering stabilizing particles (of the order of $10^2$). If we assume the elongated droplet is a "plug" or cylinder we can calculate that in order to create enough surface area from a cylinder in order to increase the surface area of a sphere with the same volume the droplet can be extended laterally in the order of $10^4$. However this would also reduce the diameter of the tube to just a few microns, so this would never be realised in our apparatus.

When the droplets are forced through the capillary the flow field will cause the elongation of the droplets thereby increasing their surface area. Due to their excess concentration the expanded oil/water interface can be fully covered by the Pickering particles during its elongated state in the capillary. Upon exiting the capillary, the droplets can no longer relax back to their spherical geometry as the adhered particles jam on the densely packed surface, hence the non-spherical shape of the droplets is preserved. (Figure 3)

In our research we used different solid stabilizers ranging from poly(methyl methacrylate) microgels,[11] titanium dioxide nanoparticles,[12] and Laponite clay-armoured cross-linked polystyrene latex.[13,14] The clay-

armoured latex particles proved to be the most versatile solid stabilizers for a range of oils, including olive oil, *n*-hexadecane, styrene, and dicyclopentadiene and also gave Pickering emulsions with the longest stability as in the other cases some coalescence of droplets occurred, suggesting a larger coverage was achieved. More details on our Laponite-armoured latex particles can be found in the Chapter 4.

In order to create the non-spherical droplets, a stable Pickering emulsion must first be created by agitating a small oil phase with a large water phase in the presence of colloidally unstable particles. The particles will adhere to the created interface to produce very stable oil in water emulsions (stable for many weeks). This emulsion is then past through a thin capillary; typical lengths of 300 mm, with inlet and outlet diameters of 686.0 μm and a minimum diameter at half-length of 273.0 μm. This capillary is thinner than the created droplets, which forces them to elongate creating the needed extra interface. The particles were pushed through the capillary in a pulsating mode to maximize mixing and promote liquid-liquid interface assembly of the dispersed Pickering stabilizers. Average residence times of the droplets inside the capillaries were approximately 15 s.

Without putting any effort into optimization the aspect ratio of the larger droplets easily exceeded 10 and their cross-sectional diameter was in accordance with the capillary geometry. Obviously, droplets of smaller size than the diameter of the capillary retained their spherical shape

(Figure 3). It should be stressed that no coalescence of droplets occurred inside the capillary. This was easily visually observed as the capillary used was transparent. The non-spherical shape was solely obtained by creating a jammed state of the adhered Pickering stabilizers upon droplet elongation induced by the confined capillary geometry.

The additional beauty of this method is that post-modification of these droplets, whilst maintaining their shape, can be carried out in ordinary weakly stirred reaction vessels. This provides an alternative to the manufacturing of non-spherical particles via droplet solidification carried out inside micro-fluidic channels. [5,15-18]

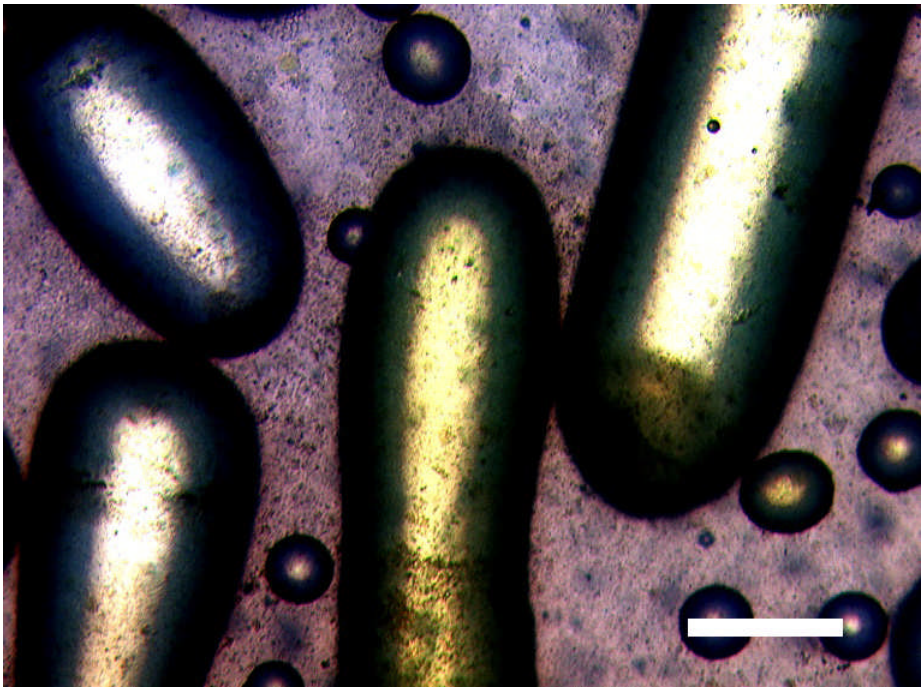

**Figure 3:** Light microscopic image of large non-spherical liquid droplets and small spherical droplets of styrene stabilized by Laponite clay armoured cross-linked polystyrene submicron spheres. Scale bar is 300.0 µm.

The second technique we shall show is that of interfacial buckling. The principle of buckling is to form a stable colloidosome with high surface coverage of particles and to remove part of the internal phase. Since the particles on the interface should be irreversibly adsorbed the size of the interface is locked. This means that as the total volume decreases, the colloidosome must change shape in order to accommodate this. We first observed this phenomena when we allowed a water droplet stabilised by polydisperse poly(divinylbenzene) evaporate in air:

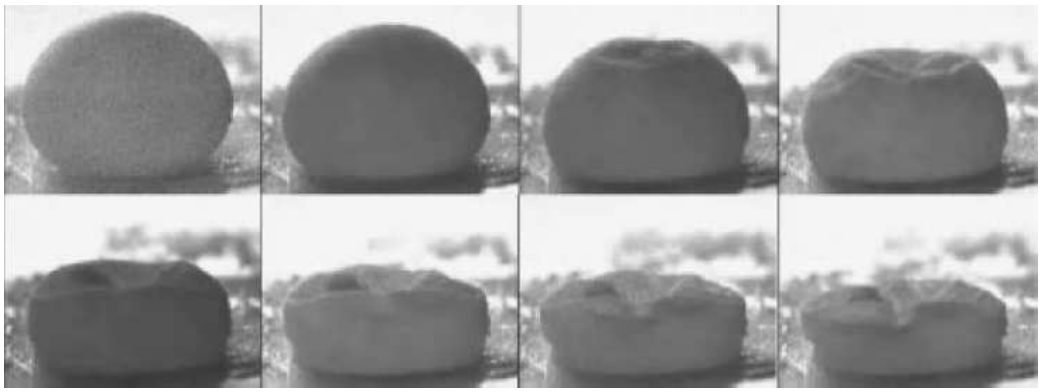

**Figure 4:** The non-spherical structure (approx. 5 mm diameter) generated by the evaporation of a water droplet stabilised by DVB particles

In order to get this approach to work for an emulsion, it was necessary to use an oil/water system. Initially, a few toluene droplets were formed in water and stabilised by poly(methyl methacrylate)/poly(divinylbenzene) latex particles using the same conditions used previously.[19] Slowly ethanol was added to the water in order to increase the solubility of toluene in the aqueous phase. The droplet was then observed under a microscope:

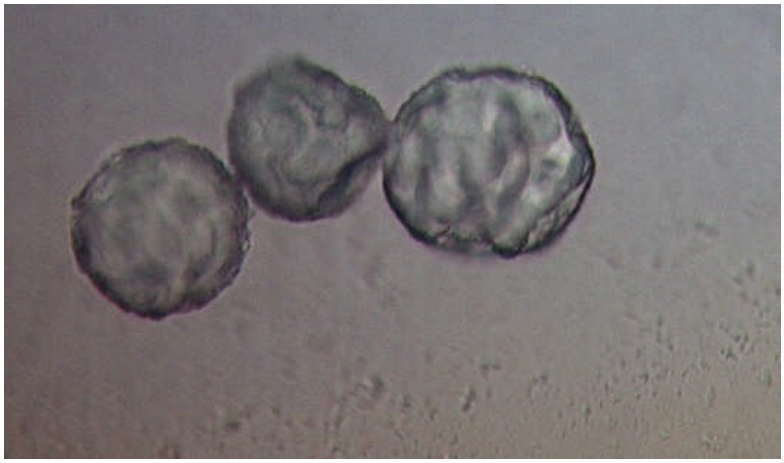

**Figure 5:** Optical microscope image of 3 buckled colloidosomes (*ca.* 50 μm dia.) consisting of an internal phase of toluene stabilised by crosslinked PMMA/DVB microgel particles

After these promising results it was decided to polymerise the droplets and attempt to vary the amounts of buckling observed. Toluene was replaced by styrene and AIBN as polymerisation initiator added. However FE-SEM analysis showed that no buckling occurred. It was postulated that perhaps there was not a high enough coverage of particles on the interface in the styrene water system to obtain a buckled system. It was decided to use Ludox TM-40 as a stabiliser using the same procedure as before, as it is known to give a high coverage in emulsion systems. Ludox TM-40 comes as a 40 wt% solution of *ca.* 25 nm silica spheres. Logically smaller droplets will be formed, since Ludox particles are an order of magnitude smaller than the microgel particles. 25 vol% of Ludox TM-40 was added to a 10 vol% mixture of styrene in water along with AIBN. The water was kept at pH 3.0 prior to ethanol addition.

Unfortunately FE-SEM images still showed limited buckling and large amounts of secondary nucleation. It is postulated that by adding ethanol to the water the wettability of the particles is affected, reducing the

energy holding them at the interface, hense they are easily removed by the buckling forces. Also due to Ludox's small size the forces holding them onto an interface are much smaller than the larger latex particles used before. Because of this another approach was needed. To overcome potential issues with radical polymerization of styrene, poly(diethoxysiloxane) (PDEOS) was employed as a scaffolding agent.[14] Hydrolysis and subsequent cross-linking of the reactive PDEOS provides mechanical reinforcement of the Pickering droplets. *n*-Pentane (60 vol% wrt. oil) was mixed with PDEOS (40 vol% wrt. oil) and droplets were generated using Laponite armoured latex particles (10 wt% wrt. oil) dispersed in a NaCl solution ( 0.1 M, 80 vol% wrt. total). To the stable emulsions nitrogen was bubbled through for different time scales to cause the *n*-pentane to evaporate. TEA was added as catalyst for the hydrolysis of the ethoxy groups after the desired evaporation time. This process yielded some, albeit limited, success:

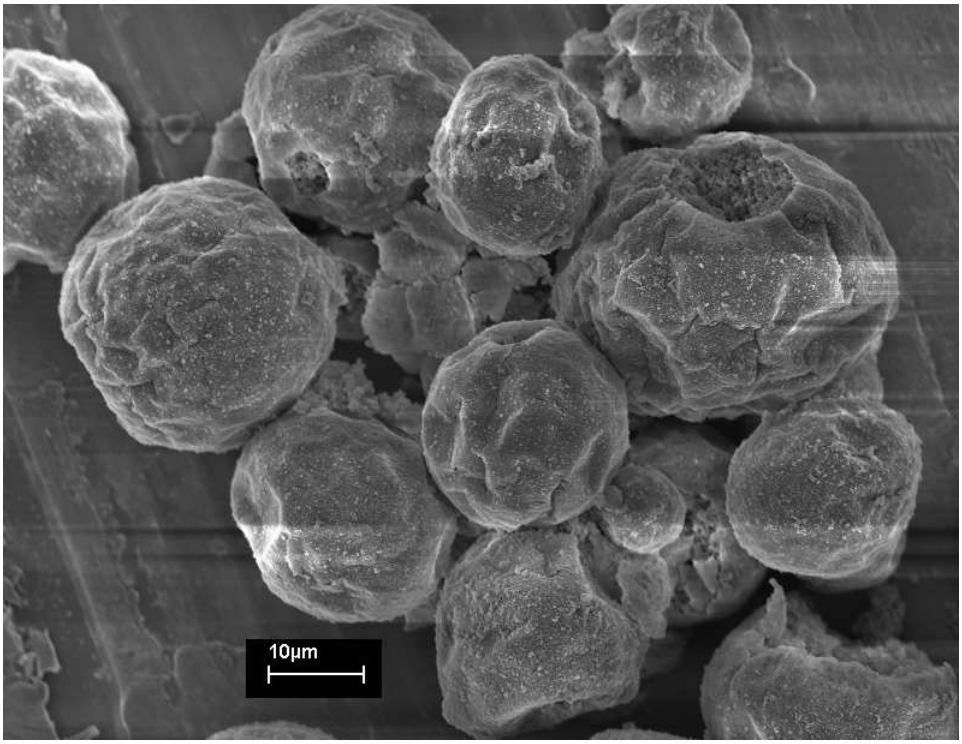


**Figure 6:** FE-SEM image of PDEOS buckled colloidosome with clay armoured polystyrene latex particles as stabiliser.

The results were not reproducible as sometimes samples bubbled through for longer would be buckled less than those obtained after shorter times and only small amounts of buckling were observed before the emulsion became destabilised.

The possible reason for this lack of reproducibility is that the droplets generated are very polydisperse, meaning each droplet behaves very differently from the others (smaller droplets will lose their internal phase much faster than larger ones). Because of this, a technique is needed to create large quantities of very monodisperse Pickering droplets. A excellent technique available to generate extremely monodisperse droplets is through a co-flow device in a microfluidic system (Figure 7).[20]

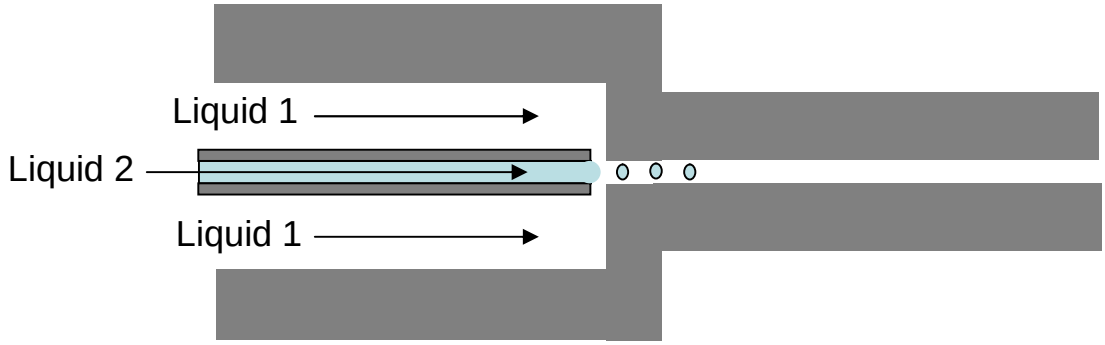


**Figure 7:** Figure depicting a microfluidic co-flow device generating monodisperse droplets.

Our group in collaboration with Kumacheva and co-workers recently showed an "inside-out" approach to monodisperse emulsion droplets stabilized by solid particles. Pickering droplets were post-polymerised via photo-initiation, and the preparation of non-spherical jammed structures was also demonstrated, in line with our previous results using glass capillaries.[21] A disadvantage is that the production of these microfludic devices is complex and requires specialist equipment and a devoted clean laboratory. McQuade showed the production of a much simpler apparatus to generate monodisperse droplets using the same principle.[22]

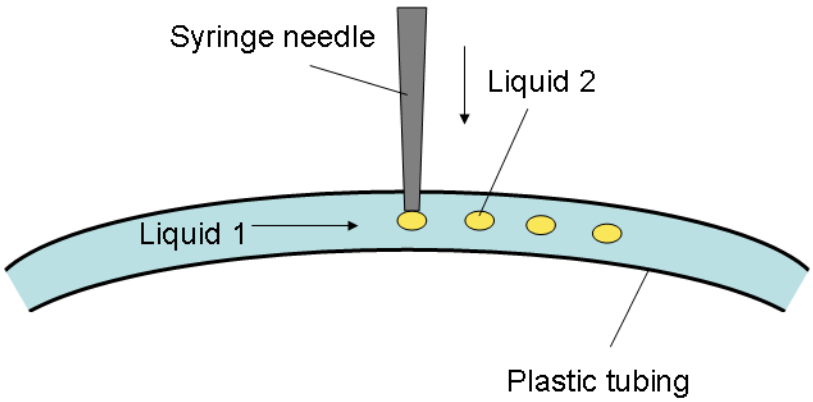


**Figure 8:** schematic representation of a simpler microfluidic device.[22]

For both systems the size of the droplets created are controlled by the size of the release aperture and by the apparent velocity of the droplet liquid. There is a limit to how small a droplet can be made with in a certain aperture. This is defined by the capillary number (Ca) which is calculated by multiplying the viscosity of liquid 1 by the apparent velocity of liquid 2 with respect to liquid 1 and dividing by the interfacial tension between the two liquids. This Ca number cannot be larger than 1 or a constant stream or jet will be produced instead of individual monodisperse droplets.

Kumacheva and Bon showed that for best results in microfluidic Pickering droplet formation the solid particles should be dispersed in the internal droplet phase, this allows rapid diffusion to the interface and means only a small excess of particles are required. This diffusion has been shown to be caused by hydrodynamic flow.[23] Moreover, it prevents fouling of the channels.

By repeating the experiments used by Kumacheva and Bon in the device created by McQuade, it should be simple to create monodisperse Pickering droplets with which to test buckling phenomena. Preliminary results look promising. *n*-Hexadecane was used as the continuous phase and methanol as the dispersed phase. The Pickering stabilisers used were poly(divinylbenzene) microspheres generated via dispersion polymerisation with small amounts of methacrylic acid (see methodology) to impart a small amount of anionic surface charge to the

particles. This small amount of charge was added to give the resulting colloidosomes some electrostatic stabilisation against coalescence. Any created droplets had to be collected in a plastic dish, as droplets would break when coming in contact with glass, possibly because the methanol wets the glass much more than the plastic. Figure 9 shows monodispersed buckled droplets created using the simplified microfluidic device with a flow rate of 40 ml/min of *n*-hexadecane (1/16" I.D. PTFE tube) and 2.5 ml/min (0.37 mm I.D. flat head syringe needle) of methanol containing 5 wt% of microspheres.

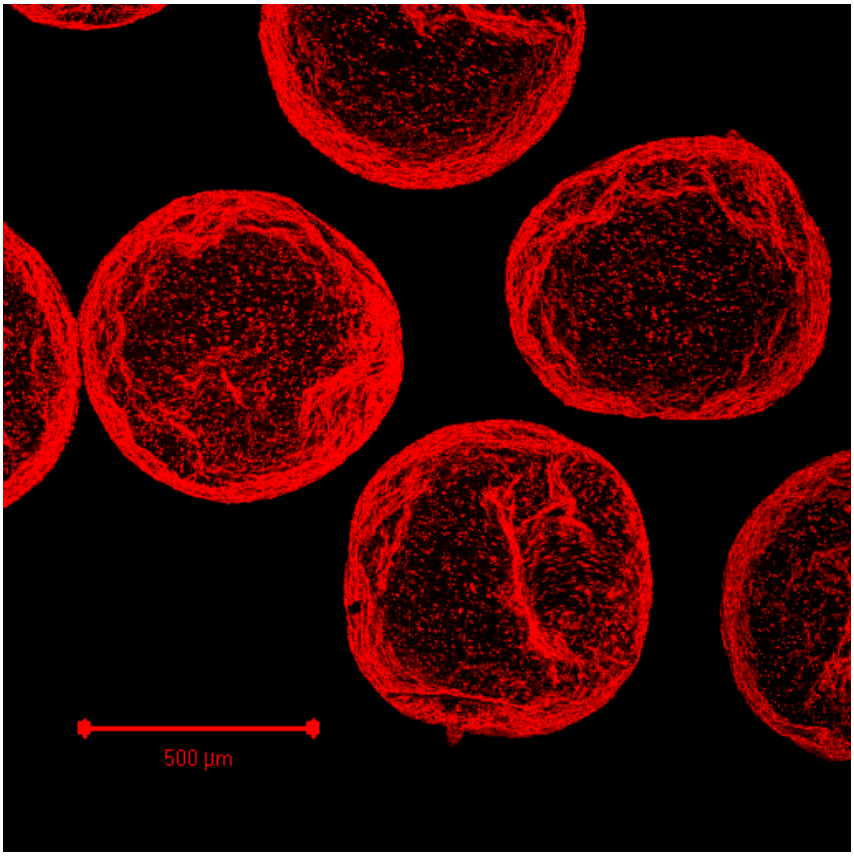


**Figure 9:** Confocal microscope image of *ca.* 550 µm methanol droplets in *n*-hexadecane. Stabilised by DVB-MAA particles labelled with hostasol methacrylate, allowed to buckle by evaporating the methanol using the heat of the laser.

## *Conclusion*

We have shown it is possible to change the shape of Pickering droplets via the post modification of a stable emulsion. They can either be elongated to give high aspect ratios or can be buckled to give a non-spherical structure with a higher surface area. This has only been done before on a drop-by-drop basis or via in-situ modification and scaffolding. Further work should be done in order to find how much force due to the buckling interface the particle can experience before the structure degrades. Also the maximum amount of buckling should be investigated when different wettabilities of particles are used.

## *Methodology*

### Apparatus

pH measurements were performed using a Knick pH meter 765 Calimetic. Micro*n*-sized colloidosomes were generated via handshaking in the case of the first example or using an IKA WERKA, Ultra Turrax, T25 basic in all others. FE-SEM images were taken on a ZEISS supra 55VP FEGSEM. Confocal imaging was performed on a ZEISS LSM 510 confocal microscope with 458 nm, 477 nm and 488 nm wavelength lasers and a LP 505 filter. The objective used was a Plan-Apochromat 5x/0.16. To make the capillaries, the tip from a standard glass pipette was broken off, then the middle was heated using an *n*-butane blow torch until glowing red,

and the hot glass was then drawn into a thin tube. The syringe pumps used to create the flow for the microfludic device were Harvard Apparatus PH 2000 infusions. The PTFE tubing was L × O.D. × I.D. 25 ft × 0.085 in. (2.1 mm) × 0.062 in. (1.58 mm) from Supelco and the syringe needle was P/N 039895 purchased from SGE analytical science.

## Dispersion polymerisation

DVB (1.9841 g), MAA (0.0312 g, 1.55 wt%), hostasol methacrylate (0.0023 g) and AIBN (0.0541 g) were dissolved in acetonitrile (100 mL) and poured into a 250 mL round bottom flask. The solution was bubbled through with nitrogen gas for 20 minutes to remove oxygen from the system. The round bottom flask was then attached to a rotary evaporator with a positive pressure of nitrogen flooding the apparatus. The flask was then rotated at 15 rpm and heated to 50 °C. After 1 hour the temperature was ramped to 70 °C over 1 hour and the reaction solution was polymerised for 24 h. The resulting polymer particles were then allowed to settle and the supernatant was removed and replaced with acetone. The particles were then allowed to settle once more and the supernatant was removed again and replaced with methanol. This procedure was repeated twice to remove any remaining monomer and initiator.

**Caution:** make sure there is an outlet for the nitrogen overpressure, otherwise pressure build up could cause the rotary evaporator to explode.

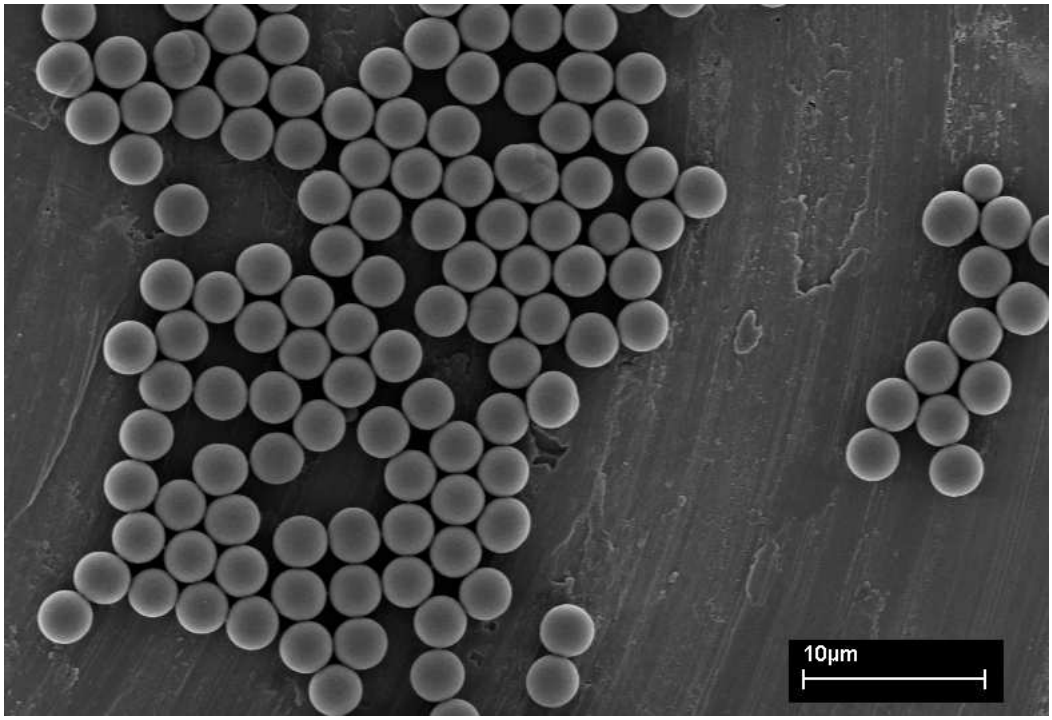


**Figure 10:** FE-SEM image of MAA-DVB (0.5:99.5 wt%) particles with average diameter of 1.8 µm, determined via average pixel measurements of *ca.* 50 particles.

(1) White, S. R.; Sottos, N. R.; Geubelle, P. H.; Moore, J. S.; Kessler, M. R.; Sriram, S. R.; Brown, E. N.; Viswanathan, S. *Nature* **2001**, *409*, 794-797.

(2) Massimo Pica, C.; Maria Domenica De, V.; Annalisa, F.; Marco, T.; Antonio, C.; Mario, N. *Phys. Rev. Lett.* **2006**, *96*, 058001.

(3) Plantard, G.; Saadaoui, H.; Snabre, P.; Pouligny, B. *Europhys. Lett.* **2006**, *75*, 335-341.

(4) Okubo, M.; Ichikawa, K.; Tsujihiro, M.; He, J. *Colloid Polym. Sci.* **1990**, *268*, 791-796.

(5) Xu, S.; Nie, Z.; Seo, M.; Lewis, P.; Kumacheva, E.; Stone, H. A.; Garstecki, P.; Weibel, D. B.; Gitlin, I.; Whitesides, G. M. *Angew. Chem. Int. Ed.* **2005**, *44*, 724-728.

(6) Hwang, D. K.; Dendukuri, D.; Doyle, P. S. *Lab Chip* **2008**, *8*, 1640-1647.

(7) Wang, S.; Mark, J. E. *Macromolecules* **1990**, *23*, 4288-91.

(8) Tamaki, K.; Matsushita, S.; Shimomura, M. *Colloids Surf. Physicochem. Eng. Aspects* **2008**, *313-314*, 630-635.

(9) Subramaniam, A. B.; Abkarian, M.; Mahadevan, L.; Stone, H. A. *Nature* **2005**, *438*, 930.

(10) Stratford, K.; Adhikari, R.; Pagonabarraga, I.; Desplat, J. C.; Cates, M. E. *Science* **2005**, *309*, 2198-201.

(11) Bon, S. A. F.; Cauvin, S.; Colver, P. J. *Soft Matter* **2007**, *3*, 194-199.

(12) T. Chen, P. J. C. S. A. F. B. *Adv. Mater.* **2007**, *19*, 2286-2289.

(13) Cauvin, S.; Colver, P. J.; Bon, S. A. F. *Macromolecules* **2005**, *38*, 7887-7889.

(14) Bon, S. A. F.; Chen, T. *Langmuir* **2007**, *23*, 9527-9530.

(15) Nisisako, T.; Torii, T. *Adv. Mater.* **2007**, *19*, 1489-1493.

(16) Dendukuri, D.; Hatton, T. A.; Doyle, P. S. *Langmuir* **2007**, *23*, 4669-4674.

(17) Shepherd, R. F.; Conrad, J. C.; Rhodes, S. K.; Link, D. R.; Marquez, M.; Weitz, D. A.; Lewis, J. A. *Langmuir* **2006**, *22*, 8618-8622.

(18) Liu, K.; Ding, H.-J.; Liu, J.; Chen, Y.; Zhao, X.-Z. *Langmuir* **2006**, *22*, 9453-9457.

(19) Bon, S. A. F.; Cauvin, S.; Colver, P. J. *Soft Matter* **2007**, *3*, 194-199.

(20) Shelley, L. A.; Nathalie, B.; Howard, A. S. *Appl. Phys. Lett.* **2003**, *82*, 364-366.

(21) Nie, Z.; Park, J. I.; Li, W.; Bon, S. A. F.; Kumacheva, E. *J. Am. Chem. Soc.* **2008**, *130*, 16508-16509

(22) Quevedo, E.; Steinbacher, J.; McQuade, D. T. *J. Am. Chem. Soc.* **2005**, *127*, 10498-10499.

(23) Subramaniam, A. B.; Abkarian, M.; Stone, H. A. *Nat. Mater.* **2005**, *4*, 553-556.

## *Chapter 4: Laponite Armoured Latex Particles Created Via Pickering Miniemulsion*[‡]

It has been shown that many materials can be used to make Pickering emulsions. We have shown in the previous chapters that these emulsions can have very different properties (chemical composition, reversibility, shape) and have many uses (filtration devices, self-healing composites). However one aspect all these examples have in common is the size of the stabilisers. The colloidal particles used are all over 100 nm in size meaning that the droplets that can be formed must all be much larger than this. Some examples do exist where nanoparticles are used. Russell *et al.* used particles such as CdSe nanoparticles as a stabiliser.[1-4] A similar approach was also more recently by Harrison *et al.*[5] Another example being our buckling work with Ludox. However the force used to create the emulsion was small, meaning large droplets were still formed. We decided to create the first Pickering miniemulsion by using small particles and a high shear force.

Commonly a miniemulsion starts with the dispersion of an oil phase in a continuous aqueous phase. The dispersion is created by applying a shear force (in this case the use of sonication), to a system consisting of water, oil, surfactant and co-surfactant and/or hydrophobe.[6-9] The surfactant stabilises the droplets, keeping them small and preventing coalescence. While the co-surfactant (typically these co-surfactants have been long-

[‡] Part of this chapter has been published: Stefan A. F. Bon and Patrick J. Colver, *Langmuir,* **2007,** *23*(16) pp 8316 - 8322

chain alkanes and alcohols but recently the use of polymeric hydrophobes has been reported) [10] can effectively retard the migration of monomer between droplets of different size, also known as Ostwald ripening.[11] It does this because the co-surfactant cannot easily diffuse into the aqueous phase, so if the monomer leaves, the concentration of the co-surfactant increases. This raises the free energy, which will therefore retard the monomer diffusion. A hydrophobe is needed to stabilize the miniemulsion because monomer dispersed in small droplets will dissolve into solution and move to larger droplets, which reduces the overall surface area of the system.[12] This effect can be described using Henry's law:

$$C_r = C_\infty e^{(2\lambda V_M / rRT)} \qquad \textbf{Equation 1}$$

Where $C_r$ (mol $L^{-1}$) is the solubility in water of the oil droplets of radius r (m), $C_\infty$ (mol $L^{-1}$) is the solubility from an infinitely large droplet, $\lambda$ (N·m) is the interfacial tension and $V_M$ ($m^3$ $mol^{-1}$) is the molar volume of the oil. The increase of the oil's solubility with decreasing r makes the small droplets thermodynamically unstable with respect to the larger ones. This makes the larger droplets grow at the expense of the smaller. Higuchi and Misra have also shown that the rate of degradation is also dependent on the radius. In fact a tenfold decrease in r gives a thousand times increase in the rate of degradation.[13]

In order to stabilise this so-called Ostwald ripening or degradation, a force acting in the opposite direction should be added. This is well

described by a review by Ugelstad and Mork[14] which discusses the following logical steps: To get a force acting in the opposite direction, a compound that can absorb the monomer and not diffuse itself is used. The swelling capacity of a compound (2) can be work out by looking at molar free energy of the monomer (1) and applying the equilibrium condition $\Delta\overline{G_1} = 0$. This expression is known as the Morton equation. [15]

$$\Delta\overline{G_1} = RT(\ln\phi_1 + (1-\frac{1}{J_2})\phi_2 + \phi_2{}^2 x + 2V_{1M}\gamma / rRT) \qquad \textbf{Equation 2}$$

$\phi$ is the volume fraction of the compound, $j_2$ is the ratio of the molar volume of compound 1 and 2. the Flory interaction parameter $x$ is an empirical free energy term which determines the deviation in free energy of mixing from what it would be when only combinatorial entropy was involved:

$$x = x_H + x_s \qquad \textbf{Equation 3}$$

$$x_H = \Delta\overline{H_1} / RT\phi_2^2 \qquad \textbf{Equation 4}$$

$$x_S = -\Delta\overline{S_1^R} / R\phi_2^2 \qquad \textbf{Equation 5}$$

Where $\Delta\overline{S_1^R}$ is denoted the residual partial entropy of mixing. In the case that $\Delta\overline{S_1^R}$ and $\Delta\overline{H_1}$ are independent of temperature, the expression for $x$ takes the form:

$$x = \alpha + \beta / T \qquad \textbf{Equation 6}$$

Equation 2 has been used for describing the swelling of polymer particles,[15] and was discussed in its use with alkanes[16]. From equation 2, follows that the best compounds for the maximum swelling are

compounds with low molecular weight that are very water insoluble.[14] This is why *n*-hexadecane is widely used and why it is used in our experiments. It is also possible that Pickering stabilisers might inhibit Ostwald ripening due to the interfacial jamming that can occur if too much of the internal phase is lost.

We wanted to develop a Pickering miniemulsion system since this would negate the need to use small-molecule surfactants which are bad for environmental reasons. Surfactants lead to surface migration in films and can also reduce barrier properties. The nanostabiliser which we decided to use was Laponite RD clay as it has previously been investigated as a Pickering stabiliser.[17] Clay has been used in polymer formulations for many years to create advantaged composites. Small quantities of added clay are known to improve the mechanical properties of polymer films[18] as well as enhancing flame retardancy[19,20]. These properties add some very interesting potential applications for clay-armoured latexes. Preparation of such composites via emulsion/suspension polymerisation include heterocoagulation of the clay minerals onto the polymer particles,[21] complexation of cationic monomers/surfactants[22] or covalent modification of the Laponite to facilitate dispersion into the polymer matrix,[23] and use as a Pickering stabiliser in conjunction with ordinary surfactant stabilisation.[24]

The clay we shall use in our miniemulsion polymerisations is Laponite RD, a synthetic trioctahedric hectorite clay composed of two tetrahedral

silica sheets and a central octahedral magnesia sheet. Its chemical formula can be expressed as $[Si_8(Mg_{5.45}Li_{0.4})O_{20}(OH)_4]Na_{0.7}$, and it has a density of 2570 kg m-$^3$. The disks have an overall negative charge caused by some of the magnesium in the crystal structure being replaced by lithium. This negative charge is neutralised by sodium ions on the surface. The edge of the Laponite disc is positively charged from broken primary bonds within the crystal structure. These are negated by hydroxyl groups. In water Laponite RD can be dispersed as individual disk-shaped colloids with a lateral diameter of ca. 25 nm and *ca.* 1 nm in thickness.[25] Laponite however will not stabilise oil-in-water emulsions on its own, as its charge is too high for flocculation onto an interface, *i.e.* the minimum of the potential energy curve, shown in the introduction to Pickering, lies in the water phase. So in order for clay to be a viable stabiliser the charges must be screened. Binks showed this by preparing many Pickering emulsions with various quantities of salt. [17]

We performed four series of Pickering miniemulsion polymerisation experiments in which we varied the amount of Laponite clay disks (series I and II; see Table 1), the amount and type of monomer (series III and IV, respectively; see Tables 2 and 3). The sodium chloride concentration was kept constant at *ca*. 0.1 moles $L^{-1}$ in all experiments. The initiator used was 2,2'-azobis(2,4-dimethyl valeronitrile) (V-65), which was premixed with the monomer. A charged water phase initiator was also used, however all attempts to polymerise in a controlled fashion failed due to excessive

coagulation. The miniemulsions were prepared via sonication (See Experimental section). This high-powered homogenization step ensures that the clay platelets can redistribute and thus are not permanently trapped at the monomer-water interface, so that it is possible to create Pickering-stabilised monomer droplets of submicron size. One interesting point is related to the fact that at salt concentrations of 0.1 M Laponite clay discs will flocculate. [26-28] Therefore it is important to first disperse the discotic platelets in water prior to the addition of the sodium chloride. A theoretical paper has been published showing the minimum energy of flocculated Laponite is a slightly overlapping structure.[29] This flocculation of the clay nanoparticles leads to an increase in overall viscosity due to this weak network created between the clay platelets. Upon addition of monomer and subsequent shear through sonication, some proportion of the clay platelets will be confined to the monomer-water interface. This leads to a lower overall viscosity of the miniemulsion in comparison to the aqueous clay dispersion in the NaCl solution. The prepared miniemulsions were degassed and polymerised overnight at 51$^{o}$C. The latexes appeared stable initially but upon storage they tended to flocculate and phase-separate into a clear upper aqueous layer and a lower turbid layer containing the polymer latex. Upon dialysis, carried out to remove the NaCl, the latexes were easily redispersed into indefinitely stable colloidal dispersions. This is because the charge screening is removed so there is now a large electrostatic

repulsion between clay particles and therefore also the clay-armoured latex particles.

## *Morphology of latexes made via Pickering miniemulsion polymerisation*

Pickering stabilisers adhere to the surface of the emulsion droplets. This ensures stability of the emulsion. The morphologies of the latexes obtained after polymerisation therefore are anticipated to be armoured polymer colloids whose surfaces are covered with Laponite clay discs. Figure 1a shows the FE-SEM image of a group of Laponite armoured polystyrene spheres made via Pickering miniemulsion polymerisation. Note that the fine-structure (sub 10 nm) is the result of the sputtered gold layer. Excess amounts of Laponite clay was observed in all samples. Figure 1b is the FE-SEM image of a film formed from these Pickering polystyrene latexes at 230 °C. This now more clearly shows the armoured structure of the individual latex particles which film-formed after limited polymer-polymer interdiffusion. Tapping mode AFM (see Figure 2) carried out on a single large Laponite clay armoured polystyrene particle clearly reveals that the Laponite discs lie flat on the surface of the particle. This behaviour is expected based on theoretical studies on acicular and discotic Pickering stabilisers. [30] [31]

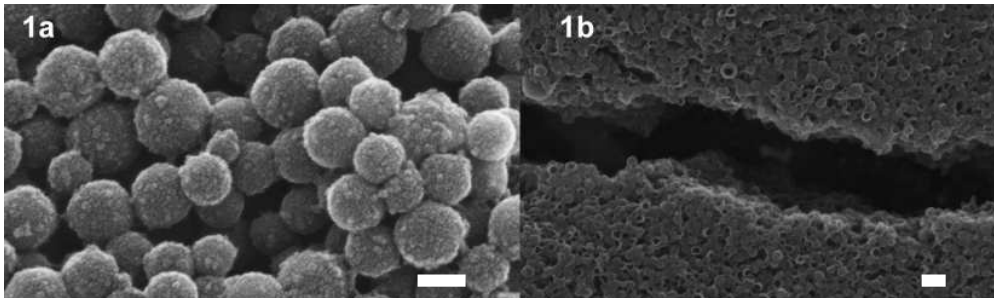


**Figure 1:** FE-SEM images of (a) Laponite armoured polystyrene latex made via Pickering miniemulsion polymerisation (scale bar = 100 nm) (b) Film formed from Laponite armoured polystyrene latex at 230°C (scale bar = 400 nm)

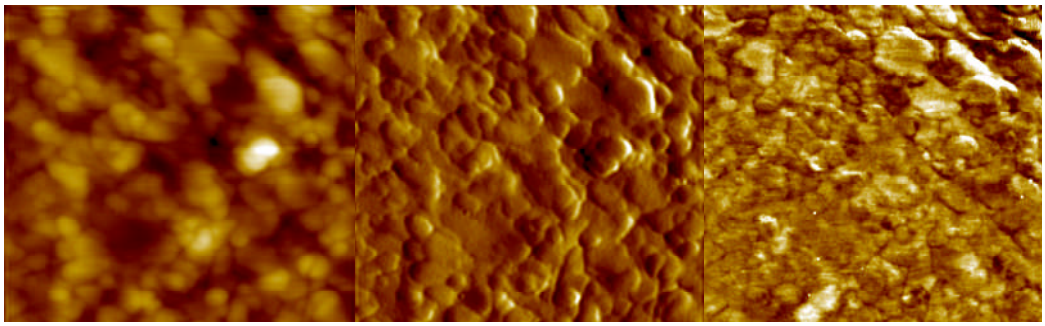

**Figure 2:** Tapping mode AFM images (250 nm × 250 nm) obtained from the surface mapping of a single large Laponite armoured polystyrene latex sphere. Left image is height (10 nm full scale), centre image is amplitude, and right image is phase.

## *Control of Particle Size in Pickering Miniemulsion Polymerisation*

We performed two series of Pickering miniemulsion polymerisations of styrene varying the amount of Laponite nanoparticles from 0.25 to 1.5 wt% with respect to water, at constant sodium chloride concentrations of 0.1 M and a constant monomer to water weight ratio of approximately 0.1 (See Table 1 for details). In these sets of experiments both 4 wt% and 8 wt% (with respect to styrene) of *n*-hexadecane as hydrophobe were employed. The reason for varying the amount of clay was to investigate its influence on the particle size distributions of the resulting latexes. In

conventional emulsion polymerisations which use low molecular weight surfactants, such as sodium dodecyl sulfate, in concentrations above the critical micelle concentration (CMC), the number of particles generated ($N_{part}$) and therefore the size of the individual particles show a strong dependence on the surfactant used concentration [S]. The straightforward Smith-Ewart model predicts a dependence of $N_{part} \propto [S]^{0.6}$, which means that the particle radius should have an exponent of -0.2.[32] More elaborate models allowing for aqueous-phase kinetics and compartmentalization predict different exponents. Antonietti *et al.* [33] and Wu[34,35] discuss simple models to predict the size of spherical microemulsions whereby monomer cores were surrounded by surfactant molecules. Analogous to these approached, we have developed a basic model to predict the average particle size of our Pickering-stabilised latexes.

There are two factors we have to take into account. Firstly, we have to realise that potentially not all solid particles, *i.e.* Laponite RD clay discs, are adhered to the interface of the miniemulsion droplets or latex particles. The overall mass balance for the solid particles therefore is:

$$C_0 = C_{surf} + C_{excess} \qquad \textbf{Equation 7}$$

In which $C_0$ is the overall concentration of solid particles in water in g/g and is given by $m_0/m_{water}$, $C_{surf}$ is the concentration of solid particles adhered to the oil-water interface *i.e.* to the monomer droplets or polymer particles, with respect to the amount of water-phase, being $m_{surf}/m_{water}$,

and $C_{excess}$ is the excess concentration of solid particles which remain in the continuous phase, in the present case water, being $m_{excess}/m_{water}$. Note that we assume that the solid particles are added to the continuous phase and not to the to-be-dispersed phase prior to preparation of the (mini)emulsions. We also assume that the energy barrier to enter the dispersed phase is too high for the solid particles to overcome and thus that there are no particles present in this phase. This is reasonable since it is impossible to disperse the clay in the organic phase without first modifying the particles.

Secondly, we have to come up with an expression that describes the surface coverage of the droplets. We assume hereby (i) that the liquid-liquid interface is "fully" covered, (ii) that the monomer droplets/polymer particles and the solid Laponite discs are uniform in size, and (iii) that the dimensions of the Laponite clay discs are negligible with respect to the size of the monomer droplets/polymer particles. The latter assumption ignores curvature and thus geometrical constraints. For simplicity we will assume here a 2-D square lateral packing of the Laponite discs. This means that the discs lie flat on the surface. The latter is plausible from theoretical studies on acicular[30] and discotic particles, [31] and in our case is confirmed experimentally (see Figure 2). The packing can easily be changed into different arrangements, such as hexagonal or random.

The interfacial area of one monomer droplet/polymer latex equals:

$$a_{oil} = \pi d_{oil}^2 \qquad \textbf{Equation 8}$$

with $d_{oil}$ being the diameter of the droplets/polymer latex.

The effective area covered by one Laponite clay disk (due to the square packing assumption) equals:

$$a_{part} = d_{part}^2 \quad \textbf{Equation 9}$$

In which $d_{part}$ being the diameter of a Laponite clay disc.

The total number of monomer droplets/polymer particles can be expressed as:

$$N_{oil} = \left(\frac{m_{oil}}{\rho_{oil}}\right) \Big/ \frac{\pi}{6} d_{oil}^3 \quad \textbf{Equation 10}$$

In which $m_{oil}$ is the combined amount of monomer/polymer and *n*-hexadecane, and in which $\rho_{oil}$ is the combined density of monomer/polymer and *n*-hexadecane.

The total number of Laponite clay discs adhered to the liquid-liquid interface can be calculated from:

$$N_{part} = 4 \left(\frac{m_{surf}}{\rho_{part}}\right) \Big/ \left(\pi\, d_{part}^2\, h\right) \quad \textbf{Equation 11}$$

With $\rho_{part}$ is the density of Laponite RD and $h$ is the height (thickness) of the discs.

When we assume full coverage the following relationship holds:

$$N_{oil}\, a_{oil} = N_{part}\, a_{part} \quad \textbf{Equation 12}$$

Substitution of equations 8-11 into equation 12 and isolation of the only unknown parameter, which is the actual amount of Laponite clay discs adhered to the interface, yields:

$$m_{surf} = \frac{3\pi}{2}\left(\frac{\rho_{part}}{\rho_{oil}}\right)\left(\frac{h}{d_{oil}}\right)m_{oil} \qquad \textbf{Equation 13}$$

The factor (3π/2) changes if one assumes a different surface packing. For example, it becomes $\sqrt{3}\pi$ when we assume hexagonal packing. Combination with the mass balance from equation 7 yields our final expression:

$$C_{excess} = C_0 - \frac{3\pi}{2}\left(\frac{\rho_{part}}{\rho_{oil}}\right)\left(\frac{h}{d_{oil}}\right)C_{oil} \qquad \textbf{Equation 14}$$

The question now is; how does this expression behave under experimental conditions? In other words, how does the diameter of the Pickering monomer droplets or polymer latex correlate with the added overall concentration of Laponite clay? Can we express $C_{surf}$ as a function of $C_0$? In generic form:

$$C_{excess} = C_0 - f\left(C_0\right) \qquad \textbf{Equation 15}$$

To answer this, we need to know the diameter of the monomer droplets and/or polymer latex particles stabilised with Laponite clay disks. We measured the particle size of dialysed Laponite armoured latexes by dynamic light scattering. The results are given in Table 1. When we insert

the experimental data from Table 1 into Equation 16 with $h$ = 1.0 nm, $\rho_{part}$ = 2570 kg m$^{-3}$, $\rho_{oil}$ as a combined value of the densities of polystyrene ($\rho_{psty}$ = 1090 kg m$^{-3}$) and *n*-hexadecane ($\rho_{hd}$ = 770 kg m$^{-3}$) their fractional contributions corrected for overall monomer conversion, $x_M$, calculated via:

$$\rho_{oil} = \frac{m_{hd}}{m_{hd} + m_{psty}} \rho_{hd} + \frac{m_{psty}}{m_{hd} + m_{psty}} \rho_{psty} \qquad \textbf{Equation 16}$$

and values for $m_{oil}$ being the sum of $m_{hd}$ and $m_{psty}$, with $m_{psty}$ being $m_{sty} \times x_M$, we can construct a plot of $C_0$ *vs.* $C_{excess}$ (See Figure 3).

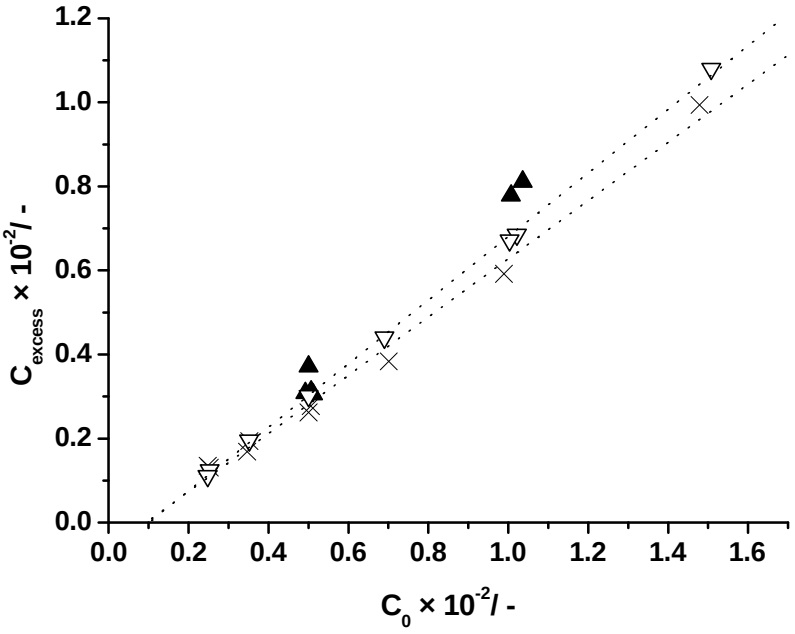


**Figure 3:** The calculated excess concentration of solid particles which remain in the continuous phase ($C_{excess}$) versus the overall concentration of solid particles in water ($C_0$) in g g$^{-1}$ (series I ∇; series II ×; series III ▲). The dotted lines are Eqs. 17 and 18.

From this Figure it is clear that there is an apparent linear behaviour for the two series of experiments carried out using two different levels of *n*-hexadecane, *i.e.* 4 wt% and 8 wt% and thus that $f(C_0)$ can be expressed as first order polynomial functions in $C_0$:

Series I with 4 wt% *n*-hexadecane (fit: $r^2 = 0.999$):

$$C_{excess} = (1 - 0.2438)\, C_0 - 7.543 \times 10^{-4} \qquad \textbf{Equation 17}$$

Series II with 8 wt% *n*-hexadecane (fit: $r^2 = 0.992$):

$$C_{excess} = (1 - 0.3076)\, C_0 - 6.468 \times 10^{-4} \qquad \textbf{Equation 18}$$

The reason why these two sets show a slightly dissimilar linear behaviour may originate in differences between the interfacial tensions. The evident linear correlation implies that, for the current range of experimental conditions, the partitioning of the Laponite clay platelets between the continuous water phase and the oil-water interface is a constant. In other words the amount of Laponite clay nanoparticles used dictates how much interface is created. This means that, for a specified amount of monomer ($m_{oil}$), the average particle size of the Pickering-stabilised emulsion droplets obtained after emulsification via in the present case sonication will have a fixed dependent value. It is important to realize that, during the emulsification process, adhesion of the particles to the oil-water interface is reversible, as a direct result of the high energy input via sonication. This reversibility of adhesion allows for the partitioning of

the Laponite clay platelets to reach equilibrium. This is directly reflected in the linear behaviour of the plots of $C_0$ *vs.* $C_{excess}$.

The average diameter of the Pickering emulsion droplets, and thus of the resulting latexes, can be predicted and calculated by first obtaining values for $C_{excess}$ using equation 18 or 19, and then calculating $d_{oil}$ from expression 15. The calculated results are given in Table 1 and show good correlation with the measured values obtained from DLS. It is noteworthy that for entry 2 and 9 in Series II, *i.e.* large particle sizes, a deviation is observed that can be ascribed to a more polydisperse particle size distribution, thereby overestimating the DLS data and possible influences of gravity on the timescale of the DLS measurements.

In order to check the robustness of our findings, we varied the amount of styrene used keeping the amount of Laponite clay constant in a third series of experiments (See Table 2). To our initial surprise entries III-1, III-4 and III-5 deviated from the expected linear relationship (Eq. 17). However, a closer look at the input values reveals that for these three experiments the ratio of Laponite clay discs to monomer and *n*-hexadecane is large. The calculated values for the diameters of the latexes for these experiments are 155, 120 and 160 nm for entries III-1, III-4 and III-5 respectively (using Eqs. 17 and 14). However, experimental values of 227, 182, and 225 nm were obtained. The predicted particle sizes are so small that one of our assumptions made in our model, *i.e.* (iii) that the dimensions of the Laponite clay discs are negligible with respect to the

size of the monomer droplets/polymer particles, does not hold. The curvature of the droplets now becomes an important factor, which can no longer be neglected. This means the clay platelet no longer sees a flat interface which is required for good adhesion since it is attached to the interface via a flat plane. We believe that this effect results in an underestimation of the true experimental values for the particle diameters.

**Table 1:** Summary of the various formulations used for the Pickering miniemulsion polymerisations of styrene stabilised by Laponite clay

| | $m_{water}$/ g | Experiment | $m_0$/ g | $m_M$/ g | $m_{Hex}$/ g | $m_I$/ g | $m_{PS}$/ g | $d_{oil}$/ nm | $C_0$/ mg $g^{-1}$ | $C_{excess}$/ mg $g^{-1}$ | Calc $C_{excess}$/ mg $g^{-1}$ | Calc $d_{oil}$/ nm |
|---|---|---|---|---|---|---|---|---|---|---|---|---|
| **Series I** | 100.2 | PJC-1-037 | 0.502 | 10.003 | 0.404 | 0.049 | 8.40 | 495.7 | 5.01 | 3.02 | 3.03 | 499.3 |
| | 100.8 | PJC-1-042 | 0.255 | 10.186 | 0.423 | 0.066 | 7.13 | 658.3 | 2.53 | 1.25 | 1.16 | 615.4 |
| | 100.5 | PJC-1-046 | 0.249 | 10.009 | 0.402 | 0.046 | 7.46 | 643.2 | 2.48 | 1.11 | 1.12 | 647.1 |
| | 101.0 | PJC-1-047 | 0.355 | 10.031 | 0.404 | 0.053 | 8.13 | 607.9 | 3.52 | 1.96 | 1.91 | 587.9 |
| | 100.4 | PJC-1-048 | 0.693 | 9.928 | 0.405 | 0.045 | 8.34 | 391.5 | 6.90 | 4.41 | 4.47 | 400.9 |
| | 99.5 | PJC-1-049 | 1.501 | 10.027 | 0.401 | 0.074 | 8.52 | 234.8 | 15.08 | 10.80 | 10.65 | 227.0 |
| | 100.0 | PJC-1-052 | 1.004 | 10.014 | 0.401 | 0.051 | 8.11 | 287.7 | 10.04 | 6.72 | 6.84 | 298.6 |
| **Series II** | 102.0 | PJC-1-021 | 1.508 | 9.966 | 0.809 | 0.050 | 9.86 | 244.3 | 14.78 | 9.94 | 9.59 | 227.9 |
| | 100.0 | PJC-1-024 | 0.253 | 10.025 | 0.810 | 0.052 | 8.26 | 846.5 | 2.53 | 1.31 | 1.10 | 724.0 |
| | 101.2 | PJC-1-025 | 0.507 | 10.021 | 0.842 | 0.047 | 8.70 | 449.3 | 5.01 | 2.62 | 2.82 | 489.9 |
| | 100.4 | PJC-1-027 | 0.354 | 10.016 | 0.808 | 0.052 | 7.39 | 589.5 | 3.52 | 1.94 | 1.79 | 538.1 |
| | 100.0 | PJC-1-028 | 0.701 | 10.030 | 0.820 | 0.052 | 8.02 | 317.1 | 7.01 | 3.84 | 4.21 | 359.0 |
| | 100.6 | PJC-1-040 | 0.995 | 10.077 | 0.803 | 0.050 | 9.57 | 294.0 | 9.89 | 5.92 | 6.20 | 316.5 |
| | 100.3 | PJC-1-043 | 0.348 | 10.014 | 0.833 | 0.048 | 8.46 | 594.2 | 3.47 | 1.69 | 1.75 | 615.0 |
| | 99.9 | PJC-1-045 | 0.505 | 10.047 | 0.817 | 0.047 | 8.44 | 461.0 | 5.06 | 2.78 | 2.86 | 477.9 |
| | 99.9 | PJC-1-050 | 0.248 | 10.009 | 0.800 | 0.045 | 7.41 | 830.3 | 2.48 | 1.35 | 1.07 | 663.9 |

**Table 2:** Summary of the various formulations used for the **a**dditional Pickering miniemulsion polymerisations of styrene stabilised by Laponite clay

| | $m_{water}$/ g | Experiment | $m_0$/ g | $m_M$/ g | $m_{Hex}$/ g | $m_I$/ g | $m_{PS}$/ g | $d_{oil}$/ nm | $C_0$/ mg $g^{-1}$ | $C_{excess}$/ mg $g^{-1}$ | Calc $C_{excess}$/ mg $g^{-1}$ | Calc $d_{oil}$/ nm |
|---|---|---|---|---|---|---|---|---|---|---|---|---|
| **Series III** | 99.6 | PJC-1-058 | 1.032 | 5.009 | 0.206 | 0.044 | 4.32 | 226.9 | 10.36 | 8.12 | 7.08 | 155.4 |
| | 101.2 | PJC-1-059 | 0.498 | 5.001 | 0.200 | 0.046 | 3.87 | 245.1 | 4.93 | 3.08 | 2.97 | 231.0 |
| | 100.1 | PJC-1-060 | 0.512 | 7.515 | 0.320 | 0.042 | 6.01 | 344.4 | 5.12 | 3.05 | 3.11 | 355.0 |
| | 100.6 | PJC-1-061 | 0.504 | 2.647 | 0.128 | 0.037 | 1.97 | 182.0 | 5.01 | 3.71 | 3.03 | 119.1 |
| | 99.7 | PJC-1-062 | 1.004 | 5.036 | 0.203 | 0.044 | 4.37 | 224.7 | 10.07 | 7.78 | 6.86 | 160.3 |
| | 99.6 | PJC-1-063 | 0.505 | 7.500 | 0.300 | 0.056 | 6.10 | 370.1 | 5.07 | 3.12 | 3.08 | 362.6 |

**Table 3:** Summary of the various formulations used for the Pickering miniemulsion polymerisations of various monomers stabilised by Laponite clay

| | $m_{water}$/ g | Experiment | $m_0$/ g | $m_M$/ g | $m_{Hex}$/ g | $m_I$/ g | $m_P$ / g | $d_{oil}$/ nm |
|---|---|---|---|---|---|---|---|---|
| **Series IV** | 101.8 | PJC-1-115(LMA) | 0.505 | 2.492 | 0.110 | 0.058 | 2.03 | 209.2 |
| | 99.4 | PJC-1-116(BMA) | 0.511 | 2.502 | 0.108 | 0.055 | 2.04 | 183.9 |
| | 98.0 | PJC-1-118(LA) | 0.250 | 2.491 | 0.105 | 0.052 | 2.03 | 285.9 |
| | 101.8 | PJC-1-119(OA) | 0.509 | 2.478 | 0.107 | 0.048 | 2.02 | 223.3 |
| | 98.5 | PJC-1-121(BA) | 0.508 | 2.568 | 0.106 | 0.054 | 2.09 | 197.4 |
| | 98.8 | PJC-1-126(2-EHA) | 0.500 | 2.532 | 0.107 | 0.050 | 2.06 | 222.1 |

## *Rate of polymerisation in Pickering miniemulsion: polymerisation of styrene*

The overall rates of polymerisation for the Pickering miniemulsion polymerisations carried out in series I, II and III were monitored by determination of monomer conversion ($x_M$) as a function of time using gravimetry. Figure 4 shows the monomer conversion *vs.* time for series I (for raw data series I to III see appendix). As one can clearly see, the overall rate of polymerisation is higher for smaller particle sizes. This is the direct result of compartmentalization of the system. In short this means that two growing polymer chains cannot undergo bimolecular termination if they are present in two separate particles, in other words they are compartmentalised, which results in an overall higher radical concentration and thus a higher rate of polymerisation.

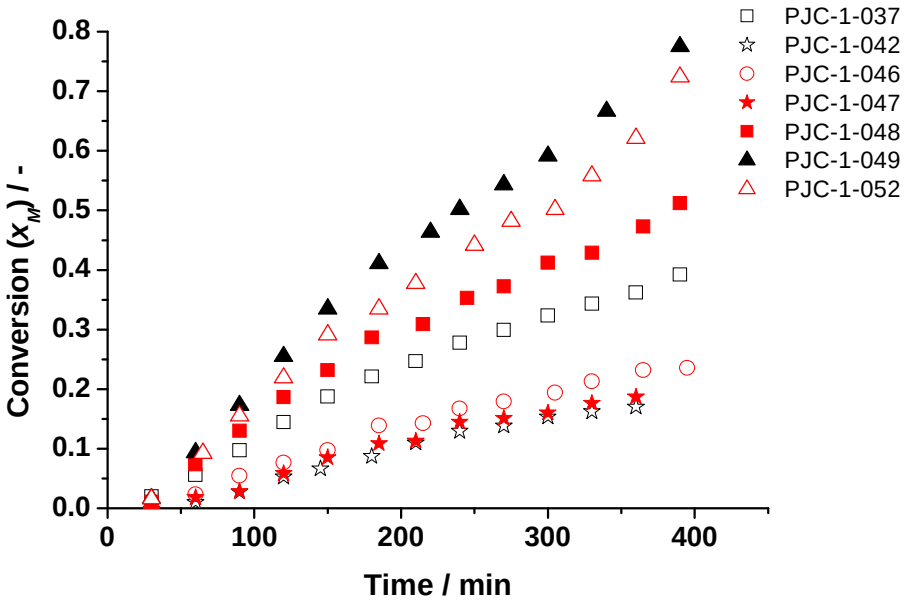


**Figure 4:** Monomer conversion ($x_M$) versus time (min) for Pickering miniemulsion polymerisations of styrene stabilised with Laponite clay (series I: see Table 1)

When we assume that the rate of polymerisation is first order in monomer concentration the following expression holds:

$$\int [R]\, dt = \frac{-\ln(1 - x_M)}{k_p} \qquad \textbf{Equation 19}$$

in which $x_M$ is the monomer conversion determined gravimetrically, [R] is the overall radical concentration in mol $dm^{-3}$, $k_p$ is the rate coefficient of propagation for the monomer, *i.e.* in the present case styrene with a $k_p$(324.15 K) = 247.1 $dm^3$ $mol^{-1}$ $s^{-1}$ , which is the IUPAC recommended value.[36] As a comparison, we carried out a bulk polymerisation for which equation 19 could be approximated at low conversion with the following linear relationship:

$$\int [R]\, dt = \frac{-\ln(1 - x_M)}{k_p} = 2.723 \times 10^{-8}\, t \qquad \textbf{Equation 20}$$

with $t$ being time in s.

The ratios of the values obtained from equation 19 for the Pickering miniemulsion polymerisations and those obtained from equation 20 for the ordinary bulk polymerisation of styrene, tentatively named φ[R], are plotted in figure 5 as a function of monomer conversion.

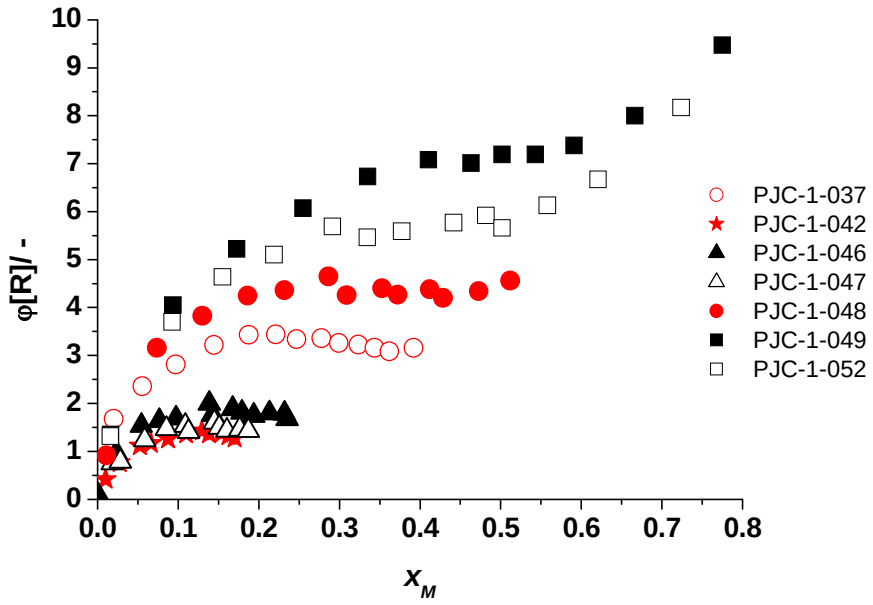


**Figure 5:** The ratios of the values obtained from Eq. 19 for the Pickering miniemulsion polymerisations and those obtained from Eq. 20 for the ordinary bulk polymerisation of styrene, *i.e.* φ[R], as a function of monomer conversion.

The obtained graphs for φ[R] show that typically values increase to reach a certain "plateau" value at intermediate monomer conversion, with a further increase at high monomer conversion. This ratio, *i.e.* φ[R], now clearly shows the effect of compartmentalization. A theoretical value of 1 would agree with ordinary bulk kinetics. "Plateau" values of 7.17, 5.74, 4.43, 3.45, 1.76, 1.54, 1.34 are obtained for particle diameters (DLS) of 234.8, 287.7, 391.5, 495.7, 643.2, 607.9, 658.3 nm, respectively. A clear increase is observed when the average particle size is reduced.

The onset behaviour to these plateau values was rather unexpected and clearly indicates that there is an inhibition and/or a retardation effect. An obvious possible explanation would be the presence of oxygen as a result of incomplete degassing of the system prior to polymerisation. We repeated some of our experiments with different degassing times (20 min, 1 h, 2 h) and found exactly the same behaviour within experimental error,

thereby ruling out oxygen as the inhibition/retardation source. From figure 5 it clearly can be observed that this behaviour becomes more pronounced and extents to higher values of monomer conversion for decreasing particle sizes. The only difference in the recipes for the Pickering miniemulsion polymerisations (series I, see Table 1) is that various amounts of clay are used. A likely cause for the onset behaviour shown in Figure 5, therefore, could be the presence of Laponite clay. The polymerisation reaction, and thus the presence of radical species, is primarily confined to the Pickering stabilised particles/emulsion droplets. It seems plausible to assume that the Laponite clay discs in direct contact with and thus at the surface of the particles/emulsion droplets can have an influence. When oil-soluble initiators are used desorption of radical species (exit) becomes more pronounced for small particle sizes.[40] A radical species exiting the particle has to cross the Laponite-covered interface. The growing polymer chain potentially could be terminated by reaction with the Laponite clay disc. This would explain why the observed onset behaviour is more pronounced for smaller particle sizes, as there are fewer radicals per clay particle, and more clay particles per unit volume.

At monomer conversions exceeding 50% we clearly see an increase in φ[R]. This can directly be ascribed to the Trommsdorff or gel effect.[37] The linear relationship used to express the bulk polymerisation of styrene in order to calculate φ[R] is only valid up to moderate monomer conversion

(Eq. 21). Not taking into account this effect of enhanced diffusion limitation for termination for the bulk polymerisation system leads to the observed increased values for φ[R]. The Trommsdorff effect occurs because, when the monomer/polymer mixture begins to gel, diffusion slows down. This controls the rate at which the growing polymer chains can move, thereby decreasing the probability of polymer-polymer termination collisions. Since monomer units can diffuse much more easily in the viscous medium, propagation is not affected to the same extent. This causes an increase in the overall rate of polymerisation.

### *Pickering miniemulsion polymerisation of various monomers*

Besides Pickering miniemulsion polymerisations of styrene, we carried out reactions using different monomers. Pickering miniemulsion polymerisations using Laponite clay discs as stabiliser and with lauryl (meth)acrylate, *n*-butyl (meth)acrylate, octyl acrylate and 2-ethylhexyl acrylate as monomer were all successful (see Table III). One common characteristic of all these monomers is their hydrophobicity. This appeared to be a crucial factor for success as reactions performed with monomers that have higher water solubilities, such as methyl acrylate or methyl methacrylate, were only partially successful under current experimental conditions. The reason for this could be that the energy created by the difference in interfacial tensions is not great enough to keep the clay at the interface of the created monomer droplets. Similar work has been reported by Bourgeat-Lami and co-workers who also

showed the production of poly(styrene–co-*n*-butyl acrylate) low $T_g$ Laponite-armoured latex particles via heterocoagulation.[38] Van Herk has also shown the inverse Pickering emulsion polymerisation of 2-hydroxyethyl methacrylate using montmorillonite as stabiliser.[39]

## *Conclusions*

We investigated the solid-stabilised, or Pickering, miniemulsion polymerisations using Laponite clay discs as a stabiliser. We showed that Pickering miniemulsion polymerisations were successful for a variety of hydrophobic monomers, *i.e.* styrene, lauryl (meth)acrylate, *n*-butyl (meth)acrylate, octyl acrylate, and 2-ethylhexyl acrylate. The Laponite-stabilised miniemulsion polymerisations yielded armoured latexes, in which the surface of the particles was covered with clay discs. Overall polymerisation kinetics of the Pickering miniemulsion polymerisations of styrene showed compartmentalization. Moreover, retardation effects up to intermediate monomer conversions were observed, which were more prominent for the smaller particles, and were ascribed to the Laponite clay. A model was presented which allows for the prediction of the average particle size of the latexes produced as a function of the amounts of monomer and Pickering stabilisers used. It shows that under specific generic conditions the amount of clay discs used correlates in a linear fashion with the total surface area of the latex particles. This is a direct result of the reversibility of the Laponite clay disc adhesion process under the emulsification conditions, *i.e.* sonication, used.

## *Methodology and raw data*

### Equipment:

pH measurements were performed on a Knick pH meter 765. Sonication was performed using a Branson digital 450W sonifier. Dynamic Light Scattering measurements were performed on a Malvern instruments, Zetasizer 3000HSA set to 25 °C, using a 0.1 M NaCl solution at pH 10 as solvent. FE-SEM measurements were performed on a ZEISS supra 55VP FEGSEM set at high vacuum EHT = 10 kV WD = 3 mm. Prior to FEG-SEM analysis samples were sputter-coated with Au for 45 seconds at 1.5 kV and 20 mA using a Quorum technologies Polaron SC7640 auto/ manual high resolution sputter coater.

### Typical recipe for Pickering miniemulsion polymerisation:

Laponite RD (1.0 g 10 wt%) was added to deoxygenated $H_2O$ (100 ml) and sonicated for 4.5 min at 70% amplitude with a 30 second pause every minute. After the first minute interval NaCl (0.57 g, 0.1 mol $dm^{-3}$) was added to the sonicating suspension. To a separate beaker, styrene (10.0 g, 0.1 mol, 8.3 %solids), *n*-Hexadecane (0.4 g, 4 wt%) and V-65 (2,2'-azobis(2,4-dimethyl valeronitrile)) (0.05g, $0.2x10^{-4}$mol, 0.5%wt) were mixed then poured into the clay suspension during agitation by Ultra Turrax set to 24,000 rpm. The emulsion was mixed until there was no visible organic layer. The emulsion was then put under ultra sound for 6.5 min at 70 % amplitude with a 30 second wait every minute with a max

temperature set at 40 $^{o}$C in order to prevent early polymerisation. The resulting emulsion was poured into a 250 ml round bottom flask, which was sealed using a rubber seal and bubbled through with $N_2$ for 20 minutes. The reaction mixture was then heated to 51$^{o}$C and gently stirred. Gravimetric analysis was performed by sampling a known mass (approx. 2 mL) of the polymerising mixture and depositing into a foil dish of known mass. The dish was then heated to 120$^{o}$C to remove any monomer and *n*-hexadecane under vacuum for 48 h to determine the solids content. Monomer conversion was obtained by taking into account the amount of clay and salt in the system. After two days the resulting latex was dialysed in distilled water made up to pH 10 by the addition of concentrated ammonia solution.

(1) Lin, Y.; Skaff, H.; Boker, A.; Dinsmore, A. D.; Emrick, T.; Russell Thomas, P. *J. Am. Chem. Soc.* **2003**, *125*, 12690-12691.

(2) Russell, J. T.; Lin, Y.; Boker, A.; Su, L.; Carl, P.; Zettl, H.; He, J.; Sill, K.; Tangirala, R.; Emrick, T.; Littrell, K.; Thiyagarajan, P.; Cookson, D.; Fery, A.; Wang, Q.; Russell, T. P. *Adv. Mater.* **2005**, *44*, 2420-2426.

(3) Lin, Y.; Skaff, H.; Emrick, T.; Dinsmore, A. D.; Russell, T. P. *Science* **2003**, *299*, 226-229.

(4) Skaff, H.; Lin, Y.; Tangirala, R.; Breitenkamp, K.; Boker, A.; Russell, T. P.; Emrick, T. *Adv. Mater.* **2005**, *17*, 2082-2086.

(5) Harrison, R. G.; Washburn, A. L.; Pickett, A. T.; Call, D. M. *J. Mater. Chem.* **2008**, *18*, 3718-3722.

(6) van Zyl, A. J. P.; Wet-Roos, D. d.; Sanderson, R. D.; Klumperman, B. *Eur. Polym. J.* **2004**, *40*, 2717-2725.

(7) Landfester, K.; Bechthold, N.; Tiarks, F.; Antonietti, M. *Macromolecules* **1999**, *32*, 5222-5228.

(8) Fontenot, K.; Schork, F. J. *Polym. React. Eng.* **1992**, *1*, 75-109.

(9) Fontenot, K. J.; Reimers, J.; Schork, F. J. *DECHEMA Monogr* **1992**, *127*, 429-38.

(10) Schork, F. J.; Luo, Y.; Smulders, W.; Russum, J. P.; Butte, A. *Adv. Polym. Sci.* **2005**, *175*, 129-255.

(11) Ostwald, W. *Lehrbuch der allgemeinen Chemie. Second edition*, 1896; Vol. II, 2; Part I.

(12) Landfester, K.; Schork, F. J.; Kusuma, V. A. *C. R. Chim.* **2003**, *6*, 1337-1342.

(13) Higuchi, W. I.; Misra, J. *J. Pharm. Sci.* **1962**, *51*, 459-66.

(14) Ugelstad, J.; Moerk, P. C.; Herder Kaggerud, K.; Ellingsen, T.; Berge, A. *Adv. Colloid Interface Sci.* **1980**, *13*, 101-40.

(15) Morton, M.; Kaizerman, S.; Altier, M. W. *J. Colloid Sci.* **1954**, *9*, 300-12.

(16) Ugelstad, J. *Makromolekul. Chem.* **1978**, *179*, 815-17.

(17) Ashby, N. P.; Binks, B. P. *Phys. Chem. Chem. Phys.* **2000**, *2*, 5640-5646.

(18) Droste, D. H.; Dibenedetto, A. T. *J. Appl. Polym. Sci.* **1969**, *13*, 2149-68.

(19) Chen, K.-H.; (Taiwan). Application: US, 2005

(20) Inan, G.; Patra, P. K.; Kim, Y. K.; Warner, S. B. *Materials Research Society Symposium Proceedings* **2003**, *788*, 289-295.

(21) Xu, Y.; Brittain, W. J.; Xue, C.; Eby, R. K. *Polymer* **2005**, *46*, 531-538.

(22) Sun, Q.; Deng, Y.; Wang, Z. L. *Macromol. Mater. Eng.* **2004**, *289*, 288-295.

(23) Herrera, N. N.; Letoffe, J.-M.; Putaux, J.-L.; David, L.; Bourgeat-Lami, E. *Langmuir* **2004**, *20*, 1564-1571.

(24) Choi, Y. S.; Xu, M.; Chung, I. J. *Polymer* **2005**, *46*, 531-538.

(25) Labbe, P.; Reverdy, G. *Langmuir* **1988**, *4*, 419-25.

(26) Ashby, N. P.; Binks, B. P. *Phys. Chem. Chem. Phys.* **2000**, *2*, 5640-5646.

(27) Mongondry, P.; Tassin, J. F.; Nicolai, T. *J. Colloid. Interface Sci.* **2005**, *283*, 397-405.

(28) Ruzicka, B.; Zulian, L.; Ruocco, G. *Langmuir* **2006**, *22*, 1106-1111.

(29) Jönsson, B.; Labbez, C.; Cabane, B. *Langmuir* **2008**, *24*, 11406-11413.

(30) Dong, L.; Johnson, D. T. *Langmuir* **2005**, *21*, 3838-3849.

(31) Nonomura, Y.; Komura, S.; Tsujii, K. *J. Phys. Chem. B.* **2006**, *110*, 13124-13129.

(32) Smith, W. V.; Ewart, R. H. *J.Chem.Phys.* **1948**, *16*, 592-599.

(33) Antonietti, M.; Bremser, W.; Muschenborn, D.; Rosenauer, C.; Schupp, B. *Macromolecules* **1991**, *24*, 6636-6643.

(34) Wu, C. *Macromolecules* **1994**, *27*, 298-299.

(35) Wu, C. *Macromolecules* **1994**, *27*, 7099-7102.

(36) Buback, M.; Gilbert, R. G.; Hutchinson, R. A.; Klumperman, B.; Kuchta, F.-D.; Manders, B. G.; O'Driscoll, K. F.; Russell, G. T.; Schweer, J. *Macromol. Chem. Phys.* **1995**, *196*, 3267-80.

(37) Trommsdorff, E.; Kohle, H.; Lagally, P. *Makromolekul. Chem.* **1948**, *1*, 169-98.
(38) Negrete-Herrera, N.; Putaux, J.-L.; David, L.; De Haas, F.; Bourgeat-Lami, E. *Macromol. Rapid Commun.* **2007**, *28*, 1567-1573.
(39) Voorn, D. J.; Ming, W.; Van Herk, A. M. *Macromolecules* **2006**, *39*, 2137-2143.

## *Chapter 5: Development of Pickering Emulsion polymerisation*

A potential improvement in the current clay miniemulsion system is the high shear force needed to generate the droplets, and the large excess of clay left in the system. One way we could try and counter this is to change our method to make it an emulsion polymerisation system. Emulsion polymerisation requires no high shear force, as it is dependent on water phase initiation of polymerisation and diffusion events to generate the polymerisation loci. The only shear required is stirring to ensure optimal dissolution of monomer in the continuous phase. In order to convert normal emulsion polymerisation into a Pickering system we need to mimic a soap-free system as solid particles will not likely produce micelles. Soap-free emulsion polymerisation has been used for many years and different mechanisms have been proposed, however the most recent and probable mechanistic scheme is that of coagulative nucleation:[1,2]

$$M + I\cdot \rightarrow I\text{-}M\cdot$$ **Scheme 1**

An initiator in the water phase decomposes to form radicals (see basic theory section). The radical then initiates a monomer molecule in the water phase

$$IM\cdot + nM \rightarrow_{n} H(M)_{n}M\cdot$$ **Scheme 2**

The monomer radical will continue to propagate in the water phase to generate an oligomer of *n* monomer units $J_n$.

$$J_{n} + mM \rightarrow_{m} J_{crit}$$ **Scheme 3**

This water-soluble oligomer can either react with another initiating radical and terminate becoming a stable water-soluble species or continue to react with monomer until it reaches sufficient size whereby it becomes water-insoluble. This size will change depending on the water solubility of the monomer in question is referred to as $J_{crit.}$

$$J_{crit} + J_{crit} + J_{crit} \rightarrow \text{Latex Particle}$$ **Scheme 4**

This insoluble polymer, now referred to as a primary particle, is often not colloidally stable, so will coagulate with other primary particles. This continues until enough charged units have been accrued to provide sufficient charge stabilisation. Other shorter species referred to as $J_z$ (oligomers large enough to be surface-active) or larger, more highly-charged species (created by two oligomeric radicals undergoing termination by coupling) may also coagulate onto this growing nucleus. From then on, this cluster of chains is referred to as a mature latex

particle. This generation process of particles is referred to as coagulative nucleation.

Simultaneously the particle swells with monomer and continues to grow and polymerise due to radical entry of the free initiator radicals (assuming zero-one kinetics, therefore no radical-radical termination) or by absorption of newly-generated growing polymer chains. This continues until all monomer has been reacted. No new nucleation sites are generated as the probability of an oligomer radical of chain length *z* entering an existing particle is much greater than the chance of further propagation in the aqueous phase. This high probability for entry exists due to the exceptionally high total surface area presented by the latex particles. When the nucleation period is fast compared to the overall polymerisation time, monodisperse particles are generated. Any difference in particle size occurs during the nucleation step, which creates very small particles. These differences become less pronounced during particle growth.

The processes in emulsion polymerisation can be categorised into the following three main steps as defined by the simplified mechanism proposed by Smith, Ewart[3] and Hawkins.[4] 1) Free monomer in solution migrates into micelles. Radicals initiate free monomer in solution and monomer in micelles. 2) Polymer chains grow only in micelles as the surface area of these is much greater than droplets of monomer. Any oligomers that grow will coagulate with existing micelles to create

nucleation sites. (This step defines the number of particles present in the system) These polymer particles will swell with any remaining monomer in free droplets 3) All free droplets of monomer disappear, leaving only water-solvated monomer and monomer in swollen latex particles. It can be seen that this model differs slightly for soap-free systems, but the basic processes are still the same.

Emulsion polymerisations have led to fascinating colloidal structures, such as core-shell[5] and hollow latexes,[6] or peanut[7] and multi-lobed particles.[8] Miniemulsion polymerisation has also led to a vast array of composite latexes, encapsulating materials such as semiconducting polymers.[9]

One interesting class of nanocomposite polymer latexes is those with morphologies that are armoured or multi-layered in nature. These potentially have great performance benefits when applied in waterborne coatings and adhesives, for example enhanced scratch resistance. These complex composite colloids, however, are not easily made. Vogt *et al.*[10] and later Caruso *et al.*[11] reported the fabrication of hollow multi-layered capsules using a layer-by-layer approach, an extension of the hetero-coagulation method to create armoured structures.[12] Disadvantages are that these methods are time-consuming and require dilute conditions. Armes *et al*. described the synthesis of poly(styrene)-silica nanocomposite particles in aqueous alcoholic media using a silica sol as stabiliser,[13] recently extending this method to in water and poly(methyl

methacrylate) using a glycerol-modified silica sol.[14] Sacanna showed that methacryloxypropyltrimethoxysilane, in presence of nanosized silica led to spontaneous emulsification in water,[15] which upon a two-step polymerisation procedure afforded armoured particles with an outer shell of poly(methyl methacrylate).[16] Müller reported the use of Janus-type polymer particles as stabilisers in emulsion polymerisation.[17]

It is our belief that if our clay miniemulsion system could be modified to use an emulsion polymerisation system it would be more industrially viable (due to the reduced energy of generating the latex) and more uptake of Pickering stabiliser might occur as there is less force removing the particles from the generated interface as there is no high shear ultrasound. In our miniemulsion system the ultrasound created a thermodynamic equilibrium with a flux of particles coming on and off the interface. In an emulsion case once the particle is adhered to the interface it should not be able to come off again, forcing any equilibrium over to full coverage.

### *Laponite miniemulsion in the presence of charge surfactants:*

In most emulsion polymerisation systems a charged initiator is used. It is therefore important to study the stability of clay as a Pickering stabiliser in the presence of charged species. Normally in a Pickering system, charged species would have a detrimental effect as these would stabilise the interface, thereby reducing the energy well keeping the solid particle at the interface.[18] Clay is known to have a cation exchange capacity (cec)

of 7.3 × $10^{-4}$ mol/g. [19] This means that positively-charged species can displace the sodium counter ion from the surface of the clay disc. Due to the fact clay is zwitterionic, two negatively-charged surfaces (top and bottom planes, reported surface area of *ca.* 750 $m^2/g$) and a weakly positively-charge rim (edge, reported surface area of *ca.* 100 $m^2/g$),[20] it should behave differently towards positive and negative species. To test this, different quantities of a positively-charged soap; cetyl trimethyl ammonium bromide (CTAB) and dioctadecyl dimethyl ammonium bromide (DODAB), and a negatively-charged soap; sodium dodecyl sulfate (SDS), were added to a standard clay miniemulsion polymerisation. It is already known that by adding different quantities of CTAB to Laponite clay the wettability can be altered.[21] we intend to investigate how this might affect our Laponite system and whether SDS has a similar affect. Pickering miniemulsion polymerisations of styrene (10 g) using Laponite clay discs (0.7 g) as stabiliser were performed in the presence and absence of different amounts of three types of surfactant, *i.e.* SDS, CTAB and DODAB all suspended in deionised water (100 mL). After the polymerisations were complete, the average particle sizes of the latexes were measured and the theoretical excess of clay was calculated by assuming 100 % coverage of the produced latex particles. This data was then plotted as a function of the amount of Laponite added with the existing data from our previous work.[22]

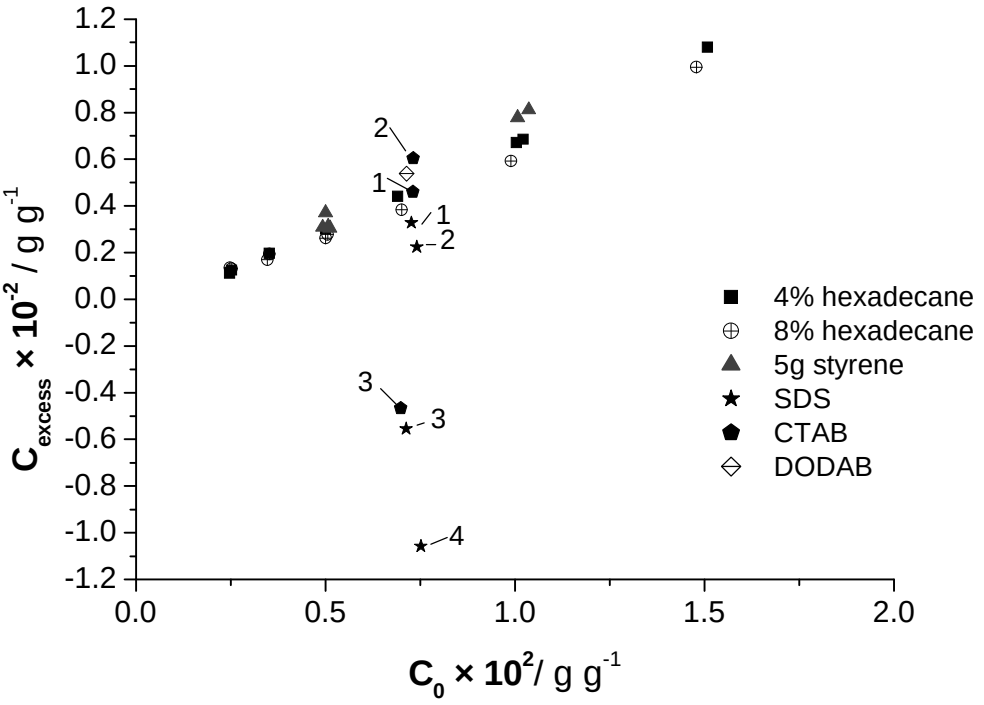


**Figure 1:** Correlation between the theoretical excess of clay and the quantity of clay added. The order of increasing concentrations of soap goes from 1-4 for SDS, 1-3 for CTAB and a single run with DODAB (0.3 g/L). The result missing from the CTAB experiments is the 3.0 g/L since it coagulated upon emulsification.

One interesting result was that when we used 3.0 g/L of either DODAB or CTAB the system coagulated upon emulsification in the Sonicator. More noticeably, the SDS system with 0.3 g/L of soap also initially coagulated. However, polymerisation of this phase-separated system led to considerable amounts of stable latex.

Apart from analysing the average particle size we investigated the polymerisation kinetics of the Pickering miniemulsion polymerisation systems, now in the presence of different surfactants. The overall rate of polymerisation was plotted relative to the rate of polymerisation of styrene under equivalent bulk conditions (See Figure 2).

This graph does not contain data for experiments with large quantities of soap (0.3 g/L SDS and 3 g/L CTAB). The small sizes of the particles generated caused the polymerisation reactions to go to completion within one hour.

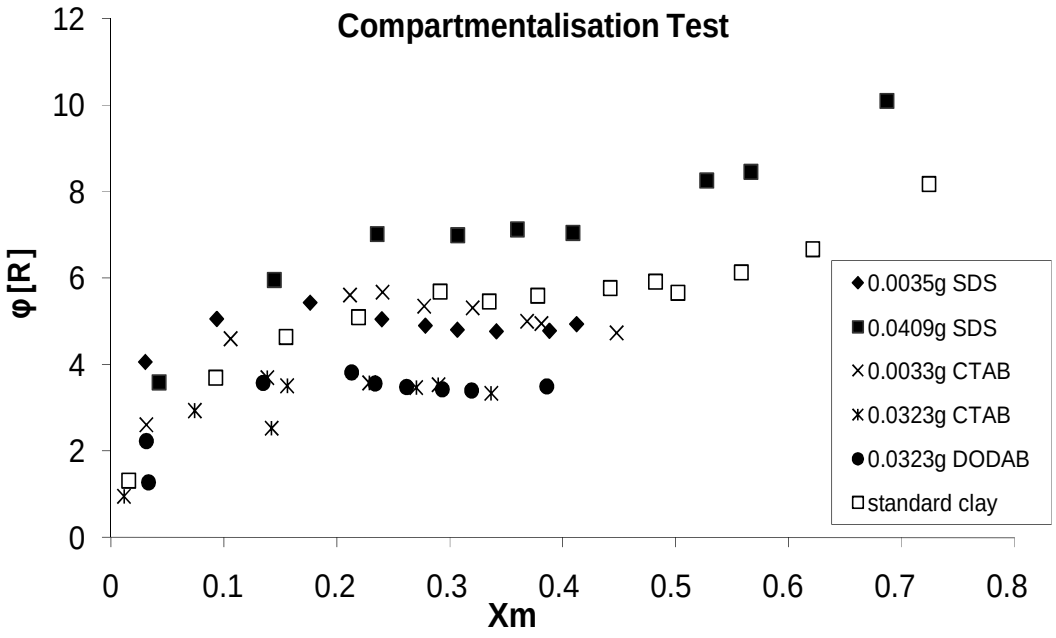


**Figure 2:** Relative rate of polymerisation compared to bulk. (φ[R]) vs. the conversion (Xm). The amounts of surfactants used are displayed for 100 mL of water.

From the results shown, it can easily be seen that soap has an obvious effect on the Laponite Pickering miniemulsion polymerisation and that the charge on the soap plays a vital role. CTAB and DODAB behave similarly, yet SDS shows a marked difference. In order to understand what is happening in these soap systems one can look at both the $C_{excess}$ graph (Figure 1) and the polymerisation rate graph (Figure 2). In the $C_{excess}$ graph for the case of cationic soaps, the theoretical $C_{excess}$ when small amounts of 0.03 g/L are used, coincided with the data obtained in Pickering miniemulsion polymerisations in the absence of soap. When we increased the amounts to 0.3 g/L, higher values of $C_{excess}$ are obtained.

This is likely due to the fact that the clay can easily adsorb very low quantities of soap and retain its normal wettability but when slightly more soap is added the wettability starts to change. The clay becomes more hydrophobic and flocculates together more so than usual. This means there is less clay available to stabilise the interface, in turn creating larger than normal droplets giving a higher theoretical excess. This increased flocculation could be due to Van der Waals interactions between soap tails. One should also take into account the fact that the hydrophobic clay aggregates can potentially partition into the monomer phase. When we further increase the amounts of cationic soap up to 3.0 g/L the surface of the clay becomes completely exchanged and the clay becomes hydrophobic, causing the platelets to fully coagulate, meaning they can no longer stabilise the monomer-water interface. The amount of CTAB able to cation-exchange with $Na^+$ ions on the surface of Laponite can be calculated as 1.9 g/L, under our experimental conditions.[19] This means that in the 3.0 g/L systems the clay has been completely exchanged. When a large excess of soap (30.0 g/L) is added, double layers of surfactant form on the clay due to the aforementioned tail/tail interaction. This causes the clay to become hydrophilic again and redisperse in water fully due to the charged surfactant heads being orientated into solution. The excess soap left in the water can then stabilise the emulsion giving purely soap-stabilised latex.

In the case of SDS the same holds for the smallest quantity of soap used, but interestingly the system coagulates a lot sooner than the cationic surfactant systems, which are already at 0.3 g/L. This is strange due to the apparent lack of an anionic exchange capacity. However the amount of soap needed to destabilise the system makes sense on a purely surface area treatment of the Laponite. The emulsions become soap-controlled on addition of more surfactant. This can clearly be seen from figure 1, as the excess becomes a lot smaller than with the non-soap system. This can be ascribed to the fact that the particles become smaller than in the pure Laponite case. The negative numbers can be explained by the soap stabilising particles so small that there isn't physically enough clay to coat the interface generated.

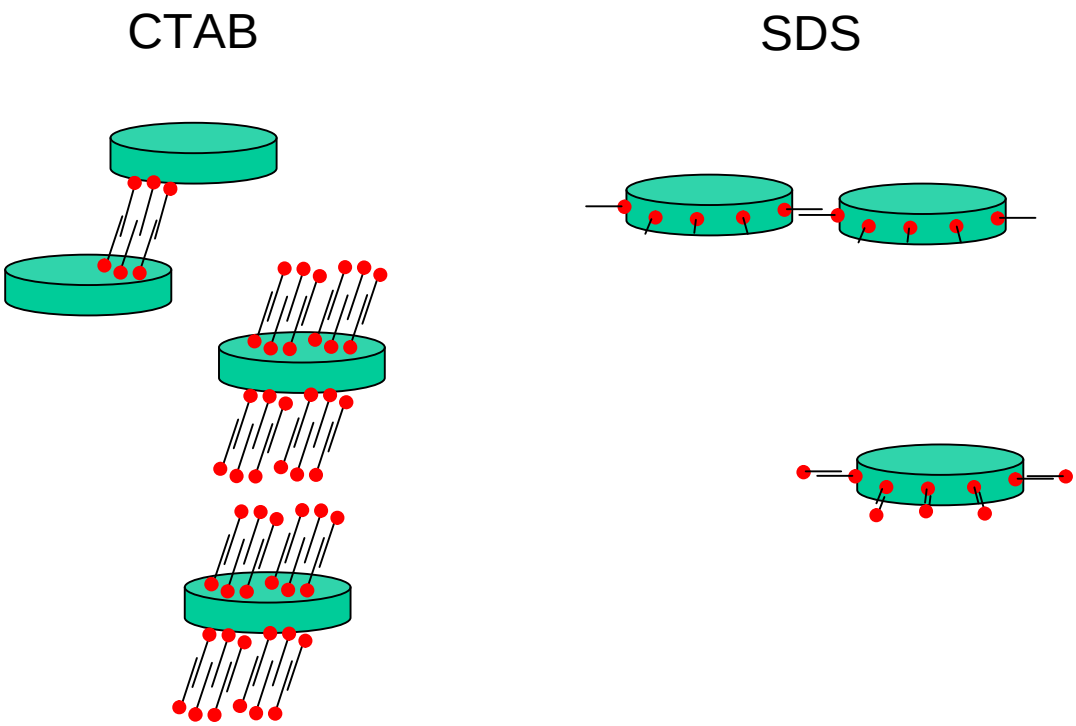


**Figure 3**: Graphical representation of soap double layer formation on clay platelets

These results can be corroborated by the rate data, which clearly shows that for the 0.03 g/L cases the rate is identical to that of the normal clay system, but when more soap is added to the cationic soap systems the rate decreases. This is due to larger particles being generated so there is less of a compartmentalization effect, whereas when more SDS is added the rate increases as smaller particles are generated. The fact that a large inhibition period is still visible suggests that the clay still plays a vital role in stabilising these systems.

These results show that the clay formulation cannot work using a negative initiator such as KPS. This is demonstrated in Figure 4, which shows that if 0.05 g of initiator is used (which is the standard amount in our experiments) the concentration of charged species leaves the known "safe zone"(greyed area) very rapidly when the 10 h half life temperature of 333 K is used.

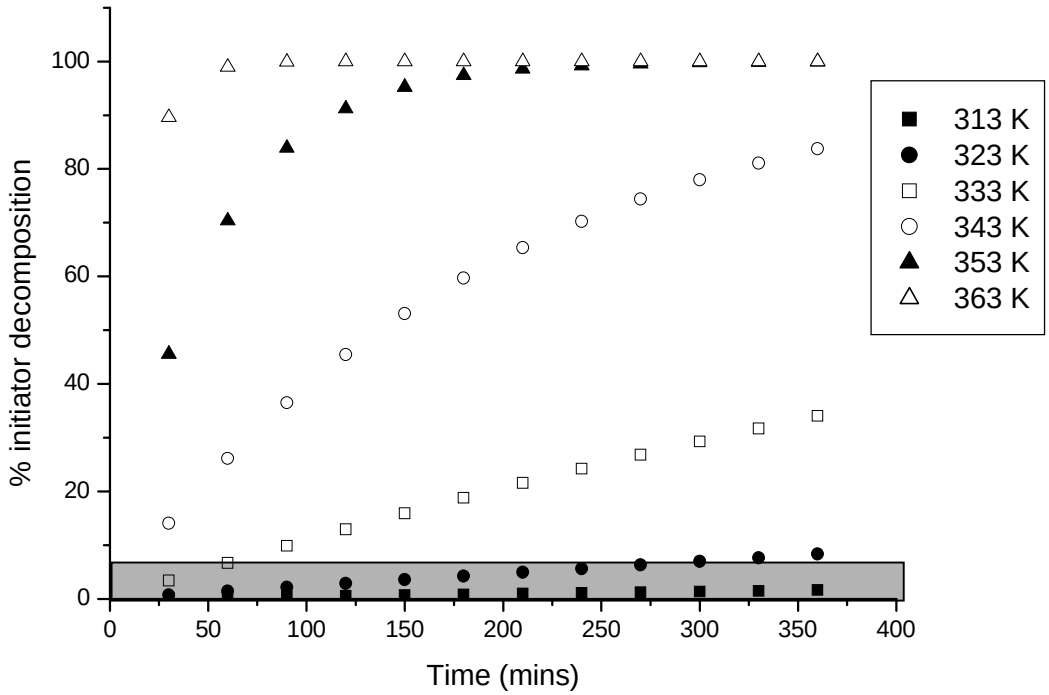


**Figure 4:** Decomposition rate of KPS over time at different temperatures. The grey region denotes the region in which it is known our clay miniemulsion system is stable for SDS

However, in theory, this also implies that cationic initiators will work because the clay system is tolerant to the levels of charged species generated during a standard polymerisation. Using the same assumptions as before, Figure 5 shows that the amount of positive species generated falls into the safe area.

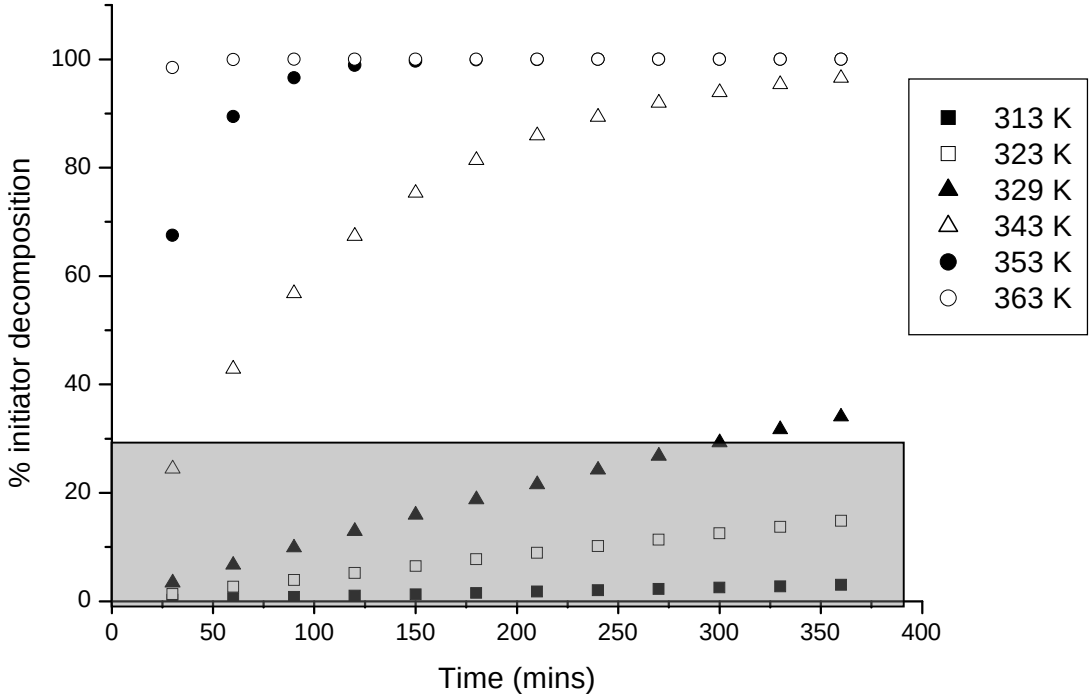


**Figure 5:** Decomposition rate of V50 at different temperatures along with the grey region in which it is known our clay miniemulsion system is stable for CTAB and DODAB

To test this theory we made up our model clay miniemulsion formulation. However, the initiator was changed to 2,2'-azobis(2-methyl propionamidine) dihydrochloride (V-50) and the miniemulsion was polymerised. Unexpectedly, the latex quickly coagulated and failed to give a stable latex. It is postulated that this is due to the initiator exchanging onto both sides of the clay particle and making the clay platelets an initiating site, causing coagulation. Another reason could be the clay forms an impenetrable barrier to radicals, meaning that no initiation can occur.

These results show that in our clay system it is not possible to perform emulsion polymerisation. Interestingly Zhao *et al*. has managed to get a clay emulsion system to succeed by grafting PDMAEMA brushes onto

the clay first.[23] If we want to get our system to work with unmodified particles, a different stabiliser needs to be used that does not have two different charges.

## *Pickering Emulsion Polymerisation using Ludox-TM40 Silica Nanoparticles as Stabilizer*

Our research group has been looking into the use of nano-silica (specifically Ludox TM40) as a stabiliser, and had successfully developed a procedure to created Ludox-armoured latex particles via Pickering miniemulsion polymerisation.[24] Ludox is supplied as a 40 wt% sol. of *ca.* 25 nm silica spheres at a pH of 10. This high pH is used to deprotonate the surface Si-OH groups to create $Si\text{-}O^{-}Na^{+}$ groups. The negative groups are the only stabilising units on the Ludox. This means they could potentially be used in conjunction with other negatively charged species and initiators (KPS or SDS). The large amount of negative charge at pH 10 creates enough stabilisation to prevent flocculation. However, when one looks at the zeta potential plot for Ludox over a range of pHs it can be seen that in its native pH it is far too charged to be used as a Pickering stabiliser. In previous work it was found that in order for Ludox to be an efficient solid stabiliser the pH must be dropped to achieve a zeta potential close to or below -30 mV.[24]

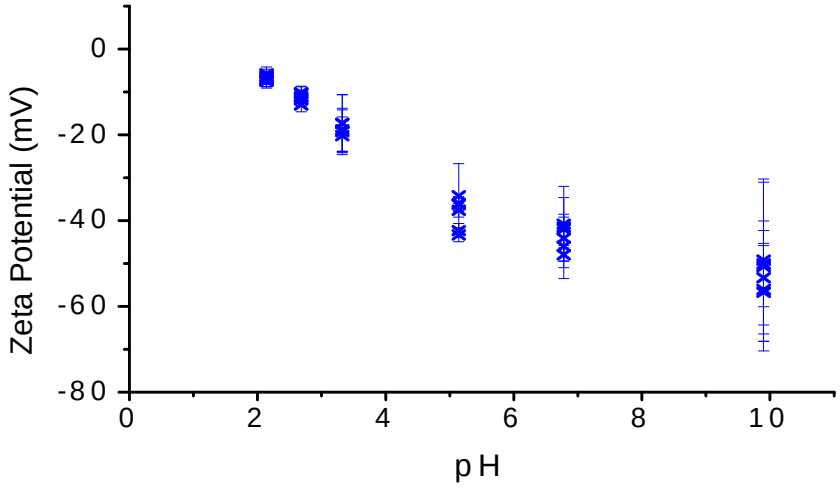


**Figure 6:** Zeta potential measurements of Ludox TM-40 at various pHs

The pH used to great success previously was 3.0. However if we want to use KPS in our system the pH must not be too acidic as this will cause the following self catalysing decomposition into non-radical species: [25-27]

$$H_2S_2O_8 + H_2O \rightarrow H_2SO_5 + H_2SO_4$$ **Scheme 5**

$$H_2S_2O_8 + H_2O \rightarrow H_2O_2 + H_2SO_4$$ **Scheme 6**

Because of this, pH 5.5 was selected as this brings the zeta potential close to -30 mV yet should be sufficiently high to prevent most of the initiator from being converted.

To investigate the use of Ludox in conjunction with charged species both CTAB and SDS were added (in the same weights as previously) to a standard Ludox miniemulsion which consisted of Ludox (5 g) dispersed in water (45 g) with styrene (5 g) as the monomer.

The resulting latexes were examined by SEM to observe their size and the location of the Ludox. CTAB even at the lowest concentrations caused the emulsion to coagulate and it only regained stabilisation at the two highest

CTAB concentrations, giving particle sizes of 200 nm and 80 nm in ascending concentration. When SDS was added, a stable latex was obtained at all concentrations. However, as can been seen from Figure 7, even at the lowest soap concentrations no Ludox particles can be found at the interface.

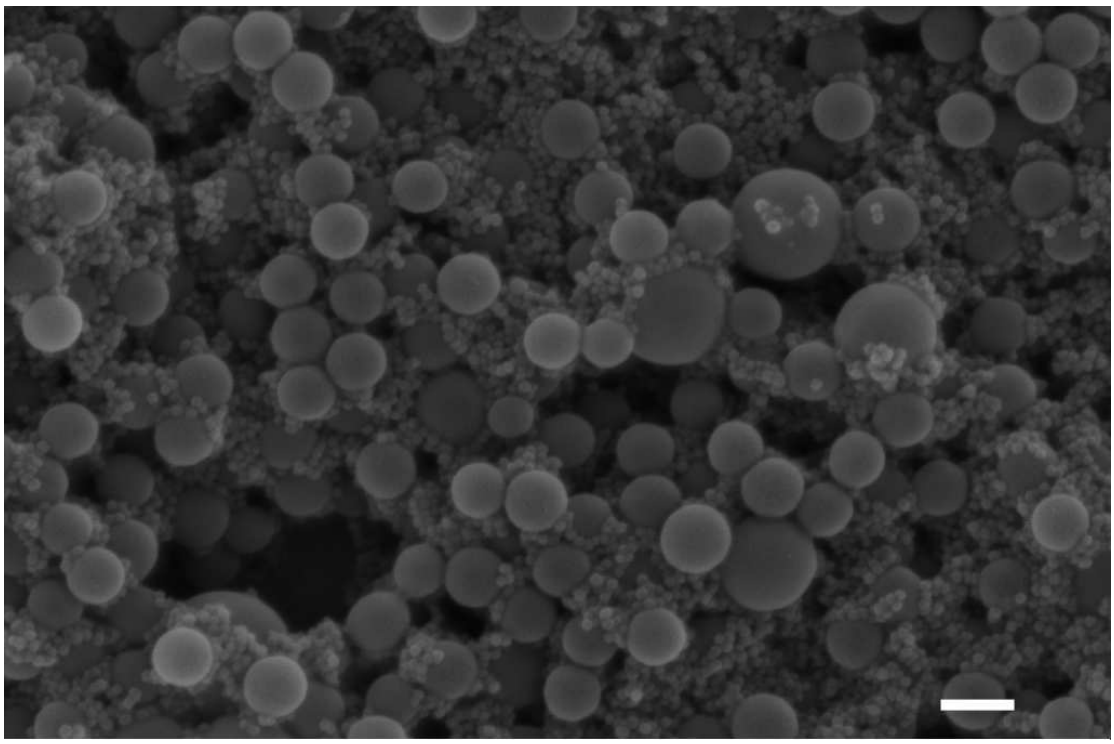

**Figure 7:** Ludox miniemulsion after polymerisation using 0.003g SDS. Large spheres are PS latex particles. Small spheres are Ludox. Scale bar 200 nm

However an interesting point is that, without Ludox, the system using 0.003 g of SDS is not stable. This implies that the Ludox still has a stabilising effect. One possibility is that the surfactant preferentially adheres to the interface of the monomer droplets and gives the interface a slight negative charge. The Ludox, which is also negatively-charged, may then act as a haloing or a depletion stabiliser.[28-30]

In order to try and get the particles to adhere to the interface of the latex particles, it was decided to use a more hydrophilic monomer to shift the energy minimum slightly more into the monomer phase. We decided to use methyl methacrylate as this is one of the most hydrophilic non-water soluble monomers and use KPS as the initiator in the miniemulsion polymerisation. Interestingly a stable latex was generated, and upon examination via SEM the polymer particles have an armoured structure (Figure 8):

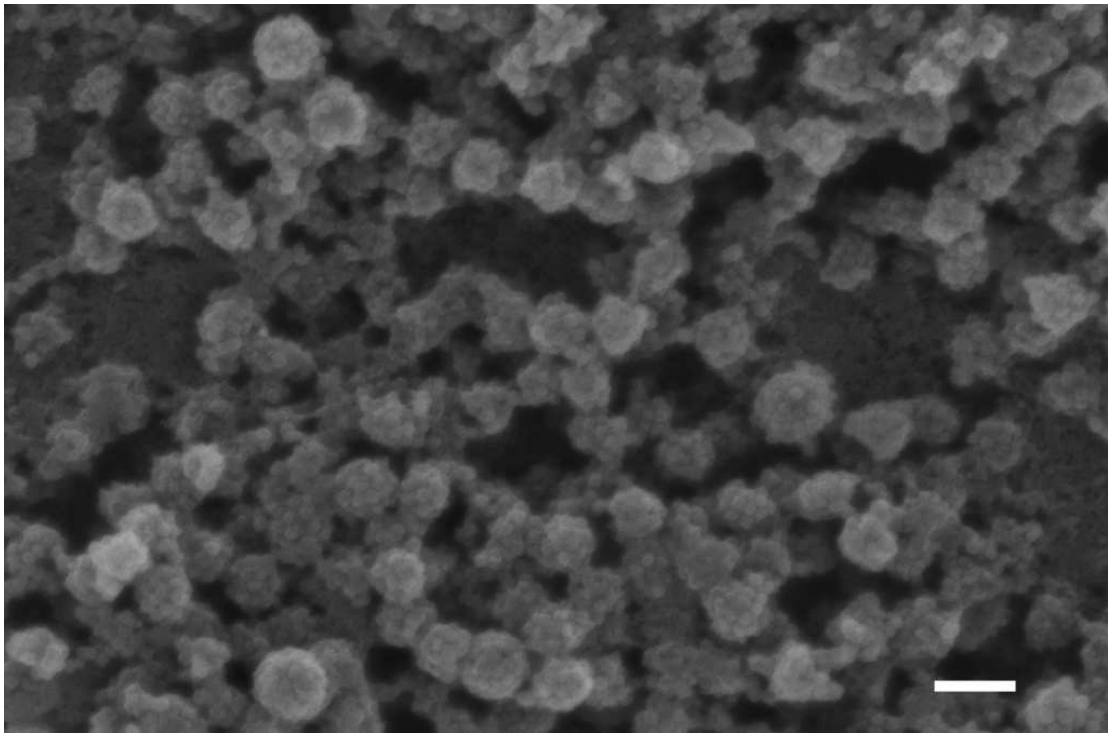

**Figure 8:** Figure showing armoured PMMA latex particles with Ludox as stabiliser. Scale bar is 200 nm

This shows that Ludox can be used as a Pickering stabiliser even in the presence of negatively-charged species. We performed various series of soap-free emulsion polymerisations in presence of Ludox nanoparticles. All reactions were carried out at 65 °C using 1.85 mM potassium persulfate as initiator, thereby providing a low and steady flux of

radicals. In our first series we used methyl methacrylate as monomer at a monomer-to-water ratio (v:v) of 0.13 and we varied the solution pH, *i.e.* 10.0, 5.5 and 3.0 to influence the surface charge densities of the growing latex particles and the silica nanoparticles. Emulsion polymerisations carried out at pH 10.0 led to full coagulation. FE-SEM analysis of the coagulum showed bare polymer latex particles, thereby indicating that no adhesion had taken place (Figure 9).

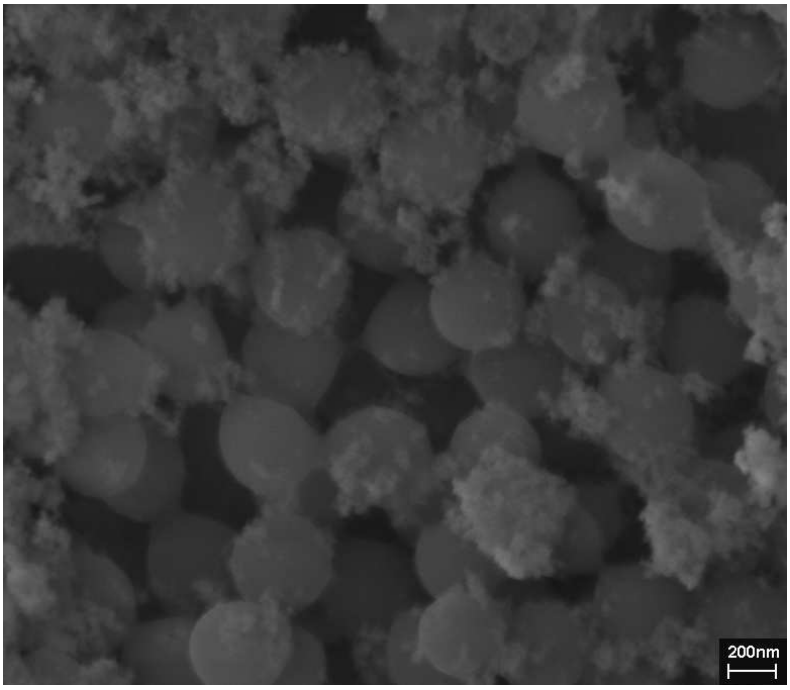


**Figure 9:** FE-SEM image of a poly(methyl methacrylate) latex prepared via emulsion polymerisation at pH 10.0 in the presence of Ludox TM-40.

At pH 3.0 a macroscopically stable latex was obtained. Dynamic light scattering, however, showed a broad particle size distribution with micro*n*-sized averages, indicating that some coagulation on a microscopic scale had occurred. This is plausible as electrostatic stabilisation through charge repulsion at this low pH is insufficient. Nevertheless, FE-SEM

analysis showed a closely-packed armoured layer of silica particles present on the polymer latex particles (Figure 10).

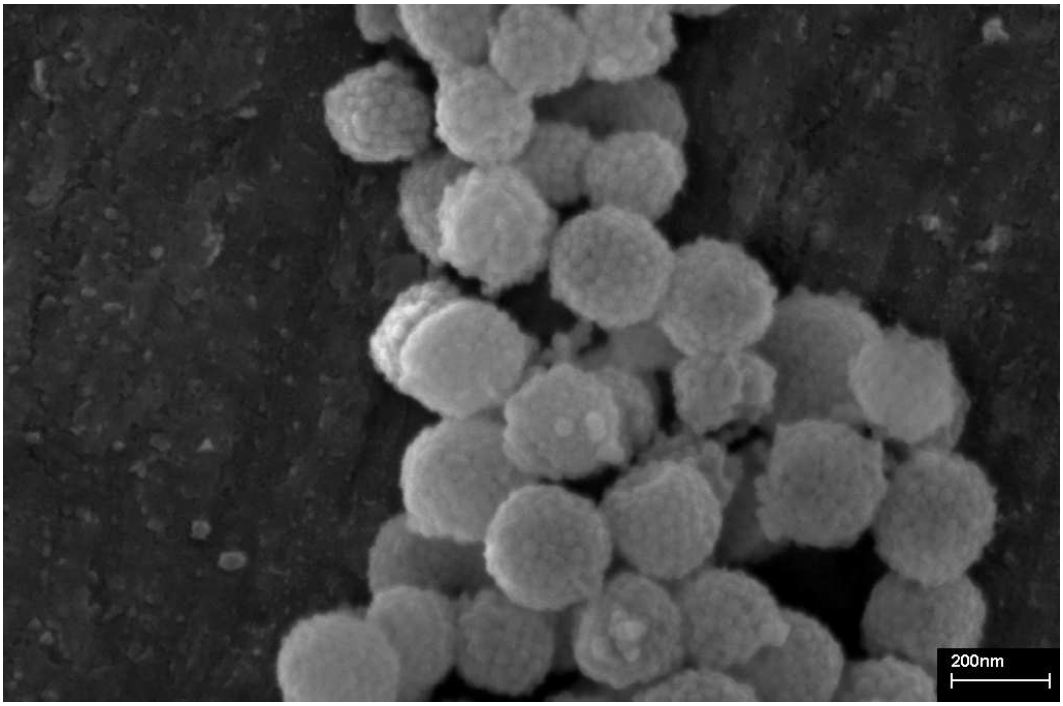


**Figure 10:** FE-SEM image of a poly(methyl methacrylate) latex armoured with Ludox TM-40 prepared via emulsion polymerisation at pH 3.0.

At pH 5.5 stable armoured polymer latexes with narrow particle size distributions were obtained. It is noteworthy that the silica nanoparticles are slightly separated on the surface as a direct result of electrostatic repulsion. All further experiments were performed at pH 5.5.

We varied the amount of silica nanoparticles, using Ludox sol to monomer volumetric ratios of 0.67, 0.83, 1.00 and 1.25, to investigate if we could control the particle size of the latexes obtained. All emulsion polymerisations led to stable armoured latexes with narrow particle size distributions, but with limited control of the average particle diameter (see table 1). However, for Ludox sol to monomer volumetric ratios of 0.5

and less, all experiments failed and led to full coagulation. This is postulated to be because, in order to get full coverage, the latex particles would have to be much larger than what would normally be generated in an emulsion system. Interestingly, in order to form a stable poly(methyl methacrylate) emulsion double the initiator concentration was needed and the system was required to be polymerised at 90 °C.

We also tried to maximize the overall solid content of our Pickering emulsion polymerisations carried out under batch conditions. We used monomer-to-water ratios of 0.14, 0.33 and 0.97 with fixed Ludox sol to monomer volumetric ratios of 1.0. Stable armoured latexes were obtained in all cases, the latter conditions reaching an overall solid content of 45 wt%. To the best of our knowledge these solid contents are not possible using normal soap-free batch processes.

In our final series we employed different monomers, ethyl methacrylate, *n*-butyl methacrylate and styrene. This was to investigate if the interfacial tension between monomer and water played a role. Reactions were performed at a monomer-to-water (v:v) ratio of 0.05, with a fixed Ludox sol to monomer volumetric ratio of 1.0. All emulsion polymerisations were successful as judged by DLS. However, FE-SEM analysis showed that, in the case of *n*-butyl methacrylate and styrene, no particles were present at the surface of the latex spheres (Figures 11a-c).

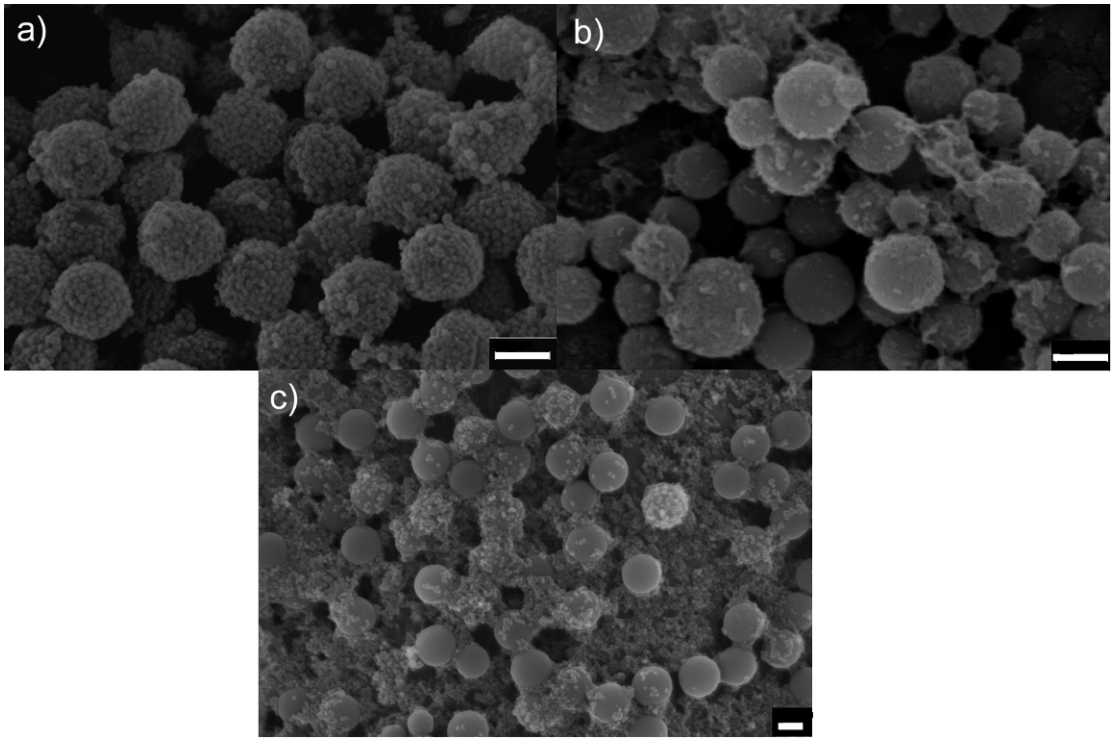


**Figure 11:** FE-SEM images of latexes generated from using a) ethyl methacrylate b) *n*-butyl methacrylate c) styrene. Scale bars are 200 nm in all cases

On the basis of our results we would like to propose the following mechanistic events for emulsion polymerisations stabilised by solid particles. When we add nanoparticles to our emulsion polymerisation system they potentially can participate in the nucleation step of the emulsion polymerisation. Growing polymer chains in the water phase can now precipitate onto a nanoparticle, under conditions whereby wetting of the nanoparticle with the polymer chain is favourable. This logically could lead to a higher number of latex particles, and thus smaller particle sizes. The second stage in emulsion polymerisation is particle growth, a process which enhances the interfacial area between latex particles and water. Growing particles need to be stabilised with sufficient surface charge or by other means, *e.g.* steric stabilisation, in

order to prevent coagulation. In the case of our solids-stabilised emulsion polymerisations the nanoparticles play a crucial role. We suggest that when a latex particle grows and thus increases its interfacial area, thereby reducing its surface charge density, it can hetero-coagulate with a nanoparticle. Upon collision, the nanoparticle adheres to the interface acting as a Pickering stabiliser and, additionally, provides extra charge to secure sufficient electrostatic repulsion between growing polymer latex particles. The latter is to avoid full coagulation of the system. The timescale of this hetero-coagulation process should be short in order to cope with expansion of the total interfacial area, which is directly linked to the overall rate of polymerisation. The following simple model estimate suggests that this timescale is of the order of ms:

Let us assume a growing latex particle with radius R does not move relative to the nanoparticles (this will underestimate the mutual diffusion coefficient and give an upper time scale for the hetero-coagulation process). Consider one of these latex particles in an infinite medium containing the nanoparticles. The initial concentration of the Ludox at the droplet is zero and in the bulk of the medium $C_0$. The rate of hetero-coagulation of particles and adhesion onto the surface of the growing latex particle of radius R is given by the Smoluchowski equation:

$$R^{het.coag.} = 4\pi RDC_0 \qquad \textbf{Equation 1}$$

The concentration of the nanoparticles can be related to their volume fraction, f, and individual spherical volume (with radius z). Using the

Stokes-Einstein equation for the diffusion coefficient of the latex particles we get:

$$R^{het.coag.} = \frac{k_B T R f}{2\pi\eta z^4} \qquad \textbf{Equation 2}$$

The number of nanoparticles needed to cover one growing latex particle can be estimated from the ratio of the surface area of the latex particle and the effective surface area covered by one nanoparticle once adhered, which is approximately $R^2/z^2$ if we assume square packing. The time needed to fully cover a growing latex particle can now be calculated from the ratio of the required number of nanoparticles and the rate of the hetero-coagulation/adhesion process. This finally results in:

$$t = \frac{2\pi\eta R z^2}{k_B T f} \rightarrow 0.191\, ms \qquad \textbf{Equation 3}$$

With the viscosity of water being *ca*. 1 mPa $s^{-1}$, the radius of a growing latex particle being 50 nm, the radius of the Ludox being 12.5 nm, the temperature being 338.15 K, and the volume fraction of Ludox in the reaction being *ca*. 5.5 vol%, this leads to a timescale in the order of 0.191 ms, which clearly is orders of magnitude faster than the overall rate of polymerisation.

In these calculations we assumed that each collision is successful. In our Pickering emulsion polymerisations the growing mature latex particles and the silica nanoparticles both have surface charges, which will lead to a repulsive interaction between the two, lowering this probability. The surface charge density of the growing particle, however, will decrease

upon its growth under our experimental conditions of low radical flux, and thus low entry rates of aqueous radical species. This will make successful collision more likely. Even if this probability of collision and adhesion of the nanoparticles onto the surface of the growing latex particles is for example only 1.0%, thereby raising the time scale to achieve full coverage to 19.1 ms in the above example, this is still orders of magnitude faster than the overall rate of polymerisation.

The calculations above imply that the nanoparticles can rearrange themselves on the interface to accommodate each new incoming nanoparticle. Whereas an individual nanoparticle adhered to the polymer/monomer-water interface is able to move on the basis of Brownian motion, it is plausible that the nanoparticles feel an attractive interaction with other nanoparticles, potentially even creating a colloidal crystal cluster. Such a cluster obviously would move much more slowly. When a nanoparticle collides with the interface of the growing latex particle at the local spot of such a cluster, it is likely that collision as a result of electrostatic and steric repulsion is unsuccessful, thereby increasing the time scale to fully cover a latex particle. Since the overall rate of polymerisation is orders of magnitude slower, this effect is not critical (and lead to coagulation) in our experiments.

This indeed shows that our suggestions are plausible. Moreover TEM analysis carried out at different times throughout our solids-stabilised emulsion polymerisation show a gradual increase in the number of

nanoparticles on the surface of growing latex particles, in support of our theory (Figure 12).

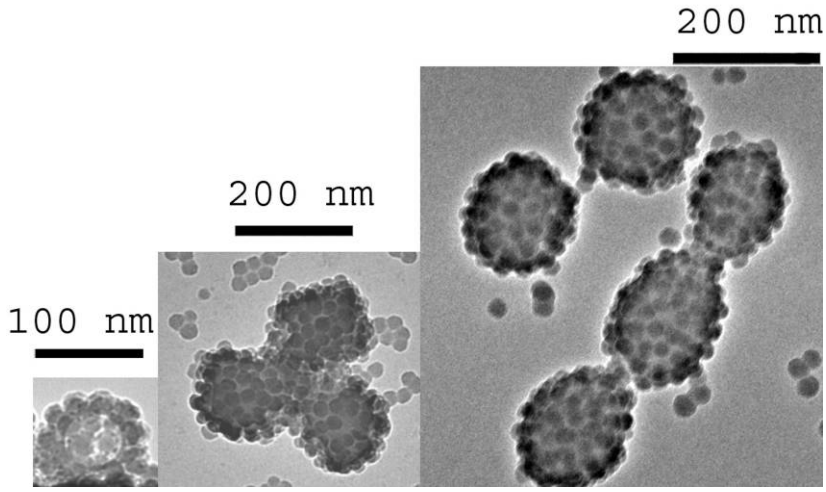


**Figure 12:** TEM pictures of a methyl methacrylate Pickering emulsion polymerisation taken from different time intervals of the reaction (20, 45, 85 min from left to right)

The elegance of our solids-stabilised emulsion polymerisation formulation provides opportunity for a straightforward second step extension that allows the fabrication of multi-layered core-shell nanocomposite polymer latex particles. We used our stable silica nanoparticle-armoured poly(methyl methacrylate) latexes as a seed and carried out a conventional monomer starved-fed emulsion polymerisation, now in presence of sodium dodecyl sulfate as surfactant. For the outer polymeric shell we used acrylonitrile, ethyl methacrylate and *n*-butyl acrylate as monomers. Seeded emulsion polymerisation of acrylonitrile afforded composite multi-layered latex particles of complex "hairy" morphology, as polyacrylonitrile is semi-crystalline (See Figure 13).

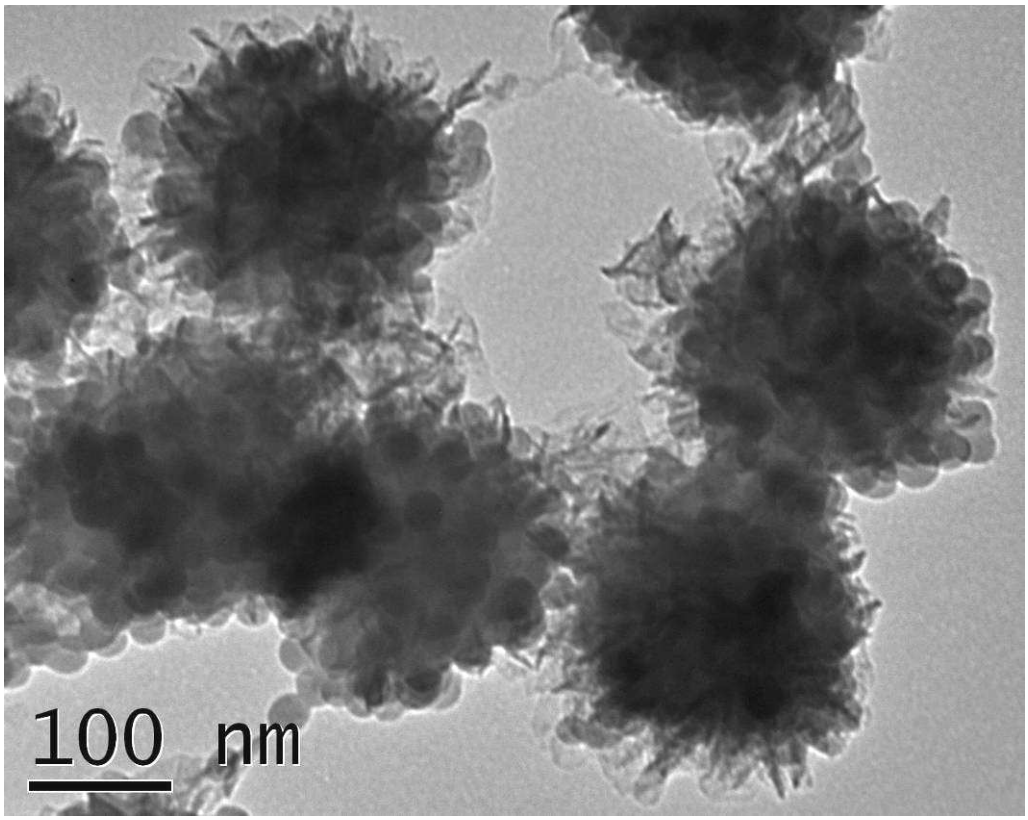


**Figure 13:** TEM image of poly(methyl methacrylate)-armoured latex particle with a crystalline polyacrylonitrile shell

Use of ethyl methacrylate provided multi-layered nanocomposite colloids with a hard outer polymeric shell and encapsulation of the silica nanoparticles. Use of *n*-butyl acrylate created a soft outer shell. Intriguingly, slow migration of the nanoparticles through the soft polymer matrix to the outer surface occurred, minimising overall surface energy and potentially gaining entropy,[31] spacing them further apart (Figure 14).

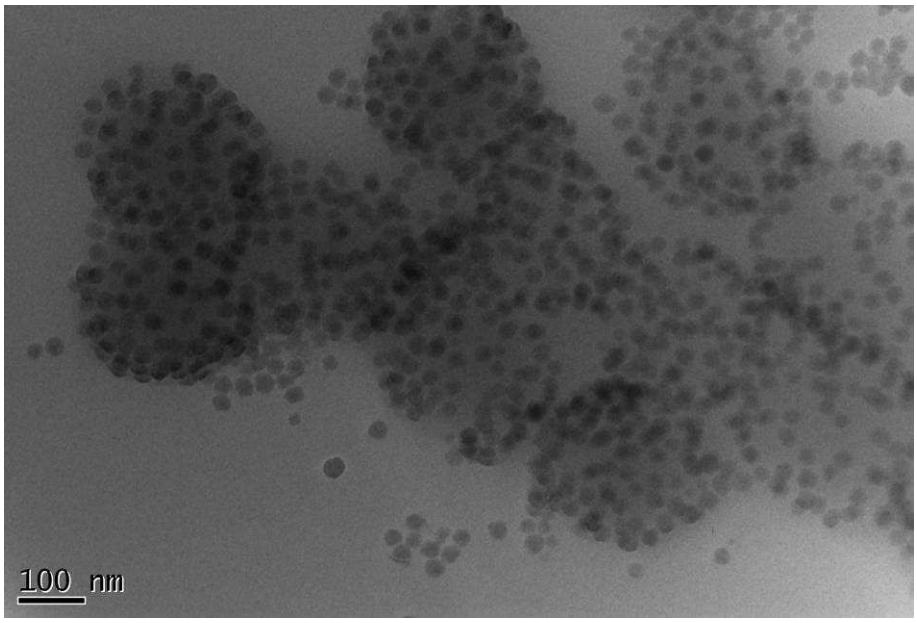


**Figure 14:** TEM image of poly(methyl methacrylate) armoured latex particles with a shell of poly(*n*-butyl acrylate)

The same experiment was repeated using ethyl methacrylate as monomer. The TEM images of the resulting core-shell emulsion shows less migration of Ludox yet retains the film formation properties. This is possibly due to the fact ethyl methacrylate is more polar. This means the Ludox is more stable so less entropy is gained by its migration.

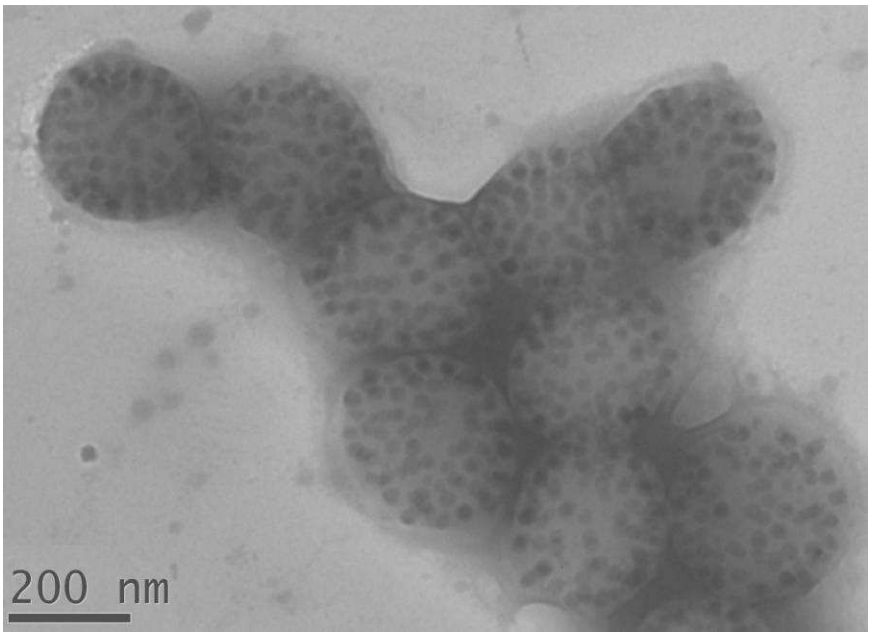


**Figure 15:** TEM image showing poly(methyl methacrylate) armoured Latex particles with a shell of poly(ethyl methacrylate).

## *Conclusion*

In conclusion, we demonstrate a versatile emulsion polymerisation process in which solid nanoparticles are used as stabiliser, thereby replacing the role of surfactants, allowing the simple fabrication of armoured nanocomposite polymer latexes. Use of a second conventional seeded emulsion polymerisation step provided a straightforward route to more complex multi-layered nanocomposite polymer colloids.

## *Methodology*

**Apparatus:**

Dynamic light scattering measurements were performed on a Malvern Zetasizer 3000HSA at 25 °C. Average particle sizes and polydispersities were determined using a Contin algorithm on the acquired data and were

averaged over 4 runs of each 10 subruns. Sonication was performed using a Branson digital 450W sonifier. Zeta potential measurements were carried out using a Malvern Zetasizer 3000HSA instrument. pH measurements were performed using a Knick pH meter 765 calimetic. FE-SEM analysis, was performed on a Zeiss Supra 55-VP instrument. Prior to FE-SEM analysis samples were sputter coated with AuPd for 45 seconds at 1.5 kV and 20 mA using a Quorum technologies Polaron SC7640 auto/manual high resolution sputter coater. TEM analyses were carried out on a JEOL 1200EX TEM, JEM2011 FasTEM LaB6 and a JEOL2000fx TEM.

**Typical Pickering Emulsion Polymerisation Procedure (I):**

A 40 wt% aqueous sol of Ludox silica nanoparticles (12.0 mL) was added to deoxygenated water (88.0 mL). The pH of the sol was reduced to pH 5.5 using dropwise addition of HCl (aq) solution. This was transferred to a 250 mL double-walled glass reactor. To this MMA (12.0 mL, 9 wt% monomer, 18 wt% total solids) was added. The mixture was then placed under a nitrogen gas inert atmosphere by bubbling through with nitrogen gas for 20 min whilst stirring, after which the system was kept under a slight overpressure of nitrogen gas. Next the mixture was heated to 65 °C and stirred at a rate such that the vortex of monomer touched the paddles of the stirrer. KPS (0.05 g) dissolved in water (1.0 mL) was injected into the system to start the polymerisation. The reaction was allowed to reach full conversion overnight at 65 °C.

**Typical Recipe for the preparation of multi-layered nanocomposite latex particles using (I) as seed:**

Armoured polymer latex prepared via Pickering emulsion polymerisation was diluted with water to reach an overall solids content of 9 wt%. The diluted latex (typically 100 mL) was transferred into a 250 mL round-bottomed flask. The seed latex was then placed under a nitrogen inert atmosphere by bubbling through with nitrogen for 20 min whilst stirring, after which the system was kept under a slight overpressure of nitrogen gas. Next, SDS (0.15 g) together with KPS (0.05 g) was dissolved in 5.0 mL of water and added to the system. The reaction mixture was heated to 65 °C whilst stirring gently with a magnetic stirrer bar. The second monomer of choice, *i.e.* EMA, BA, or ACN, (4.5 mL) was added by syringe pump at a rate of 0.7 mL/h. The polymerisation was allowed to continue to reach full conversion overnight at 65 °C.

## Raw Data

**Table 1:** Experimental data and results

| Exp No. | M:W (v:v)/ - | L:M (v:v)/ - | Particle diameter (DLS)/ nm[#] | Polydispersity Index (DLS)/ - |
|---|---|---|---|---|
| **1) pH** | | | | |
| pH = 3.0 | 0.13 | 0.83 | 1010 | 0.440 |
| pH = 10.0 | 0.13 | 0.83 | - | - |
| pH = 5.5 | 0.13 | 0.83 | 323 | 0.062 |
| **2) Monomer** | | | | |
| styrene | 0.05 | 1.00 | 394 | 0.017 |
| ethyl methacrylate | 0.05 | 1.00 | 284 | 0.056 |
| *n*-butyl methacrylate | 0.05 | 1.00 | 413 | 0.054 |
| **3)Ludox concentration*** | | | | |
| 3.1 | 0.13 | 0.67 | 321 | 0.019 |
| 3.2 | 0.13 | 0.67 | 315 | 0.017 |
| 3.3 | 0.13 | 0.83 | 342 | 0.074 |
| 3.4 | 0.14 | 1.00 | 284 | 0.024 |
| 3.5 | 0.14 | 1.00 | 283 | 0.016 |
| 3.6 | 0.14 | 1.25 | 278 | 0.013 |
| **4) Solids content** | | | | |
| 4.1 | 0.33 | 1.00 | 315 | 0.017 |
| 4.2 | 0.97 | 0.93 | 454 | 0.067 |

Note: monomer (M), water (W), ludox sol (L)

[#]Diameters are an average taken from the $Z_{ave}$ of 4 runs, each consisting of 10 sub runs

*The repeated experiments in section 3 show the reproducibility of the method.

(1) Feeney, P. J.; Napper, D. H.; Gilbert, R. G. *Macromolecules* **1987**, *20*, 2922-2930.
(2) Feeney, P. J.; Napper, D. H.; Gilbert, R. G. *Macromolecules* **1984**, *17*, 2520-9.
(3) Smith, W. V.; Ewart, R. H. *J. Chem. Phys.* **1948**, *16*, 592-9.
(4) Harkins, W. D. *J. Am. Chem. Soc.* **1947**, *69*, 1428-1444.
(5) Hergeth, W. D.; Schmutzler, K.; Wartewig, S. *Makromol. Chem., Macromol. Symp.* **1990**, *31*, 123-42.
(6) McDonald Charles, J.; Devon Michael, J. *Adv. Colloid Interface Sci.* **2002**, *99*, 181-213.
(7) Mock, E. B.; Bruyn, H. D.; Hawkett, B. S.; Gilbert, R. G.; Zukoski, C. F. *Langmuir* **2006**, *22*, 4037-4043.
(8) Okubo, M.; Ichikawa, K.; Tsujihiro, M.; He, J. *Colloid Polym. Sci.* **1990**, *268*, 791-796.
(9) Kietzke, T.; Neher, D.; Landfester, K.; Montenegro, R.; Guentner, R.; Scherf, U. *Nature Materials* **2003**, *2*, 408-412.
(10) Pommersheim, R.; Schrezenmeir, J.; Vogt, W. *Macromol. Chem. Phys.* **1994**, *195*, 1557-67.
(11) Caruso, F.; Caruso, R. A.; Moehwald, H. *Science* **1998**, *282*, 1111-1114.
(12) Vincent, B.; Young, C. A.; Tadros, T. F. *J. Chem. Soc., Faraday Trans. 1* **1980**, *76*, 665-73.
(13) Schmid, A.; Fujii, S.; Armes, S. P.; Leite, C. A. P.; Galembeck, F.; Minami, H.; Saito, N.; Okubo, M. *Chem. Mater.* **2007**, *19*, 2435-2445.
(14) Schmid, A.; Tonnar, J.; Armes, S. P. *Adv. Mater.* **2008**, *20*, 3331-3336.
(15) Sacanna, S.; Kegel, W. K.; Philipse, A. P. *Phys. Rev. Lett.* **2007**, *98*, 158301-158304.
(16) Sacanna, S.; Philipse, A. P. *Adv. Mater.* **2007**, *19*, 3824-3826.
(17) Walther, A.; Hoffmann, M.; Muller Axel, H. E. *Angew Chem Int Ed Engl* **2008**, *47*, 711-4.
(18) Subramaniam, A. B.; Mejean, C.; Abkarian, M.; Stone, H. A. *Langmuir* **2006**, *22*, 5986-5990.
(19) Capovilla, L.; Labbe, P.; Reverdy, G. *Langmuir* **1991**, *7*, 2000-3.
(20) Labbe, P.; Reverdy, G. *Langmuir* **1988**, *4*, 419-25.
(21) Zhang, S.; Lan, Q.; Liu, Q.; Xu, J.; Sun, D. *Colloids Surf. Physicochem. Eng. Aspects* **2008**, *317*, 406-413.
(22) Bon, S. A. F.; Colver, P. J. *Langmuir* **2007**, *23*, 8316-8322.
(23) Zhang, J.; Chen, K.; Zhao, H. *J. Polym. Sci., Part A: Polym. Chem.* **2008**, *46*, 2632-2639.
(24) S. Fortuna, C. A. L. C., A. Troisi, S.A.F. Bon **submitted**.
(25) Beylerian, N. M.; Vardanyan, L. R.; Harutyunyan, R. S.; Vardanyan, R. L. *Macromol. Chem. Phys.* **2002**, *203*, 212-218.
(26) Palme, H. *Zeitschrift fuer Anorganische und Allgemeine Chemie* **1920**, *112*, 97-130.
(27) Kolthoff, I. M.; Miller, I. K. *J. Am. Chem. Soc.* **1951**, *73*, 3055-9.
(28) Chavez-Paez, M.; Gonzalez-Mozuelos, P.; Medina-Noyola, M.; Mendez-Alcaraz, J. M. *Physica A* **2004**, *341*, 1-22.
(29) Tohver, V.; Smay, J. E.; Braem, A.; Braun, P. V.; Lewis, J. A. *PNAS* **2001**, *98*, 8950-8954.
(30) Karanikas, S.; Louis, A. A. *Phys. Rev. Lett.* **2004**, *93*, 248303.
(31) Gupta, S.; Zhang, Q.; Emrick, T.; Balazs, A. C.; Russell, T. P. *Nat. Mater.* **2006**, *5*, 229-233.

# *Chapter 6: Material Properties of Laponite Armoured Latex Particles*

It is known that fillers can improve the properties of polymer materials. A composite is a material where inorganic particles are added to an organic substrate in order to bestow some of their favourable properties upon the mixture. These improvements are usually created because the hard inorganic component can prevent crack propagation and hinders movement of polymer chains during forced rearrangement.[1] Polymer composite materials have been made for many years by adding materials such as talc, carbon black, and glass fibres. Usually advantageous properties can only be achieved with high loadings of filler (generally between 20 and 40 wt%).[2] This however suppresses other useful properties of the substrate material *i.e.* malleability and shock resistance.

When nanoparticles are used as a filler, one speaks of a nanocomposite, or originally a hybrid material.[2] These can be superior to normal composites. Typically less filler is needed to bestow the same improved properties (typically 2-6 wt%) as the surface area to weight ratio is far higher (this can only be achieved if full dispersion of the nanoparticles can be achieved). The need for smaller quantities of filler allows fabrication of materials which are lighter in weight at a cheaper cost, and also retention of the polymer's favourable properties can be achieved.[1] The use of nano-sized fillers was first proposed by Takayanagi *et al.* who created a hybrid material of nylon and aramide fibres of 30 nm.[3] This idea

was first made into an industrially used material by the Toyota Central Research and Development Laboratories Inc. in 1986 when they made a Nylon6-clay hybrid which showed remarkable properties:[4] It's tensile strength was increased by 55%, the tensile modulus by 91% and the heat distortion temperature increased by 134% relative to pristine Nylon. This material is now used in most automotive plastics.[4]

Blumstein was the first to show that clays can modify polymer properties.[5] However many other papers have been publish on this subject since. Superior properties include; improved modulus and strength, reduced gas permeation and better barrier properties.[1,2,6,7] Most composites rely on dispersing the inorganic particles inside the polymer matrix to ensure maximum surface contact. Our Pickering (mini)emulsion polymerisation techniques deliver armoured structures which potentially should show different physical and mechanical behaviour to traditionally blended nanocomposite materials. We therefore would like to investigate the influence of armoured structures on material properties. Some work in this area has been already undertaken. For example, Bourgeat-Lami *et al.* looked at the mechanical and thermal properties of poly(styrene-co-butyl acrylate) Laponite latexes.[8]

## *Heat resistance*

Clay is known to impart increased thermal stability and decreased flammability to polymers.[9] The later effect is because the clay promotes

char formation and this char layer prevents heat transfer to the polymer and also prevents gas exchange.[6] The thermal stability is thought to arise from a decrease in thermal motion of the polymer chains when in contact with clay,[5] or from the inhibition of flow of volatile degradation products.[10] The heat transfer resistance due to charring is important when open flames are used. However, for just thermal stability, the stabilising effect is due to the inhibition of mass transfer due to the barrier of clay and the decreased thermal motion. It is known that, during heat treatment of clay nano-composites, clay migrates to the surface of a film to form a protective barrier.[11] However, in our system all latex particles have this barrier already in place. Because of this, it was decided to analyse some of our armoured latex via TGA (thermal gravimetric analysis). Different composite polystyrene latexes of varying sizes were analysed, as well as normal soap free polystyrene latex particles prepared with no clay and with added clay in the proportions present in our Pickering systems. The samples chosen for the composites all contained 0.5 g of clay but used different amounts of styrene as monomer (having clay wt% wrt. to polymer of 4.8, 6.4, 9.1 and 16.6). Polystyrene latex and Laponite clay colloidal blends were made by mixing polystyrene latexes made via soap-free emulsion polymerisation with clay to give approximate comparisons with the 4.8 wt% and 9.1 wt% formulations. The program used for the TGA experiments was to first hold at 100 °C for 10 minutes in order to drive off any water, then the sample was heated to

800 °C at a rate of 5 °C min-1. The following temperature versus weight traces were obtained:

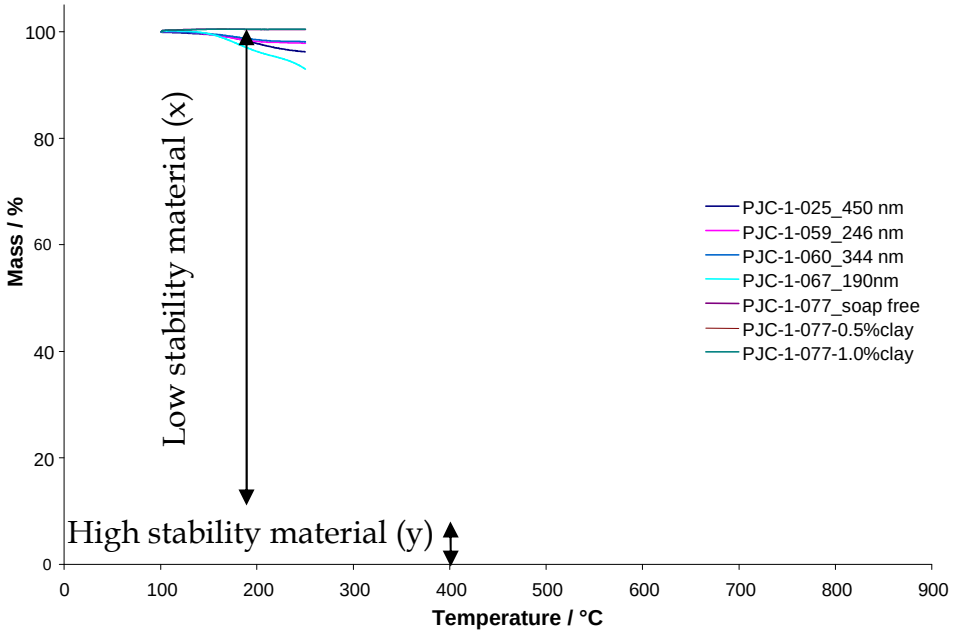


**Figure 1:** Thermal gravimetric analysis curves obtained for the 7 samples analysed. The graph has been normalised by removing the mass of left over material, in order to make comparisons easier.

This figure shows a few very intriguing points. Firstly and very interestingly a larger amount of material that degrades at a higher temperature at higher clay loadings. This must be polymer, not clay as in the blend system there is only a small amount of this thermally stable material. Since this material is not clay, the only other factor that changes between the samples is the particle size. It is hypothesised that this more stable polymer is in contact with the clay on the interface, as the smaller the particle, the high the surface area to volume ratio. (As stated previously, adding more clay to the miniemulsion system decreases the final latex particle size). This can be examined further by comparing the amount of high stability material to the surface area to volume ratio of

the latex particles. The ratio of high stability material can be calculated by dividing the percentage of material left (the plateau after the main polymer decomposition) by 100, minus this percentage (ratio = % at plateau / 100 - % at plateau). The surface area to volume ratios were calculated from the particle sizes given by DLS. The results are plotted in Figure 2.

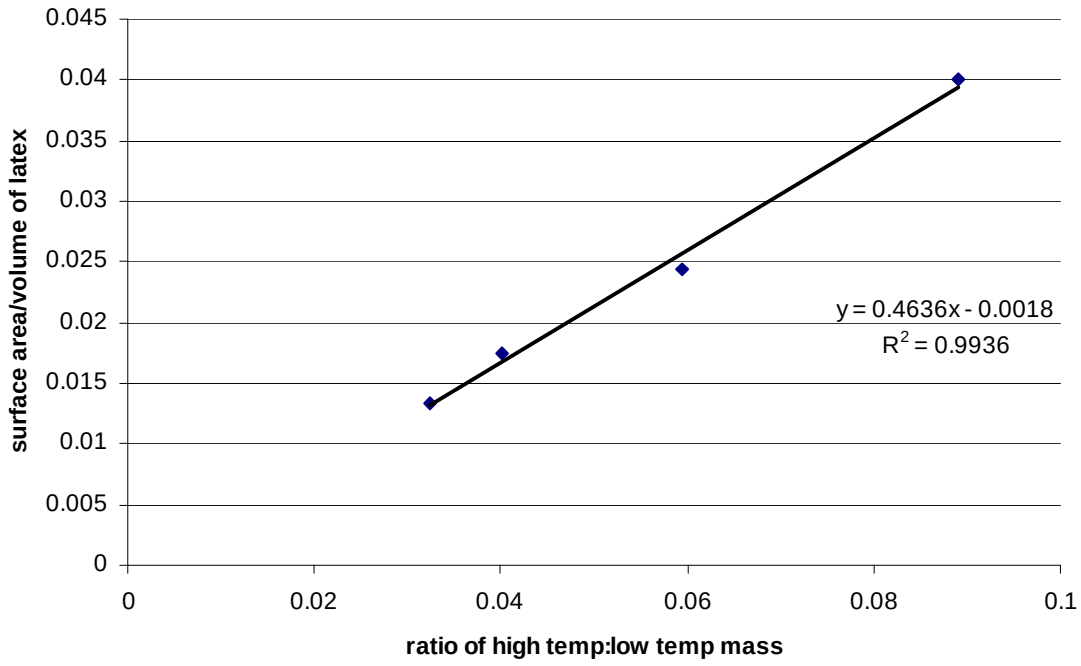


**Figure 2:** Correlation between the proportions of high stability material relative to the amount of polymer in contact with clay

The best fit equation is linear with a near zero intercept. This is logical, as for an infinitely large sphere there can be no contact of clay to the polymer, so there will be no high stability material. Also the $R^2$ value is almost 1 meaning our assumption that the amount of stable material is due to its contact with clay is strengthened. For the soap-free system with blended-in clay, there is only a sparse amount of stable material at elevated temperatures. If the latex particles were very large, this would

mean there is no increase in stability using our Pickering system. However, the particle size in our soap-free emulsion polymerisation is 158 nm, which is even smaller than the smallest armoured structure. This implies that by creating our armoured structures via a Pickering route we get better thermal stability than by just blending. If we continue with the assumption that the high stability material is in contact with clay, one can calculate the thickness of the polymer that is affected.

This can be done by comparing the ratio of different temperature material to the ratio of the volume of a hollow sphere of diameter "x" to that of a whole one with known diameter "z". Diameter x can be calculated back from the area of the smaller sphere, which can be found by multiplying the percentage of low temperature material by the volume of the whole latex particle. The thickness of the high temperature layer (y) is then found by subtracting x from the original radius z.

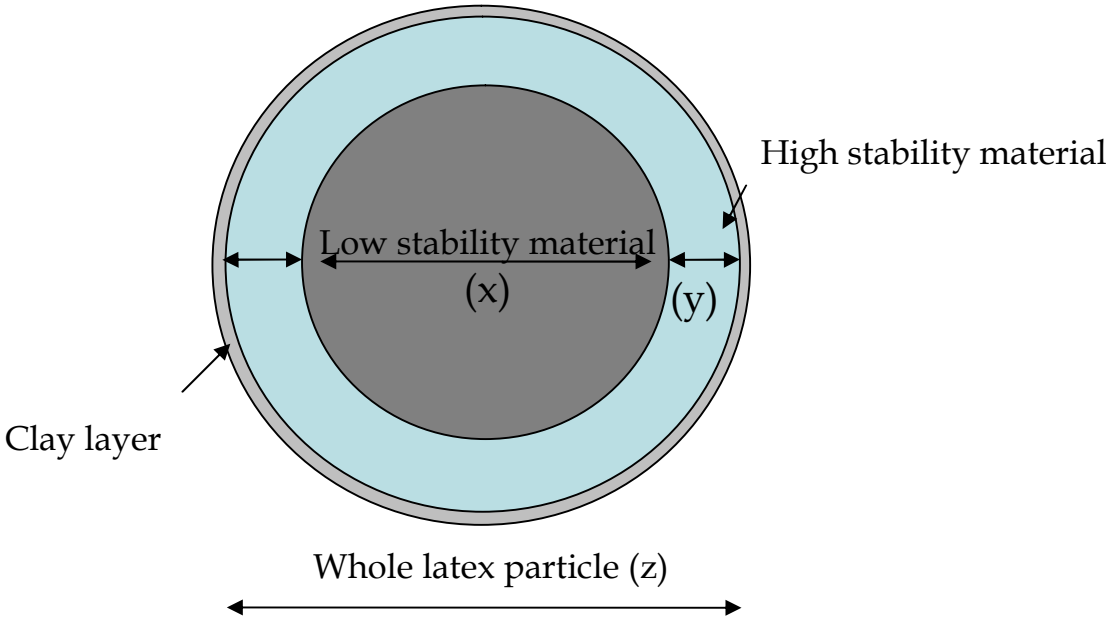


**Figure 3:** Schematic illustration of the theoretical volumes taken up by the high and low temperature material

By doing this we get a ring of polymer, surrounded by clay, of thickness between 6.3-6.6 nm. This is smaller than the radius of gyration (the effective volume taken up by the polymer chain) of polystyrene in polystyrene melt for a sensible molecular weight range (80 Å for 152K $M_w$).[12,13] This implies that the polymer chains are attracted to the clay and are pulled flatter against it.

The second observation that can be made from the TGA data is that the period of time needed to degrade the main bulk of the polymer is much longer for samples containing more clay. This can clearly be seen as the gradient of the TGA trace becomes smaller on addition of more clay. The longer time frame is probably due to the clay acting as a barrier to the

removal of the volatile products. The clay forces these products to take a lot longer to leave the film, creating this extended time frame.

The final observation is that the onset temperature of decomposition is much lower for the polymer in all the clay systems. This is unexpected, but has been reported once before in work by Bourgeat-Lami and co-workers, who commented on the TGA traces from their low $T_g$ Laponite latexes.[8] The onset of degradation was actually earlier for the composites, yet the overall temperature of degradation was higher; no other work has reported this. We originally thought this might be due to the thermal conductivity difference between clay and polystyrene (polystyrene *ca.* 0.18 $Wm^{-1}K^{-1}$,[14] clay *ca.* 0.25 $Wm^{-1}K^{-1}$)[26] . However due to the slow heat ramping and the large temperature difference this is unlikely. Another explanation could be that silica/metal oxide materials are used in the catalytic cracking of hydrocarbons.[15] This cracking would create a layer of coke over the Laponite. It could be this coke material that exhibits high stability to degradation. The amount of coke is easily calculated by looking at the percentage of material left over and subtracting the percentage of clay added. One can then plot this percentage of material against the surface area to volume ratio calculated earlier.

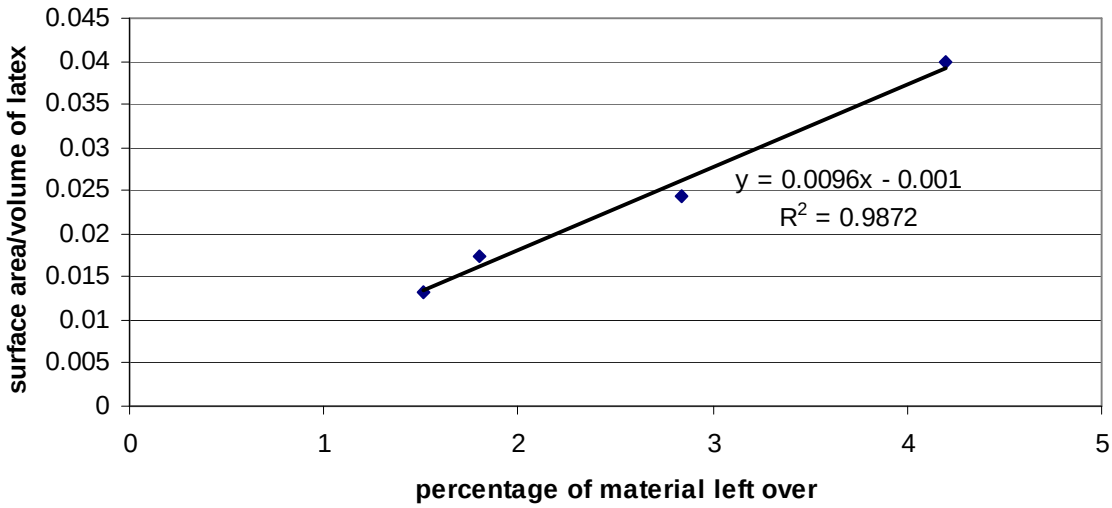


**Figure 4:** Correlation between the percentage of coke deposits and the surface area to volume ratio of the latex particles

This clearly shows there is also a linear correlation between the coke deposits and clay contact area with the polymer. We believe that the Laponite acts as a cracking catalyst for the degradation of the polystyrene, giving a lower onset temperature. Due to this cracking, a coke layer is formed around the Laponite (the high temperature material shown in Figure 3). This coke layer prevents the evolution of gaseous material, slowing down the weight loss, and therefore extending the whole degradation time frame. At the end of the TGA run a porous honeycomb of Laponite with a thin layer of coke around it is formed. This formed material could have uses as a flame retardant coating due to its porous nature and high thermal stability.

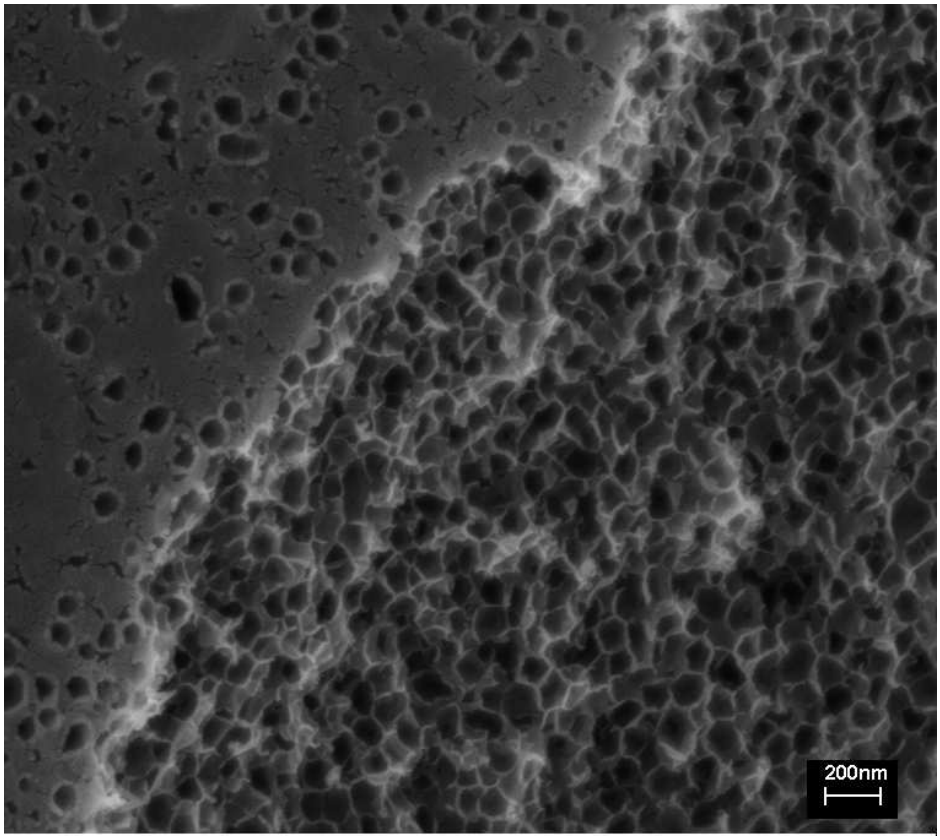


**Figure 5:** Figure showing a cross-section of the honeycomb material created by heating a film of our smallest clay-armoured latex particles at 600 °C for several hours

## *Tacisity in Pressure Sensitive Adhesives.*

Recent work by Keddie *et al.* has shown that by adding small quantities of filler (in this case carbon nanotubes) can greatly increase the effectiveness of pressure sensitive adhesives (PSAs).[16] It was decided to test our composites for use in PSAs to see if we could achieve similar success.

A PSA is a substance that will instantly adhere to almost any surface without the use of covalent bonding or activation.[17] A good PSA will stick very strongly to a substrate and a probe, but will leave nothing behind on the probe when it is removed. The PSA should also dissipate a lot of energy via deformation. To do this effectively, the material must be

neither too liquid nor too stiff. Figure 5 shows the process the PSA undergoes during probe removal.

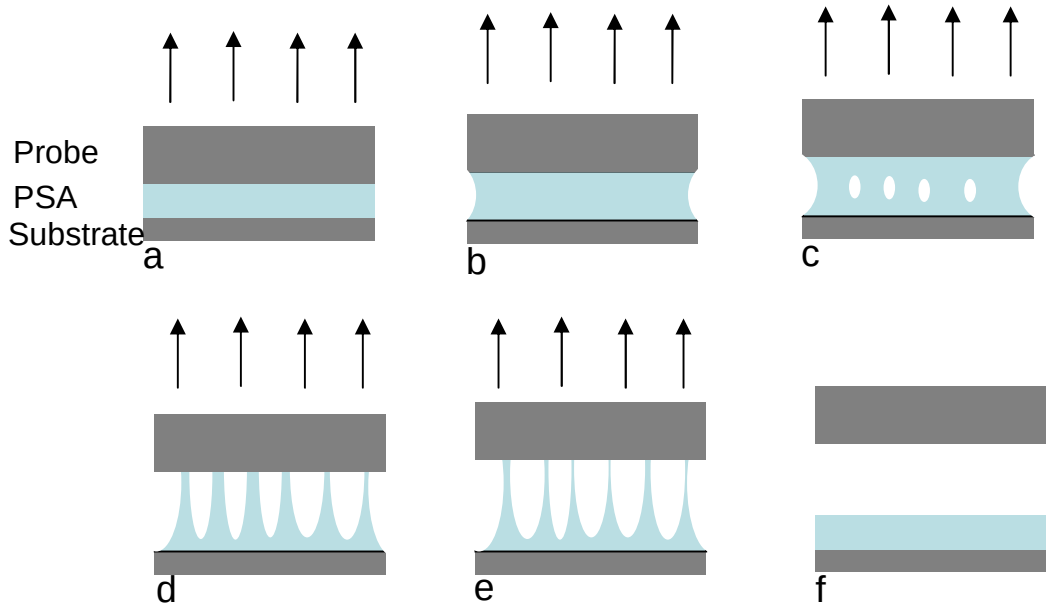


**Figure 6:** Summary of the processes involved in a PSA when an adherent is removed from the surface. a through to f show increasing distance of the probe from the substrate.

Figure 6a shows both surfaces coming into contact with the PSA and the top surface being slowly withdrawn. 6b shows the PSA being stretched upwards and deforming slightly to accommodate the larger volume created. At greater seoaration distances the PSA can no longer stretch to fill the increased volume (critical stress, $\sigma_o$, is achieved), so cavity nucleation occurs, see 6c.[18,19] These cavities expand laterally and vertically until fibrils are generated in 6d. The fibrils can be stretched until a given extension ($\varepsilon_f$) is reached, giving a plateau where the fibrils become so thin that they can no longer adhere to the top substrate and either detach or break.[20,21] The PSA will then deform back into its original shape (6f). An ideal PSA will allow a long extension of the fibrils, yet the fibrils need to be resilient in order to dissipate the energy. If the PSA is

too stiff there will be no fibril formation, but if the PSA is too liquid-like the fibrils will be too weak to hold the two surfaces together. The energy involved in cavity formation and fibril extension contributes to the overall energy of adhesion $E_a$.[22] Keddie *et al.* showed that by adding SWNT to their PSA matrix, the PSA became stiffer yet could dissipate energy better at the same time, which both contribute to an increase in $E_a$. Li *et al.* published some interesting work on the use of montmorillonite as a filler in acrylate PSAs.[7] Their results however showed that clay, while increasing the shear strength of the polymer, greatly reduced the $E_a$.

An elegant way of measuring $E_a$ and therefore adhesive performance of a PSA is via probe-tack experiments, where the energy of removing a probe from a surface is measured by recording the force pulling back on the probe as it is removed at a constant rate from the PSA.[22,23] A graph is then generated of stress versus strain. Stress and strain are size-independent measurements of force and distance respectively. The area under the curve is $E_a$. Another experiment that can be performed on a film to test its potential as a PSA is Dynamic Mechanical Analysis. This technique gives two values: tan δ and storage modulus. Tan δ represents the time needed for the material to reach its maximum extension (strain) after the maximum force (stress) has been applied. This gives an indication of the energy dissipation potential of the material. The storage modulus of a material represents how far it will stretch with a certain force; this therefore gives an idea of the stiffness. A good PSA will have a high tan δ,

modulus and $E_a$; however, most fillers that increase the stiffness of a material also cause a decrease in $E_a$. This is usually because the created fibrils break earlier during extension or have insufficient wettability for the adherent.

To test whether our composites might make a good PSA, both probe-tack and DMA measurements were performed. The composite we chose for the experiments was the poly(lauryl acrylate) armoured latex created previously, as this is a hydrophobic low Tg polymer. A more hydrophobic monomer was used as these give better results for the miniemulsion preparation, as mentioned previously. This composite was blended with a high solids PBA latex (the same latex used in Keddie's previous work) at different concentrations. Our composite was blended into the pure latex for two reasons. Firstly a high solids latex is needed to create coherent films and secondly a pure composite contains too much free clay, which forms a barrier on the surface of the film thus preventing adhesion to the probes surface. To test that our results are due to the composite, rather than the addition of PLA or free clay, experiments were also performed using just a colloidal mixture of clay and the PBA latex, as well as a latex blend of PBA and various quantities of PLA latex made via traditional soap containing miniemulsion polymerisation.

Firstly we shall look at just adding Laponite to our system at low concentrations. Our results showed that at very small quantities of Laponite the adhesive properties of PBA increased (*i.e.* the maximum

strain, $\varepsilon_f$, is larger, giving a higher $E_a$), but when larger quantities were used $\varepsilon_f$ actually becomes lower than normal. Figure 7 shows that the maximum $\varepsilon_f$ is achieved using 0.15 wt% of Laponite. This Figure also shows that the stress plateau also becomes higher, which also contributes to the higher $E_a$. Also shown is the reduction in the adhesive properties when large wt% of clay are used. However, the higher plateau level still remains, even though $\varepsilon_f$ is reduced. These data suggest that the clay enhances the stiffness of our PSA, but too much clay causes the stiffness to increase above a critical value, whereby the fibres detach from the probe instead of being extended. These results agree to some extent with the paper by Li and co-workers,[7] as the stiffness does increase, however, contrary to their data, our results show some improvements to the PSA properties. This disagreement may be because Li *et al.* used large quantities of clay, meaning that possible improvements at low concentrations were not examined, or possibly the size difference of the two clays has an additional effect (montmorillonite being *ca.* 1 μm by 1 nm and laponite being *ca.* 25 nm by 1 nm).

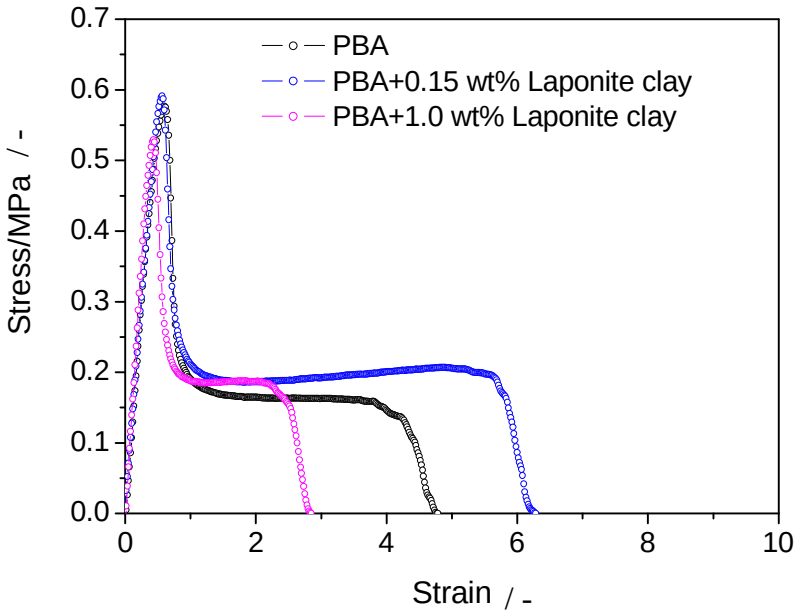


**Figure 7**: Adhesion stress-strain curves of PBA physically blended with Laponite. An example showing the adhesive improvement at Laponite concentration of 0.15 % (maximum achieved) and a reduction in performance at high Laponite content (1.0 %) are shown here.

The next experiment performed was the probe-tack analysis of PBA-PLA blended films. Figure 8 shows that, at low PLA loading, the PSA properties are virtually unchanged. However, when higher loadings are used, a marked improvement is observed. This shows that PLA is a better polymer for use in PSAs. However, if a specific polymer is needed for chemical or biological reasons, the fact that large quantities are needed for an improvement to be observed makes the addition of PLA less attractive as a filler.

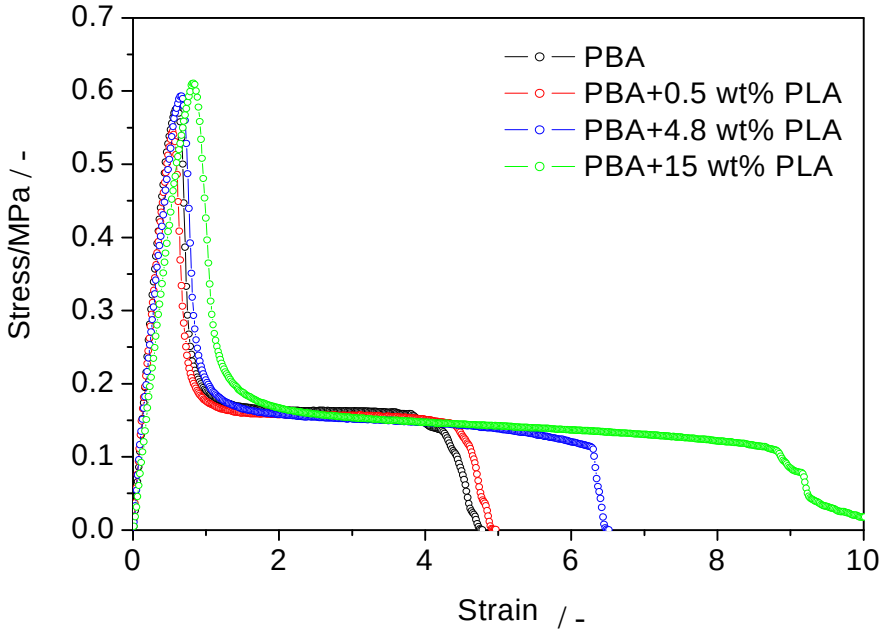


**Figure 8:** Adhesion stress-strain curves of PBA physically blended with PLA. No improvement at low PLA content, but better adhesion at high PLA content

Logically the next analysis to perform was probe-tack experiments using our composite material. Figure 9 shows some remarkable results. By only adding very small quantities of our composite, a large increase in the adhesion energy is observed (approximately 75 %). However, on addition of more that 2.7 wt% $E_a$ began to fall back to normal values.

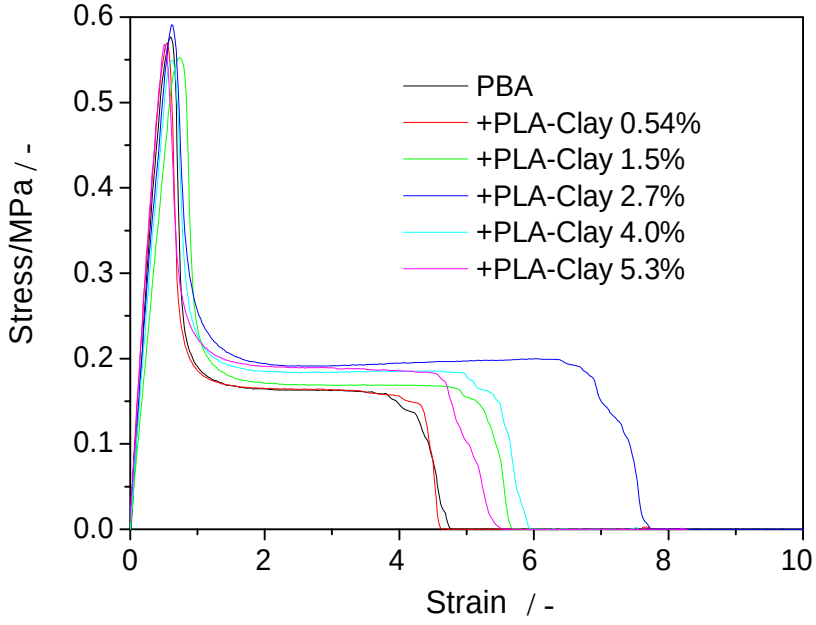


**Figure 9:** Adhesion stress-strain curves of PBA/PLA-Clay nanocomposite.

In order to understand what is going on, and to judge if the increase in adhesion energy is due to the composite or just the separate materials, the increase in adhesion energies for all experiments were plotted together. For easy comparison the wt% of clay was plotted on a different axis and normalised to correspond to the amount of clay in the composite system. Figure  shows that, for small amounts of filler (below 6 wt%), the composite gives a much larger increase in adhesion energy. Inspecting Figure 10, it can be seen that, in the systems that are not composites, there is little or no increase in $E_a$. This implies that some difference in the composite system causes this increase, rather than just a mixing of the two separate components.

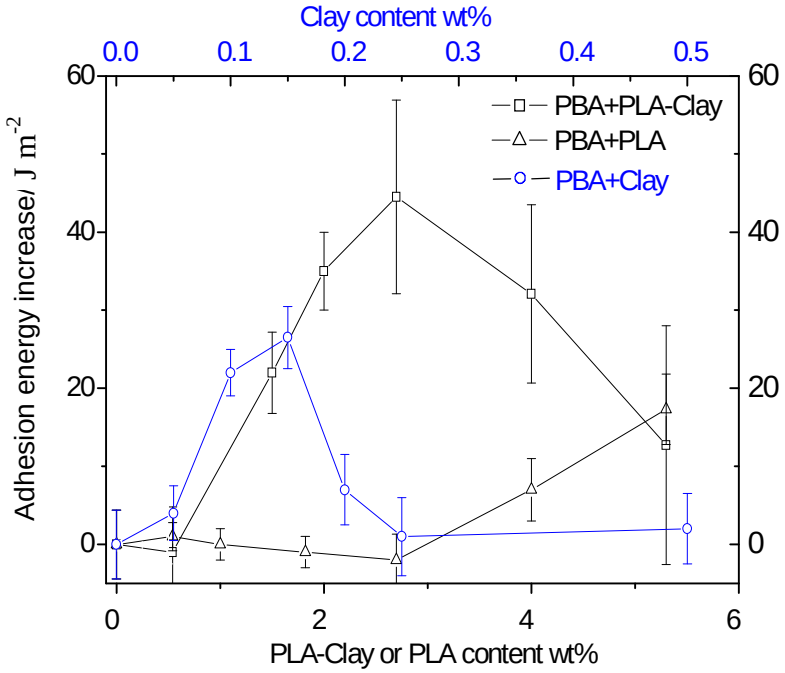


**Figure 10:** The synergy effect of armoured soft hybrid particles on adhesion energies of nanocomposite adhesives.

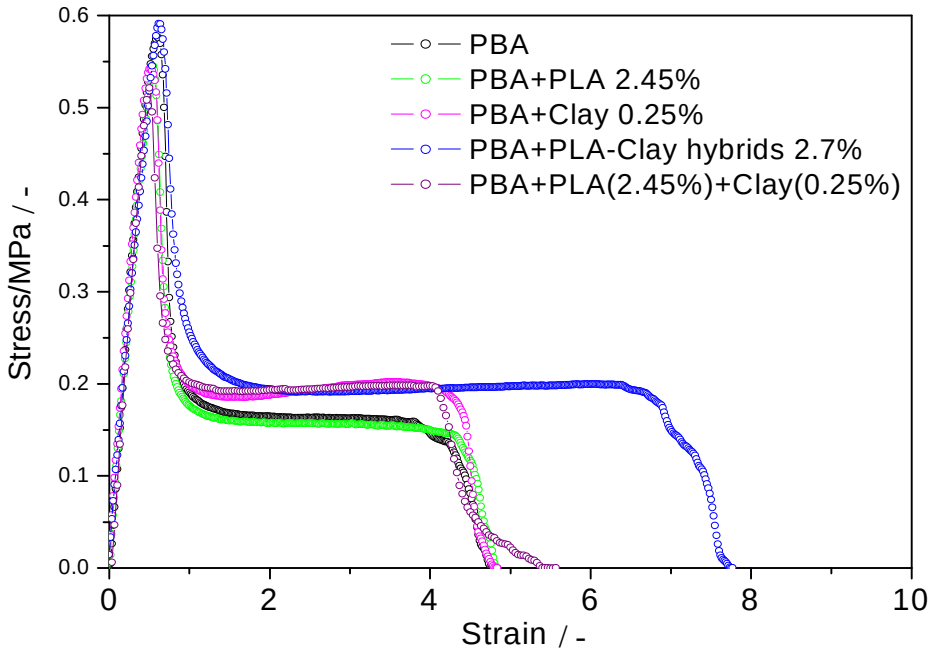


**Figure 11:** Adhesion stress-train curve comparison of PBA, PBA/PLA, PBA/clay, PBA/PLA + free clay and PBA/PLA-clay nanocomposite with the same amount of PLA (2.45 %) or clay content (0.25 %) as in PBA/PLA-clay nanocomposite.

To gain a better understanding of why our nanocomposite has better adhesive properties, we performed dynamic material analysis on our Laponite dispersion, composite and pure PBA films.

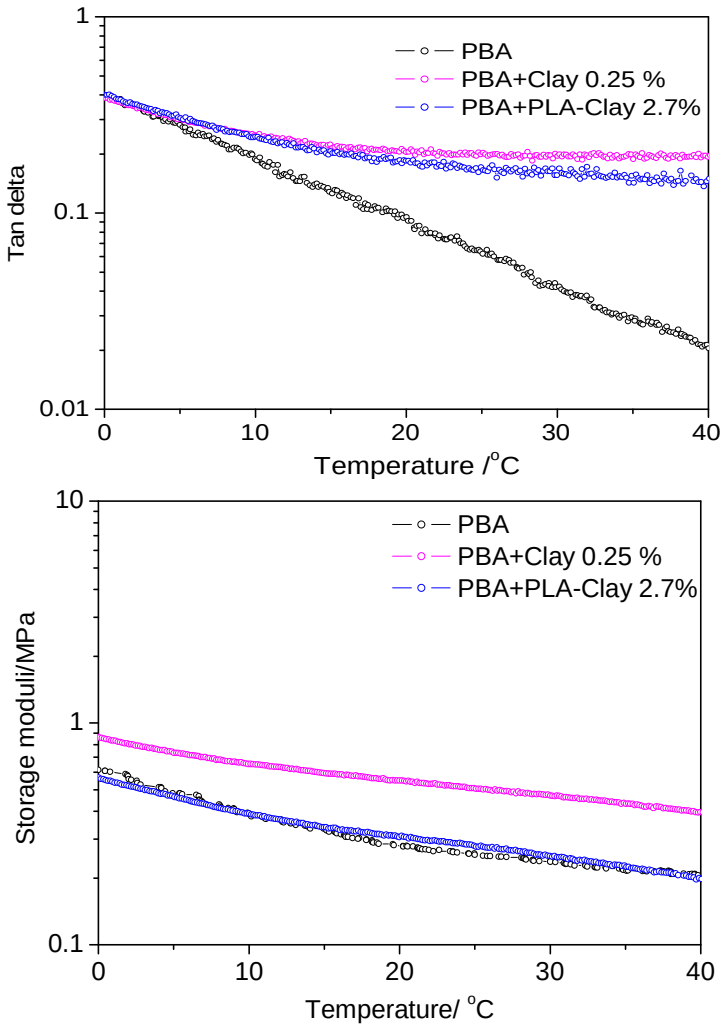


**Figure 12:** Dynamic mechanical analysis of PBA, PBA/Clay (with the same amount of clay, 0.25 %, as in PBA/Clay nanocomposite) and PBA/PLA-Clay nanocomposite.

Theses two graphs show very interesting results. Firstly, both the free clay and the composite material increase the tan δ of the material, meaning that the energy dampening properties have been improved in both cases. However, the storage modulus for the free clay system has also increased compared to the pure system. This shows that the material is much stiffer. Coupled with the lower $E_a$, this implies that although the created fibrils can dampen the energy very effectively, they detach from the probe surface prematurely. The storage modulus of the clay composite remains unchanged, however. This may be due to the fact

most of the clay is confined to the outside of the armoured latex particles, meaning the bulk PBA is relatively unchanged, while pockets of the armoured structures dampen the energy during extension. This can easily be seen by looking at table 1, which compares the data at 20 °C.

**Table 1:** Viscoelasticities of adhesive blends with different fillers

| Materials | Storage modulus, E' (MPa) | Energy dissipation rate, tan δ | Tan δ/E' |
|---|---|---|---|
| Model adhesive | 0.30 | 0.11 | 0.36 |
| Model adhesive + nanoclay | 0.55 | 0.20 | 0.36 |
| Model adhesive + hybrids | 0.30 | 0.18 | 0.60 |

The presence of 0.25 wt% nanoclay increases the E' from 0.3 MPa to 0.55 MPa. However, the value of tan δ /E' is unchanged compared to that of the model adhesive. As a result of the high stiffness, the adhesive energy during the debonding process is reduced. With the presence of 2.7 wt% hybrid particles, the E' is not affected, so tan δ is higher, and the tan δ /E' ratio is nearly doubled (increases from 0.36 to 0.6). This strong effect on tan δ /E' explains why hybrid particles increase the tack adhesion energy.[16,24]

The reduction of $E_a$ with increased armoured latex concentrations may be due to the fact there is still excess clay in the emulsion. This means that the PBA will become stiff when sufficient clay is added. This could be prevented if the excess clay could be removed. However a simple method

of doing this has yet to be found. This can be somewhat examined by looking at the data in Figure 10. To do this we can subtract the contribution of the PLA from the adhesion energy and find where the addition of composite returns back to its normal value. We can then compare this to where the addition of free clay also returns back to normal. The PLA curve crosses the composite curve at a value of 5 wt%, whereas the curve for free clay returns to base values at *ca.* 0.25 wt%. The total amount of clay in the system when 5 wt% of composite is added is 0.45 wt%, whereas when one looks at the excess clay there is 0.30 wt%. This is close to the 0.25 wt% observed, giving some validity to the assumption that the drop is due to the excess clay. However, it is possible we have more than 100% coverage on our interface, giving a smaller excess. In fact, if we did have 0.25 wt% of free clay in our system we would have 120 % coverage. This is a possibility, as it is known that when clay aggregates (as it would at the interface of the particle) there is an overlap[25] and this has also been observed in the AFM images of our particle interfaces.

## *Conclusion*

We have shown that the armoured latex particles have interesting material applications, namely heat resistance and increased PSA properties. These unique properties require our armoured structure and are not obtainable by using a standard blend system.

## *Methodology*

### Apparatus

Probe-tack measurements were taken on a MicroSystems Texture Analyser, Godalming, UK. DMA measurements were performed using a Q800, TA Instruments, New Castle, DE, USA. FE-SEM images were taken using a Zeiss Supra 55-VP. Prior to FEG-SEM analysis, samples were sputter-coated with AuPd for 45 seconds at 1.5 kV and 20 mA using a Quorum technologies Polaron SC7640 Auto/manual High resolution sputter coater. All TGA measurements were run on a STARe TGA system.

### Latex preparation

All Laponite-armoured latex particles were prepared as per Chapter 4. Full details on the preparation of the pure PBA latex can be found in Keddie's previous work.[16] To create the soap-free polystyrene latex, sodium 4-styrenesulfonate (0.0831 g) and sodium hydrogen carbonate (0.0520 g) was dissolved in water (100 g). To this solution, styrene (10.0 g) was added. The whole mixture was purged with $N_{2(g)}$ for 20 mins, then

isolated with an over-pressure to prevent oxygen re-entering the system. The reaction was then stirred at a speed where the layer of styrene became mixed by the rotor blades and was heated to 70 °C. Once the reaction was up to temperature KPS (0.0831 g) was added and was left for 24 hrs to ensure complete conversion.

**Probe-tack analysis of adhesive properties**

Probe-tack adhesive analysis of the nanocomposite films on glass plates followed the Avery method using a spherical steel probe. The probe was lowered onto the film with a load of 4.9 N and allowed 1 second of contact before being withdrawn from the film surface at a constant velocity of 100 μm/sec. This corresponds to an initial strain rate of 1.7 Hz. Films were formed using a 250 μm gap film-forming block pulled across a glass plate.

**DMA analysis**

Nanocomposite specimens (10 mm x 1 mm x 1 mm) for dynamic mechanical analysis (DMA) were obtained by casting the wet latex blends in Teflon moulds. Dynamic mechanical analysis of these samples were performed in tensile mode with a strain of 0.25% and a frequency of 1 Hz, which is comparable to the strain rate in the tack measurements.

(1) Sengupta, R.; Chakraborty, S.; Bandyopadhyay, S.; Dasgupta, S.; Mukhopadhyay, R.; Auddy, K.; Deuri, A. S. *Polym. Eng. Sci.* **2007**, *47*, 1956-1974.
(2) Okada, A.; Usuki, A. *Macromol. Mater. Eng* **2006**, *291*, 1449-1476.
(3) Takayanagi, M.; Ogata, T.; Morikawa, M.; Kai, T. *J. Macromol. Sci., Phys.* **1980**, *B17*, 591-615.
(4) Okada, A.; Kawasumi, M.; Kurauchi, T.; Kamigaito, O. *Polymer Preprints* **1987**, *28*, 447-8.
(5) Blumstein, A. *J. Polym. Sci. A.* **1965**, *3*, 2665-2672.
(6) Inan, G.; Patra, P. K.; Kim, Y. K.; Warner, S. B. *Materials Research Society Symposium Proceedings* **2003**, *788*, 289-295.
(7) Li, H.; Yang, Y.; Yu, Y. *J. Adhes. Sci. Technol.* **2004**, *18*, 1759-1770.
(8) Negrete-Herrera, N.; Putaux, J.-L.; David, L.; De Haas, F.; Bourgeat-Lami, E. *Macromol. Rapid Commun.* **2007**, *28*, 1567-1573.
(9) Gilman, J. W. *Applied Clay Science* **1999**, *15*, 31-49.
(10) Burnside, S. D.; Giannelis, E. P. *Chem. Mater.* **1995**, *7*, 1597-1600.
(11) Gilman, J. W.; Jackson, C. L.; Morgan, A. B.; Harris, R.; Manias, E.; Giannelis, E. P.; Wuthenow, M.; Hilton, D.; Phillips, S. H. *Chem. Mater.* **2000**, *12*, 1866-1873.
(12) Sikka, M., Cerini L. N., Ghosh S. S., Winey, K. I. *J. Polym. Sci., Part B: Polym. Phys.* **1996**, *34*, 1443-1449.
(13) Terao, K.; Mays, J. W. *Eur. Polym. J.* **2004**, *40*, 1623-1627.
(14) Bashirov, A. B.; Shermergor, T. D. *Mech. Compos. Mater.* **1975**, *11*, 474-476.
(15) Jang, B.-S.; Cho, K.-H.; Kim, K.-H.; Park, D.-W. *React. Kinet. Catal. Lett.* **2005**, *86*, 75-82.
(16) Wang, T.; Lei, C.-H.; Dalton, A. B.; Creton, C.; Lin, Y.; Fernando, K. A. S.; Sun, Y.-P.; Manea, M.; Asua, J. M.; Keddie, J. L. *Adv. Mater.* **2006**, *18*, 2730-2734.
(17) Satas, D. *Handbook of Pressure Sensitive Adhesives*; 3rd ed ed.; Van Nostrand Reinhold, New York, 1989.
(18) Yamaguchi, T.; Morita, H.; Doi, M. *Eur. Phys. J. E* **2006**, *20*, 7-17.
(19) Yamaguchi, T.; Doi, M. *Eur. Phys. J. E* **2006**, *21*, 331-339.
(20) Lakrout, H.; Creton, C.; Ahn, D.; Shull, K. R. *Macromolecules* **2001**, *34*, 7448-7458.
(21) Creton, C.; Hooker, J.; Shull, K. R. *Langmuir* **2001**, *17*, 4948-4954.
(22) Lakrout, H.; Sergot, P.; Creton, C. *J. Adhes.* **1999**, *69*, 307-359.
(23) Zosel, A. *Int. J. Adhes. Adhes.* **1998**, *18*, 265-271.
(24) Wang, T.; Lei, C.-H.; Liu, D.; Manea, M.; Asua, J. M.; Creton, C.; Dalton, A. B.; Keddie, J. L. *Adv. Mater.* **2008**, *20*, 90-94.
(25) Jönsson, B.; Labbez, C.; Cabane, B. *Langmuir* **2008**, *24*, 11406-11413.
(26) http://www.newton.dep.anl.gov/askasci/env99/env140.htm

# *Chapter 7: Technical and Basic Theory*

## *Polymerisation*

Polymerisation is a simple way of solidifying a liquid phase. The process of polymerisation is the covalent linking of many smaller molecules or "monomer" units into much larger high molecular weight chains. This process was first described as a polymerisation reaction by Berthelot in 1866.[1] Polymers are now one of the highest earning chemical industries in the world. The most common way to form high molecular weight material is the free radical polymerisation of vinyl molecules, most commonly styrenics and acrylates. The basic scheme for a peroxide free radical polymerisation can be seen in Figure 1, where $K_d$, $K_i$, $K_p$, $K_{tc}$ and $K_{td}$ are the rate constants of dissociation, initiation, propagation, termination by combination and termination by disproportionation, respectively. A free radical polymerisation can be defined as a "chain polymerisation in which each polymer molecule grows by addition of monomer to a terminal free-radical reactive site known as an active centre". Free radicals are defined as "… independently existing species which possess an unpaired electron and normally are highly reactive with short lifetimes".[2] In order to understand and predict this process, kinetic expressions need to be developed. Firstly, it is assumed that $K_t$ ($K_{tc}$+$K_{td}$) and $K_p$ are independent of the chain length of the polymer chain. This is acceptable as long as the growing end of the chain has

sufficient freedom of movement. Due to this one can omit $M_n$ and $M_m$ nomenclature.

Initiation:

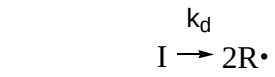

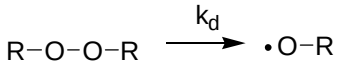

Followed by:

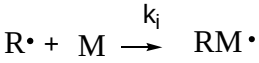

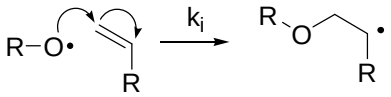

Propagation:

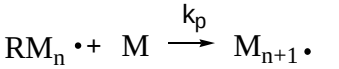

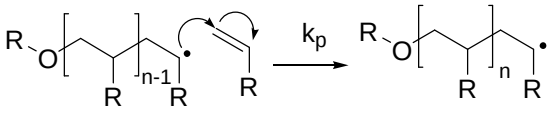

Termination:

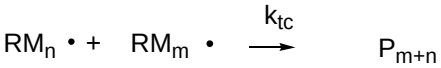

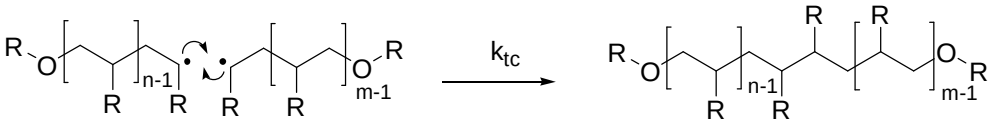

Or:

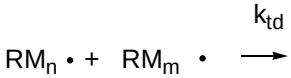

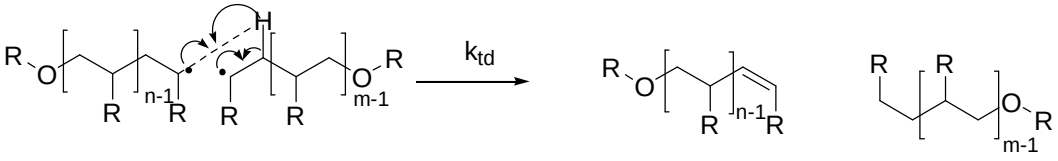

**Figure 1:** Basic reaction scheme for a free radical polymerisation reaction using a vinyl monomer

From the scheme in Figure 1 it can be seen that the rate of monomer disappearance can be written as:

$$\frac{-d[\mathrm{M}]}{dt} = k_i[\mathrm{R}\cdot][\mathrm{M}] + k_p[\mathrm{M}\cdot][\mathrm{M}] \qquad \textbf{Equation 1}$$

And for a polymerisation for growing long chains, $k_i[\mathrm{R}\cdot][\mathrm{M}]$ << $k_p[\mathrm{M}\cdot][\mathrm{M}]$ meaning that this expression can be rewritten as:

$$\frac{-d[\mathrm{M}]}{dt} = k_p[\mathrm{M}\cdot][\mathrm{M}] \qquad \textbf{Equation 2}$$

Also the rate of growing chain disappearance can be written as follows:

$$\frac{d[\mathrm{M}\cdot]}{dt} = k_i\mathrm{R}\cdot[\mathrm{M}] - 2k_t[\mathrm{M}\cdot]^2 \qquad \textbf{Equation 3}$$

A major problem with these equations is that the concentration of radicals over time is either very difficult or impossible to measure. So in order for them to become useful, any radical concentration term must be eliminated. This is easily done using the steady state assumption. This allows us to equate the previous equation to zero:

$$Ki[\mathrm{R}\cdot][\mathrm{M}] = 2k_t[\mathrm{M}\cdot]^2 \qquad \textbf{Equation 4}$$

This allows us to form the following expression, where f is the efficiency of the initiator (typically between 0.5-1.0):

$$\frac{d[\mathrm{R}\cdot]}{dt} = 2fk_d[\mathrm{I}] - k_i[\mathrm{R}\cdot][\mathrm{M}] = 0 \qquad \textbf{Equation 5}$$

Combining equations 1-4 one gets:

$$\frac{-d[\mathrm{M}]}{dt} = k_p[\mathrm{M}](k_d f[\mathrm{I}]/k_t)^{1/2} \qquad \textbf{Equation 6}$$

Which in short form gives the final equation:

$$R_p = k_p[\mathrm{M}](\mathrm{R}_i/2k_t)^{1/2} \qquad \textbf{Equation 7}$$

Where $R_p$ is the rate of polymer chain growth and $R_i$ is the rate of polymer chain initiation.[3]

There are three main ways of creating radicals for initiating a polymerisation reaction: 1) thermal cleavage of a covalent bond, 2) photochemical cleavage and 3) redox process

1) Thermal initiation works by heating a molecule above the dissociation energy of one of its bonds, usually yielding two identical radicals. These bonds are typically azide or peroxide linkages. Two commonly used initiators being azobisisobutyronitrile (AIBN) an oil-soluble initiator and potassium peroxide (KPS) a water-soluble initiator. Thermal initiators are usual classified by their 10 hr half-life temperatures, which is the temperature at which half of the initiator will have decomposed. (65 °C for AIBN and 60 °C for KPS).[4]

The $k_d$ of an initiator can be determined from its half-life at a given temperature using the equation $k_d$=Ln2/t, where t is the half-life in s.

2) Photochemical cleavage works in a very similar way to thermal dissociation. However, the energy needed to break the weakest bond is taken from an absorbed photon (usually from UV light). This is possible as the energy of a photon has the same magnitude as a weak covalent bond (200-400 kJ)[3]

3) Most redox processes that form radicals occur by a one electron transfer step. Two widely used reactions for producing radicals are ammonium persulfate (APS) and N, N, N', N'-tetramethylethylenediamine (TEMED), or cumyl hydroperoxide and $Fe^{2+}$, which both can undergo a redox process to form radicals at room temperature.

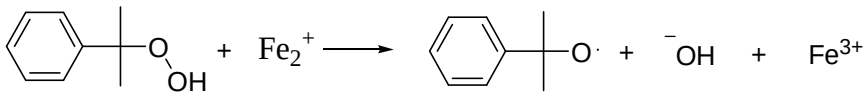


**Figure 2:** The one electron step involved in the redox reaction between cumyl hydroperoxide and $Fe^{2+}$

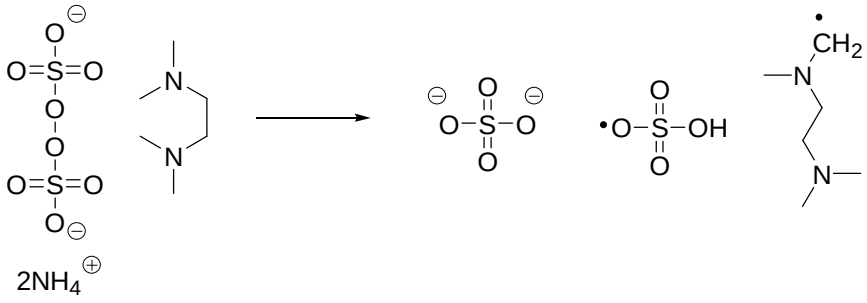


**Figure 3:** Reaction between TEMED and APS to form radical species[5]

## *Dynamic Light Scattering*

During the measurement, laser light is beamed into the sample. The particles cause the light to be diffracted. The diffracted light is detected at a constant angle by a single photon counter. The intensity of the scattered light is monitored over time and this fluctuates as the particles diffuse through the liquid medium. A correlation function is used to analyse the non-randomness of the intensity fluctuation over time. The correlation of the particle positions over time is plotted. Since smaller particles diffuse faster, they will have moved into a new (random) position sooner. This will mean the correlation will fall to zero much quicker. Therefore the exponential curve generated by this correlation vs. time expression will give the diffusion rate of the particles. When used in conjunction with the Stokes-Einstein equation, this can be used to obtain the hydrodynamic radius of the particle. Different angles of detection can be used in order to calculate the particle size by using Mie theory to give the relative intensity of the beam for different angles and particle sizes. It can be seen from figure 1 that 90 degrees is used as the normal angle of detection, because there is little fluctuation in intensity from different particle sizes.

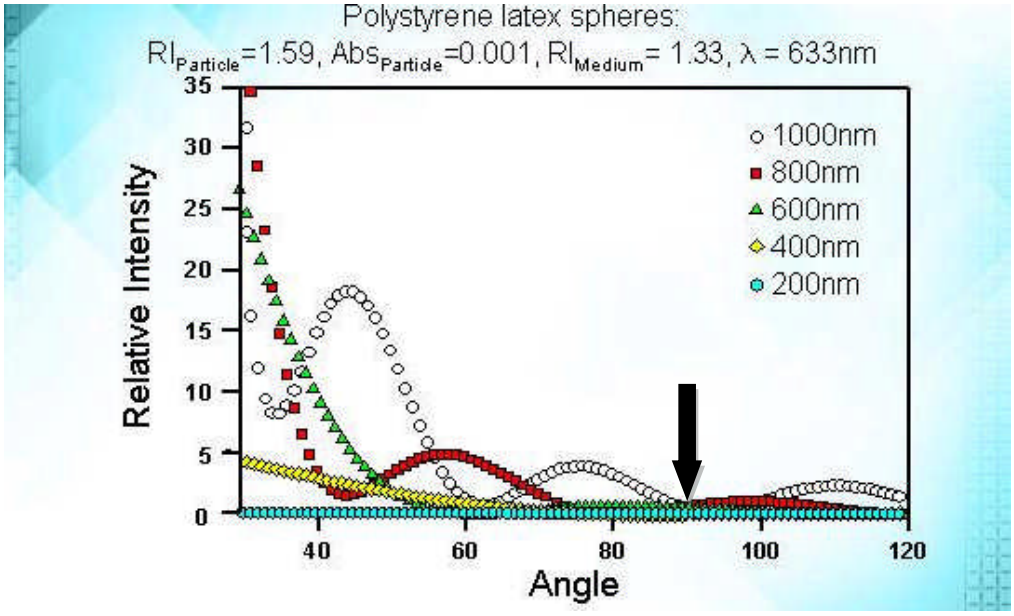


**Figure 4:** Plot showing the relative intensities at multiple angles for different particle sizes using Mie theory[‣]

## *Scanning Electron Microscope*

SEM works in a very similar way as normal optical microscopy in reflectance mode except electrons are used as the probe. To visualise a sample an electron beam is focused into a small spot onto the surface of the media by a series of electro-magnets. The spot is scanned across the surface of the media and the intensity of the backscattered electrons are detected. From the intensity at each spot, an image can be built up by matching the intensity of the electrons detected with the intensity of the pixel on the VDU. As electrons are used instead of photons, this allows a much high magnification to be used as the pixel size in microscopy is limited by the size of the scanning beam. The smallest wavelength normally available for a photon is ca. 250 nm but the wavelength of an electron is less than 1 nm.

‣ Taken from Malvern's online knowledge base

### *Transmission Electron Microscope*

TEM uses an electron beam like SEM but works by detecting the electrons that pass through the sample. The image is generated because thicker areas of the sample will prevent more electrons from passing through giving a darker image. Also some materials are more transparent to electrons than others. This gives TEM an advantage over SEM in that it can more easily analyse composites, as some materials will show up darker than others. Also, because the electron beam passes through the sample it allows analysis of objects imbedded inside another material. The disadvantage of TEM over SEM is that the sample must be very thin for the beam to be transmitted.

### *Confocal Microscopy*

Confocal Microscopy differs from conventional microscopy because, instead of flooding the sample with light, a point source is used with a pinhole to filer out any non-focused light. This allows an image to be generated in a narrow plane only by scanning across the surface being viewed. A 3D map can also be generated by scanning multiple planes at different heights and rebuilding one on top of the other.

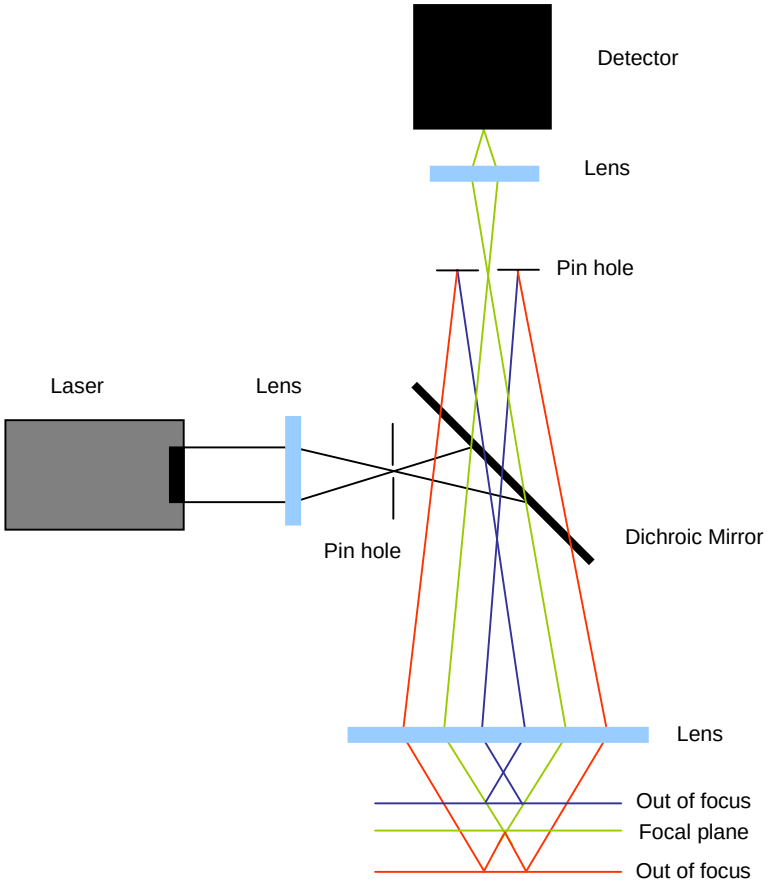


**Figure 5:** Schematic representation of a confocal microscope.

## *Probe-tack*

In probe tack measurements, a probe is lowered onto the substrate of known thickness until a pre-decided resistance is detected. The probe is then removed from the substrate at a given speed. The force pulling on the probe is measured by detecting the weight of the probe during surface removal. From the data obtained, a force/distance curve can be generated. This data is dependent on the probe used and the thickness of the film. So in order to obtain a stress/strain curve, one must divide the force by the contact area of the probe, and divide the extension distance

by the thickness of the film used. When this is done, the following graph will be generated:

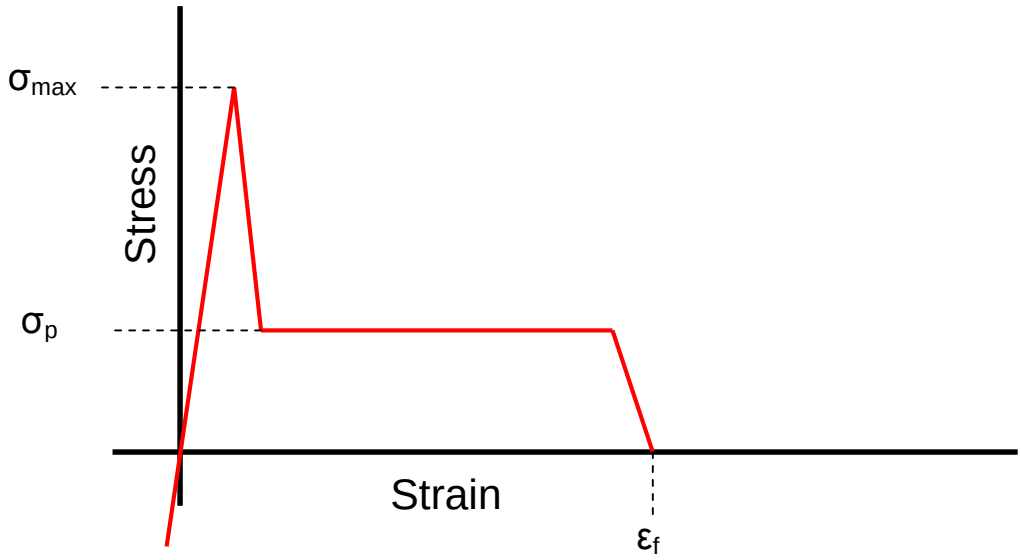


**Figure 6:** Schematic representation of a probe-tack stress strain curve

As the probe is pulled away from the substrate, the film will deform and pull back on the probe. The more the film has to deform, the larger the force that pulls back on the probe. The force will continue to increase until a maximum strain is reached ($\sigma_{max}$); this is where the film cannot deform any more and cavities are generated. This reduces the force pulling back on the probe. The cavities will continue to grow, further reducing the strain until fibrils are created. The fibrils will then stretch and exert a uniform force upon the probe, resulting in the plateau in strain ($\sigma_p$). Once the fibrils get to a certain extension they will start to break or detach from the probe until no contact is left at the maximum stress ($\varepsilon_f$), reducing the stain back to zero.

## *Dynamic Mechanical Thermal Analysis (DMTA)*

Dynamic Mechanical Thermal Analysis, sometimes known as Dynamic Mechanical Rheological Testing (DMRT), is a laboratory test method in which mechanical properties of a material are calculated by applying an oscillating strain to a sample and measuring the resulting stress.

Polymers are viscoelastic materials and give interesting stress-strain curves. The stress signal generated by a viscoelastic material can be separated into two components: an elastic stress component which gives a direct increase of stress with a given strain, and a viscous component that is 90° out of phase with the strain. The elastic stress measures the degree to which the material behaves as an ideal solid; the viscous stress, the degree to which the material behaves as an ideal fluid. By analysing the curve generated in a DMTA run both the viscous and elastic components can be extrapolated by looking at the following expressions:

$$\sigma = \sigma_0 \sin(\omega t + \delta) \text{ and } \varepsilon = \varepsilon_0 \sin \omega t \qquad \textbf{Equation 8}$$

Where δ is the relative angular displacement of the stress to strain. The stress can be expanded to be:

$$\sigma = \sigma_0 \sin \omega t \cos \delta + \sigma_0 \cos \omega t \sin \delta \qquad \textbf{Equation 9}$$

From this equation the viscous and the elastic components can be resolved with the in phase contribution being $\sigma_0 \cos\delta$ and the out of phase contribution being $\sigma_0 \sin\delta$.

By comparing the ratio of the elastic contribution to the applied strain, one gets the storage modulus of a material $E' = (\sigma_0/\varepsilon_0)\cos\delta$ , whereas the ratio of the viscous contribution to strain gives the loss modulus E'' $= (\sigma_0/\varepsilon_0)\sin\delta$ .

The ratio between the storage and the loss modulus (E''/E') gives the dampening factor tanδ.


(1) M. Berthelot, *Ann Chim Phys*; **1866**, 9, 446

(2) Young, R. J., Lovel, P. A., *Introduction to Polymers*; Second edition ed.; Chapman and Hall, 1991.

(3) Walling, C. *Free Radicals in Solution*; John Wiley, New York., 1957.

(4) Brandrup, J., Immergut, E. H., Grulke, E. A., Bloch, D.; "*Polymer Handbook*"; 4th edition ed.; John Wiley, New York., 1999.

(5) Feng, X. D., Guo, X. Q., Qui, K. Y.; *Die Makromole. Chem*. **1988**, *189*, 77-83.

# *Chapter 8*

## *Final Words*

We have shown that by changing the type of stabiliser used in our Pickering systems, many structures with different sizes and morphologies can be generated. These structures can have properties that can only be obtained using this versatile technique. We have also demonstrated that these systems can replace the use of surfactants in most polymer emulsion systems. Most importantly I hope we have shown that Pickering stabilisation is not only interesting academically but allows access to very important systems for industrial use.

## *Quotes:*

**Q:** It's an unknown - isn't that enough??

**Picard:** If you'd earned that uniform you're wearing, you know it's the unknown that brings us out here!

**Star trek next generation:** *Encounter at Farpoint*

**Frodo:** I wish it need not have happened in my time

**Gandalf:** So do I and so do all who live to see such times. But that is not for them to decide. All we have to decide is what to do with the time that is given us."

**Lord of the Rings:** *Chapter 'The Shadow of the Past'*

# *Appendix*

## *Raw data: Chapter 4*

**Series I**

| PJC-1-037 | Time/ mins | Empty | Full | Dry | Initiator/g | X |
|---|---|---|---|---|---|---|
| 0.5 g clay | 30 | 1.0833 | 3.1965 | 1.1083 | 0.0485 | 0.020 |
| | 60 | 1.086 | 3.1641 | 1.1172 | | 0.056 |
| | 90 | 1.0867 | 3.105 | 1.1245 | | 0.097 |
| | 120 | 1.0891 | 3.004 | 1.1331 | | 0.145 |
| | 150 | 1.0898 | 3.006 | 1.1412 | | 0.188 |
| | 180 | 1.0853 | 3.1141 | 1.1458 | | 0.221 |
| | 210 | 1.0881 | 3.1391 | 1.154 | | 0.247 |
| | 240 | 1.0879 | 3.1142 | 1.1586 | | 0.278 |
| | 270 | 1.0912 | 3.1708 | 1.1678 | | 0.299 |
| | 300 | 1.0908 | 3.1654 | 1.1717 | | 0.324 |
| | 330 | 1.0892 | 2.9965 | 1.167 | | 0.344 |
| | 360 | 1.0877 | 3.1965 | 1.1772 | | 0.362 |
| | 390 | 1.0852 | 3.0924 | 1.1758 | | 0.392 |
| | | 1.0873 | 3.1622 | 1.2648 | | 0.843 |
| PJC-1-042 | | | | | | |
| 0.25 g clay | 30 | 1.084 | 3.1573 | 1.1001 | 0.0656 | -0.002 |
| | 60 | 1.0773 | 3.1548 | 1.0957 | | 0.010 |
| | 90 | 1.0809 | 2.9971 | 1.1009 | | 0.028 |
| | 120 | 1.0785 | 3.1866 | 1.1053 | | 0.053 |
| | 145 | 1.0861 | 3.0701 | 1.1138 | | 0.066 |
| | 180 | 1.0795 | 3.1027 | 1.1116 | | 0.087 |
| | 210 | 1.0879 | 3.1927 | 1.1256 | | 0.110 |
| | 240 | 1.0839 | 3.0697 | 1.123 | | 0.130 |
| | 270 | 1.0867 | 3.073 | 1.1274 | | 0.138 |
| | 300 | 1.0894 | 3.1976 | 1.1355 | | 0.154 |
| | 330 | 1.0866 | 3.1908 | 1.1343 | | 0.162 |
| | 360 | 1.0872 | 3.1497 | 1.1354 | | 0.170 |
| | | 1.0844 | 3.5206 | 1.2592 | | 0.704 |
| PJC-1-046 | | | | | | |
| 0.25 g clay | 30 | 1.0948 | 3.1185 | 1.1106 | 0.0456 | 0.001 |
| | 60 | 1.0911 | 3.0178 | 1.11 | | 0.023 |
| | 90 | 1.0905 | 3.14 | 1.1163 | | 0.054 |
| | 120 | 1.0898 | 3.0728 | 1.1187 | | 0.077 |
| | 150 | 1.0972 | 3.1455 | 1.1309 | | 0.098 |
| | 185 | 1.0973 | 3.0484 | 1.1366 | | 0.139 |
| | 215 | 1.096 | 2.9597 | 1.1342 | | 0.143 |
| | 240 | 1.099 | 3.1896 | 1.1465 | | 0.168 |
| | 270 | 1.0947 | 3.1648 | 1.1439 | | 0.179 |
| | 305 | 1.0893 | 3.1348 | 1.1406 | | 0.194 |
| | 330 | 1.092 | 3.3297 | 1.152 | | 0.213 |
| | 365 | 1.0912 | 3.1485 | 1.1498 | | 0.232 |
| | 395 | 1.0931 | 3.2848 | 1.1562 | | 0.235 |
| | | 1.093 | 2.3365 | 1.1865 | | 0.753 |

| PJC-1-047 | Time/ mins | Empty | Full | Dry | | X |
|---|---|---|---|---|---|---|
| 0.35 g clay | 30 | 1.0897 | 3.0348 | 1.106 | 0.0527 | -0.004 |
| | 60 | 1.0933 | 2.9427 | 1.1124 | | 0.018 |
| | 90 | 1.0962 | 3.312 | 1.1211 | | 0.028 |
| | 120 | 1.095 | 3.0552 | 1.1223 | | 0.058 |
| | 150 | 1.0894 | 3.1976 | 1.1238 | | 0.085 |
| | 185 | 1.091 | 3.2258 | 1.1303 | | 0.109 |
| | 210 | 1.0969 | 3.1893 | 1.1362 | | 0.113 |
| | 240 | 1.0911 | 2.9818 | 1.132 | | 0.145 |
| | 270 | 1.0996 | 3.083 | 1.1436 | | 0.151 |
| | 300 | 1.1004 | 3.5075 | 1.1558 | | 0.160 |
| | 330 | 1.0994 | 3.1447 | 1.1494 | | 0.176 |
| | 360 | 1.1029 | 3.0822 | 1.1532 | | 0.187 |
| | | 1.0926 | 2.8762 | 1.2364 | | 0.806 |
| PJC-1-048 | | | | | | |
| 0.7 g clay | 30 | 1.0839 | 3.2349 | 1.1114 | 0.0554 | 0.011 |
| | 60 | 1.0756 | 3.3177 | 1.1167 | | 0.074 |
| | 90 | 1.077 | 3.2891 | 1.1286 | | 0.130 |
| | 120 | 1.0786 | 3.2089 | 1.1389 | | 0.186 |
| | 150 | 1.0814 | 3.2361 | 1.1511 | | 0.232 |
| | 180 | 1.0815 | 3.2646 | 1.1627 | | 0.287 |
| | 215 | 1.0788 | 3.1945 | 1.1617 | | 0.309 |
| | 245 | 1.0794 | 3.3078 | 1.1754 | | 0.353 |
| | 270 | 1.0876 | 3.2042 | 1.1824 | | 0.372 |
| | 300 | 1.0869 | 3.2151 | 1.1897 | | 0.412 |
| | 330 | 1.0835 | 3.1344 | 1.1856 | | 0.429 |
| | 365 | 1.0847 | 3.143 | 1.1952 | | 0.473 |
| | 390 | 1.0818 | 3.2457 | 1.2055 | | 0.512 |
| | | 1.0819 | 2.9581 | 1.2434 | | 0.838 |
| PJC-1-049 | | | | | | |
| 1.5 g clay | 30 | 1.0824 | 3.2019 | 1.126 | 0.0737 | 0.016 |
| | 60 | 1.0849 | 3.1816 | 1.1425 | | 0.093 |
| | 90 | 1.0812 | 3.0192 | 1.1482 | | 0.173 |
| | 120 | 1.0853 | 3.0605 | 1.1681 | | 0.255 |
| | 150 | 1.0833 | 3.0698 | 1.1808 | | 0.335 |
| | 185 | 1.0887 | 3.171 | 1.205 | | 0.411 |
| | 220 | 1.0841 | 3.1841 | 1.2113 | | 0.463 |
| | 240 | 1.0851 | 3.0375 | 1.2101 | | 0.502 |
| | 270 | 1.0835 | 3.1511 | 1.2235 | | 0.543 |
| | 300 | 1.0835 | 3.0805 | 1.2273 | | 0.591 |
| | 340 | 1.0752 | 3.1422 | 1.238 | | 0.667 |
| | 390 | 1.0818 | 3.0739 | 1.258 | | 0.775 |
| | | 1.0795 | 2.8052 | 1.2442 | | 0.853 |

| PJC-1-052 | Time/ mins | Empty | Full | Dry | | X |
|---|---|---|---|---|---|---|
| 1.0 g clay | 30 | 1.0786 | 3.0703 | 1.1104 | 0.0509 | 0.016 |
| | 65 | 1.0799 | 3.0386 | 1.1246 | | 0.093 |
| | 90 | 1.0806 | 3.0089 | 1.1354 | | 0.155 |
| | 120 | 1.0832 | 2.9674 | 1.1475 | | 0.219 |
| | 150 | 1.0836 | 3.0764 | 1.1645 | | 0.291 |
| | 185 | 1.0822 | 3.1842 | 1.1757 | | 0.335 |
| | 210 | 1.0828 | 2.957 | 1.1733 | | 0.377 |
| | 250 | 1.0814 | 2.9326 | 1.1814 | | 0.442 |
| | 275 | 1.075 | 2.9894 | 1.1853 | | 0.482 |
| | 305 | 1.0792 | 3.0021 | 1.1934 | | 0.502 |
| | 330 | 1.0779 | 3.0864 | 1.2073 | | 0.558 |
| | 360 | 1.0817 | 3.1131 | 1.224 | | 0.621 |
| | 390 | 1.0835 | 3.0443 | 1.2389 | | 0.724 |
| | | 1.0802 | 2.9931 | 1.2598 | | 0.888 |
| **Series II** | | | | | | |
| PJC-1-021 | | | | | | |
| 1.5 g clay | 30 | 1.0851 | 3.1389 | 1.129 | | 0.032 |
| | 60 | 1.0841 | 3.205 | 1.146 | | 0.122 |
| | 90 | 1.0868 | 3.1773 | 1.1706 | | 0.248 |
| | 120 | 1.0821 | 3.0694 | 1.1769 | | 0.336 |
| | 150 | 1.0874 | 3.0906 | 1.1979 | | 0.422 |
| | 180 | 1.0872 | 3.0276 | 1.2086 | | 0.507 |
| | 210 | 1.0891 | 3.0061 | 1.2218 | | 0.584 |
| | 240 | 1.0813 | 3.0789 | 1.2468 | | 0.741 |
| | 270 | 1.0881 | 3.0643 | 1.2656 | | 0.821 |
| | 300 | 1.083 | 3.0729 | 1.2705 | | 0.872 |
| | 330 | 1.0823 | 2.8379 | 1.2457 | | 0.859 |
| | 360 | 1.0853 | 3.2493 | 1.2955 | | 0.906 |
| | | 1.0823 | 3.0894 | 1.2917 | | 0.989 |
| PJC-1-024 | | | | | | |
| 0.25 g Clay | 30 | 1.0793 | 3.2689 | 1.0984 | | 0.010 |
| | 60 | 1.0884 | 2.9972 | 1.1054 | | 0.012 |
| | 90 | 1.0794 | 3.1386 | 1.0999 | | 0.024 |
| | 120 | 1.0784 | 2.8856 | 1.1001 | | 0.047 |
| | 150 | 1.0814 | 3.1708 | 1.1096 | | 0.063 |
| | 180 | 1.077 | 2.9685 | 1.1043 | | 0.074 |
| | 210 | 1.0784 | 3.1543 | 1.1105 | | 0.085 |
| | 245 | 1.0802 | 3.0286 | 1.1123 | | 0.097 |
| | 270 | 1.0775 | 2.9438 | 1.1091 | | 0.102 |
| | 300 | 1.0827 | 3.0088 | 1.1207 | | 0.133 |
| | 330 | 1.0854 | 3.0384 | 1.123 | | 0.128 |
| | 360 | 1.0849 | 2.9124 | 1.1231 | | 0.146 |
| | | 1.0888 | 3.1443 | 1.257 | | 0.825 |

| PJC-1-025 | Time/ mins | Empty | Full | Dry | X |
|---|---|---|---|---|---|
| 0.5 g clay | 30 | 1.0803 | 2.9689 | 1.0997 | 0.004 |
| | 60 | 1.0872 | 3.1883 | 1.1092 | 0.006 |
| | 90 | 1.0784 | 3.0151 | 1.1132 | 0.091 |
| | 120 | 1.0809 | 3.0757 | 1.1236 | 0.129 |
| | 150 | 1.0824 | 3.1306 | 1.1312 | 0.157 |
| | 180 | 1.0799 | 3.1179 | 1.1367 | 0.202 |
| | 220 | 1.0828 | 2.9479 | 1.1418 | 0.245 |
| | 240 | 1.0817 | 3.0562 | 1.1434 | 0.241 |
| | 270 | 1.0822 | 2.9283 | 1.1425 | 0.257 |
| | 300 | 1.0827 | 2.9222 | 1.1452 | 0.271 |
| | 330 | 1.0858 | 3.1056 | 1.1624 | 0.316 |
| | | 1.089 | 3.2165 | 1.2737 | 0.868 |
| PJC-1-027 | | | | | |
| 0.35 g clay | 30 | 1.085 | 3.0793 | 1.1018 | -0.002 |
| | 60 | 1.0891 | 3.0303 | 1.1065 | 0.004 |
| | 90 | 1.0866 | 2.9873 | 1.1053 | 0.013 |
| | 120 | 1.0879 | 3.124 | 1.1125 | 0.039 |
| | 150 | 1.0899 | 3.116 | 1.1177 | 0.057 |
| | 180 | 1.0842 | 3.1463 | 1.1194 | 0.094 |
| | 210 | 1.0884 | 3.1334 | 1.1262 | 0.110 |
| | 240 | 1.0861 | 3.0128 | 1.1262 | 0.136 |
| | 270 | 1.0794 | 3.0554 | 1.1253 | 0.163 |
| | 300 | 1.0786 | 3.1165 | 1.1289 | 0.180 |
| | 330 | 1.0836 | 3.0428 | 1.1335 | 0.189 |
| | 360 | 1.0846 | 3.0195 | 1.1356 | 0.198 |
| | 390 | 1.0849 | 3.0902 | 1.1419 | 0.222 |
| | | 1.0839 | 3.1239 | 1.236 | 0.738 |
| PJC-1-028 | | | | | |
| 0.7 g clay | 30 | 1.086 | 3.0581 | 1.1142 | 0.028 |
| | 60 | 1.0847 | 3.1214 | 1.1208 | 0.067 |
| | 90 | 1.0835 | 3.077 | 1.1295 | 0.126 |
| | 120 | 1.0865 | 3.2933 | 1.1512 | 0.196 |
| | 150 | 1.0829 | 3.1123 | 1.1544 | 0.262 |
| | 180 | 1.0873 | 3.1492 | 1.1729 | 0.333 |
| | 210 | 1.0872 | 3.0667 | 1.1752 | 0.365 |
| | 240 | 1.0842 | 3.1224 | 1.1833 | 0.412 |
| | 270 | 1.0836 | 3.1059 | 1.1873 | 0.442 |
| | 300 | 1.0825 | 3.016 | 1.189 | 0.484 |
| | 330 | 1.0913 | 3.0113 | 1.1939 | 0.466 |
| | 360 | 1.0865 | 3.0618 | 1.201 | 0.517 |
| | | 1.0872 | 2.9691 | 1.244 | 0.800 |

| PJC-1-040 | Time/ mins | Empty | Full | Dry | | X |
|---|---|---|---|---|---|---|
| 1.0 g clay | 30 | 1.0858 | 3.197 | 1.1174 | 0.0498 | 0.008 |
| | 60 | 1.083 | 3.2205 | 1.137 | | 0.123 |
| | 90 | 1.0889 | 3.1789 | 1.1484 | | 0.159 |
| | 120 | 1.0844 | 3.1623 | 1.157 | | 0.232 |
| | 150 | 1.0865 | 3.1866 | 1.1736 | | 0.305 |
| | 180 | 1.0879 | 3.1119 | 1.1791 | | 0.345 |
| | 210 | 1.0868 | 3.1579 | 1.1914 | | 0.406 |
| | 245 | 1.0909 | 3.168 | 1.2026 | | 0.443 |
| | 280 | 1.0878 | 3.1731 | 1.2113 | | 0.504 |
| | 305 | 1.0959 | 3.1624 | 1.2267 | | 0.550 |
| | 335 | 1.0908 | 3.136 | 1.2296 | | 0.601 |
| | 360 | 1.0838 | 3.113 | 1.2363 | | 0.683 |
| | 390 | 1.086 | 3.1975 | 1.2632 | | 0.782 |
| | | 1.0895 | 2.5539 | 1.2346 | | 0.952 |
| PJC-1-043 | | | | | | |
| 0.35 g clay | 30 | 1.0755 | 3.1308 | 1.0957 | 0.0475 | 0.013 |
| | 60 | 1.0866 | 3.2416 | 1.1119 | | 0.035 |
| | 95 | 1.0745 | 3.0846 | 1.1065 | | 0.082 |
| | 120 | 1.0779 | 3.0751 | 1.1146 | | 0.109 |
| | 150 | 1.0793 | 3.1568 | 1.1222 | | 0.135 |
| | 190 | 1.0832 | 3.0926 | 1.1308 | | 0.169 |
| | 215 | 1.0774 | 3.1295 | 1.1306 | | 0.194 |
| | 240 | 1.0809 | 3.1095 | 1.1361 | | 0.208 |
| | 270 | 1.0849 | 3.1367 | 1.1446 | | 0.229 |
| | 300 | 1.0831 | 3.0743 | 1.1459 | | 0.257 |
| | 340 | 1.0852 | 3.1434 | 1.1552 | | 0.284 |
| | 360 | 1.0815 | 3.1824 | 1.1569 | | 0.305 |
| | 390 | 1.0782 | 3.1614 | 1.1575 | | 0.330 |
| | | 1.0781 | 3.0294 | 1.2422 | | 0.845 |
| PJC-1-045 | | | | | | |
| 0.5 g clay | 30 | 1.0812 | 2.9838 | 1.1009 | 0.0466 | 0.004 |
| | 70 | 1.0768 | 3.0558 | 1.1061 | | 0.053 |
| | 90 | 1.0816 | 3.0247 | 1.1146 | | 0.078 |
| | 120 | 1.0797 | 2.9756 | 1.1208 | | 0.130 |
| | 155 | 1.0835 | 3.0628 | 1.1327 | | 0.165 |
| | 185 | 1.0864 | 3.0232 | 1.1368 | | 0.178 |
| | 210 | 1.0861 | 3.203 | 1.1491 | | 0.220 |
| | 250 | 1.0918 | 3.12 | 1.156 | | 0.241 |
| | 275 | 1.0894 | 2.9595 | 1.1528 | | 0.266 |
| | 305 | 1.0939 | 2.9703 | 1.1608 | | 0.285 |
| | 335 | 1.0924 | 3.3481 | 1.1756 | | 0.299 |
| | 370 | 1.0918 | 3.0551 | 1.1688 | | 0.325 |
| | 405 | 1.0959 | 2.9489 | 1.1732 | | 0.353 |
| | | 1.0928 | 2.9353 | 1.2505 | | 0.842 |

| PJC-1-050 | Time/ mins | Empty | Full | Dry | | X |
|---|---|---|---|---|---|---|
| 0.25 g clay | 30 | 1.0943 | 2.9621 | 1.1088 | 0.045 | 0.000 |
| | 60 | 1.1015 | 2.9776 | 1.1187 | | 0.016 |
| | 90 | 1.0979 | 3.206 | 1.1211 | | 0.036 |
| | 125 | 1.0932 | 2.9551 | 1.1179 | | 0.062 |
| | 150 | 1.0945 | 3.0165 | 1.1259 | | 0.096 |
| | 180 | 1.0954 | 3.2918 | 1.1348 | | 0.114 |
| | 210 | 1.0969 | 3.1236 | 1.1364 | | 0.131 |
| | 240 | 1.0889 | 3.2194 | 1.1328 | | 0.143 |
| | 270 | 1.0982 | 3.0845 | 1.1431 | | 0.166 |
| | 305 | 1.0845 | 2.9838 | 1.1304 | | 0.183 |
| | 330 | 1.086 | 3.2584 | 1.1419 | | 0.200 |
| | 360 | 1.0867 | 3.1208 | 1.141 | | 0.211 |
| | 390 | 1.0919 | 3.1271 | 1.1476 | | 0.219 |
| | | 1.0892 | 2.7661 | 1.213 | | 0.737 |
| **Series III** | | | | | | |
| PJC-1-058 | | | | | | |
| 1.0 g clay, 5.0 g St | 30 | 1.1004 | 3.155 | 1.1354 | 0.044 | 0.033 |
| | 60 | 1.0993 | 2.9508 | 1.1452 | | 0.197 |
| | 90 | 1.0875 | 3.1189 | 1.1588 | | 0.416 |
| | 120 | 1.0867 | 3.1731 | 1.1729 | | 0.548 |
| | 150 | 1.0843 | 3.1947 | 1.195 | | 0.785 |
| | 180 | 1.0887 | 3.0201 | 1.1905 | | 0.791 |
| | 215 | 1.0885 | 3.1162 | 1.1969 | | 0.806 |
| | 240 | 1.0859 | 3.2219 | 1.2019 | | 0.824 |
| | 270 | 1.0893 | 3.0689 | 1.1976 | | 0.833 |
| | 300 | 1.0909 | 3.0855 | 1.1992 | | 0.824 |
| | 330 | 1.092 | 3.2393 | 1.2108 | | 0.846 |
| | 360 | 1.0945 | 3.0966 | 1.2046 | | 0.839 |
| | 390 | 1.0886 | 3.1518 | 1.2029 | | 0.848 |
| | | 1.09 | 3.2178 | 1.2093 | | 0.862 |
| PJC-1-059 | | | | | | |
| 0.5 g clay, 5.0 g St | 30 | 1.0905 | 3.3723 | 1.1132 | 0.0461 | -0.010 |
| | 60 | 1.0887 | 3.2547 | 1.1158 | | 0.045 |
| | 90 | 1.0854 | 3.1944 | 1.1172 | | 0.101 |
| | 120 | 1.0828 | 3.1872 | 1.1221 | | 0.178 |
| | 150 | 1.0851 | 3.2176 | 1.1304 | | 0.233 |
| | 180 | 1.0912 | 3.3471 | 1.142 | | 0.261 |
| | 210 | 1.091 | 3.3013 | 1.1456 | | 0.308 |
| | 240 | 1.086 | 3.2398 | 1.1432 | | 0.347 |
| | 270 | 1.0842 | 3.2088 | 1.1438 | | 0.380 |
| | 300 | 1.0831 | 3.2473 | 1.1483 | | 0.424 |
| | 330 | 1.0932 | 3.2414 | 1.1604 | | 0.449 |
| | 360 | 1.091 | 3.2171 | 1.1629 | | 0.503 |
| | 390 | 1.0886 | 3.2661 | 1.1673 | | 0.553 |
| | | 1.0884 | 3.2363 | 1.1881 | | 0.774 |

| PJC-1-060 | Time/ mins | Empty | Full | Dry | | X |
|---|---|---|---|---|---|---|
| 0.5 g clay, 7.5 g St | 30 | 1.0916 | 3.2563 | 1.1155 | 0.0422 | 0.010 |
| | 60 | 1.093 | 3.0481 | 1.1223 | | 0.068 |
| | 90 | 1.0937 | 2.9647 | 1.1288 | | 0.122 |
| | 120 | 1.0844 | 3.0145 | 1.1285 | | 0.182 |
| | 155 | 1.0853 | 3.0582 | 1.1394 | | 0.248 |
| | 180 | 1.0841 | 3.1309 | 1.1441 | | 0.276 |
| | 210 | 1.0824 | 3.1053 | 1.1475 | | 0.317 |
| | 240 | 1.0764 | 3.1382 | 1.1475 | | 0.351 |
| | 270 | 1.0743 | 2.9256 | 1.1413 | | 0.375 |
| | 300 | 1.0776 | 2.9779 | 1.1499 | | 0.402 |
| | 330 | 1.0807 | 2.9598 | 1.1568 | | 0.438 |
| | 360 | 1.0761 | 3.0852 | 1.1644 | | 0.488 |
| | 395 | 1.0775 | 3.1403 | 1.179 | | 0.564 |
| | | 1.0785 | 3.3836 | 1.2294 | | 0.800 |
| PJC-1-061 | | | | | | |
| 0.5 g clay, 2.5 g St | 30 | 1.0762 | 3.2468 | 1.0979 | 0.0369 | -0.026 |
| | 60 | 1.0798 | 3.171 | 1.1023 | | 0.004 |
| | 90 | 1.0823 | 3.1232 | 1.1113 | | 0.140 |
| | 120 | 1.0752 | 3.1775 | 1.114 | | 0.308 |
| | 150 | 1.0795 | 3.1654 | 1.1204 | | 0.353 |
| | 180 | 1.0767 | 3.1432 | 1.1229 | | 0.462 |
| | 210 | 1.0741 | 3.1674 | 1.1262 | | 0.562 |
| | 240 | 1.0747 | 3.1833 | 1.1296 | | 0.607 |
| | 270 | 1.0831 | 3.1465 | 1.1397 | | 0.662 |
| | 300 | 1.0765 | 3.1996 | 1.1369 | | 0.702 |
| | 335 | 1.0788 | 3.1747 | 1.1369 | | 0.673 |
| | 360 | 1.0807 | 3.1797 | 1.1413 | | 0.719 |
| | 390 | 1.0828 | 3.1389 | 1.1414 | | 0.704 |
| | | 1.0821 | 3.1414 | 1.1429 | | 0.745 |
| PJC-1-062 | | | | | | |
| 1 g clay, 5.0 g St | 30 | 1.0796 | 3.0669 | 1.1095 | 0.0444 | -0.001 |
| | 65 | 1.0816 | 3.2212 | 1.1329 | | 0.188 |
| | 90 | 1.079 | 3.0111 | 1.1388 | | 0.335 |
| | 120 | 1.0796 | 3.144 | 1.1562 | | 0.465 |
| | 150 | 1.0801 | 3.0675 | 1.1675 | | 0.611 |
| | 180 | 1.0775 | 3.0953 | 1.1806 | | 0.761 |
| | 210 | 1.0769 | 3.0274 | 1.1822 | | 0.823 |
| | 240 | 1.0786 | 3.0259 | 1.1836 | | 0.821 |
| | 270 | 1.0839 | 3.0036 | 1.1881 | | 0.829 |
| | 300 | 1.0841 | 3.056 | 1.1928 | | 0.847 |
| | 330 | 1.0839 | 3.1149 | 1.196 | | 0.848 |
| | 360 | 1.0799 | 3.1966 | 1.1959 | | 0.840 |
| | 390 | 1.0834 | 3.0295 | 1.1869 | | 0.806 |
| | | 1.0834 | 3.0397 | 1.1932 | | 0.868 |

| PJC-1-063 | Time/ mins | Empty | Full | Dry | | X |
|---|---|---|---|---|---|---|
| 0.5 g clay, 7.5 g St | 35 | 1.0853 | 3.2014 | 1.1074 | 0.0562 | 0.002 |
| | 60 | 1.0845 | 3.1681 | 1.1089 | | 0.021 |
| | 90 | 1.0877 | 3.2114 | 1.1172 | | 0.052 |
| | 120 | 1.0864 | 3.2175 | 1.121 | | 0.086 |
| | 150 | 1.0861 | 3.1817 | 1.1246 | | 0.117 |
| | 180 | 1.0856 | 3.1867 | 1.1297 | | 0.155 |
| | 210 | 1.0873 | 3.2139 | 1.1346 | | 0.173 |
| | 240 | 1.0881 | 3.1913 | 1.1422 | | 0.223 |
| | 270 | 1.0814 | 3.1825 | 1.1391 | | 0.249 |
| | 300 | 1.0776 | 3.1613 | 1.1386 | | 0.275 |
| | 330 | 1.0794 | 3.1859 | 1.1447 | | 0.300 |
| | 360 | 1.0831 | 3.1218 | 1.1492 | | 0.320 |
| | 390 | 1.0889 | 3.1654 | 1.1584 | | 0.335 |
| | | 1.0852 | 3.3402 | 1.2353 | | 0.814 |